INFORMATION TO USERS

This material was produced from a microfilm copy of the original document. While the most advanced technological means to photograph and reproduce this document have been used, the quality is heavily dependent upon the quality of the original submitted.

The following explanation of techniques is provided to help you understand markings or patterns which may appear on this reproduction.

1. The sign or "target" for pages apparently lacking from the document photographed is "Missing Page(s)". If it was possible to obtain the missing page(s) or section, they are spliced into the film along with adjacent pages. This may have necessitated cutting thru an image and duplicating adjacent pages to insure you complete continuity.

2. When an image on the film is obliterated with a large round black mark, it is an indication that the photographer suspected that the copy may have moved during exposure and thus cause a blurred image. You will find a good image of the page in the adjacent frame.

3. When a map, drawing or chart, etc., was part of the material being photographed the photographer followed a definite method in "sectioning" the material. It is customary to begin photoing at the upper left hand corner of a large sheet and to continue photoing from left to right in equal sections with a small overlap. If necessary, sectioning is continued again — beginning below the first row and continuing on until complete.

4. The majority of users indicate that the textual content is of greatest value, however, a somewhat higher quality reproduction could be made from "photographs" if essential to the understanding of the dissertation. Silver prints of "photographs" may be ordered at additional charge by writing the Order Department, giving the catalog number, title, author and specific pages you wish reproduced.

5. PLEASE NOTE: Some pages may have indistinct print. Filmed as received.

Xerox University Microfilms

300 North Zeeb Road
Ann Arbor, Michigan 48106

76-19,131

FITZWATER, Susan Jane, 1950-
FORMULATION AND STUDY OF AB INITIO ETHANE AND MODIFIED UREY-BRADLEY HYDROCARBON FORCE FIELDS; MOLECULAR STRUCTURES OF N-BUTANE AND N-HEXADECANE BY ELECTRON DIFFRACTION.

The University of Michigan, Ph.D., 1976
Chemistry, physical

Xerox University Microfilms, Ann Arbor, Michigan 48106

FORMULATION AND STUDY OF AB INITIO ETHANE AND MODIFIED UREY-BRADLEY HYDROCARBON FORCE FIELDS; MOLECULAR STRUCTURES OF N-BUTANE AND N-HEXADECANE BY ELECTRON DIFFRACTION

by

Susan Jane Fitzwater

A dissertation submitted in partial fulfillment
of the requirements for the degree of
Doctor of Philosophy
(Chemistry)
in The University of Michigan
1976

Doctoral Committee:

Professor Lawrence S. Bartell, Chairman
Professor Seymour M. Blinder
Associate Professor Paul G. Rasmussen
Assistant Professor C. M. Venkatachalam

ACKNOWLEDGEMENTS

I would like to thank Dr. L. S. Bartell for his many helpful discussions during the course of this research, and for his advice during the writing of this dissertation. If the research detailed herein seems interesting and worthwhile, it is so largely as a result of his guidance and imagination.

I also wish to thank the members of the electron diffraction group, past and present, for their assistance. Particularly thanks are due to Mr. David Romenesko for introducing me to molecular mechanics. The electron diffraction group has provided me with a congenial and intellectually stimulating work environment; I would like to express my appreciation to all concerned.

I express special thanks to my parents, whose support has helped me get over a number of rough spots.

Finally, I wish to express my gratitude for financial support from the National Science Foundation and from the Department in the form of Eastman Kodak, Carpenter, Institute of Science and Technology, and Knoller Fellowships. A generous allowance of computing time from The University of Michigan Computer Center is gratefully acknowledged. I also wish to thank Dr. Warren J. Hehre of the University of California at Irvine for running certain computations.

TABLE OF CONTENTS

ACKNOWLEDGEMENTS ii

LIST OF TABLES iv

LIST OF FIGURES vi

LIST OF APPENDICES vii

I. A FORCE FIELD FOR ETHANE: INVESTIGATION OF AB INITIO AND MODEL CONSTANTS, AND CALCULATION OF SECONDARY ISOTOPE EFFECTS UPON MOLECULAR STRUCTURE 1

Derivation and Description of the Force Field . 2
The Secondary Isotope Effect upon the C-C Bond Length in Ethane 29
References 50

II. FORMULATION AND TESTING OF A MODIFIED UREY-BRADLEY MODEL FORCE FIELD AND AN INVESTIGATION OF THE "GAUCHE HYDROGEN EFFECT" 52

Introduction 52
Formulation of MUB-2 56
Computer Programs Used 70
Evaluation of MUB-2 71
Investigation of the Gauche Hydrogen Hypothesis 99
References 109
Appendix 111

III. GAS-PHASE ELECTRON DIFFRACTION DETERMINATIONS OF THE STRUCTURES OF N-ALKANES: N-BUTANE AND N-HEXADECANE 121

Determination of the Structure of n-Butane . . 121
Determination of the Structure of n-Hexadecane. 140
References 182
Appendices 183

LIST OF TABLES

PART I

I.	Symmetry Coordinates of Ethane	7
II.	*Ab Initio* Symmetry Force Constants for Ethane.	10
IV.	General Valence Force Constants for C_2H_6	16
V.	Selected Anharmonic Force Constants for Ethane	17
VI.	Transformation of symmetry Force Constants to Valence Force Constants	21
VII.	Differences Between the Mean-Square Amplitudes of the Symmetry Coordinates of Protiated and Deuterated Ethane	34
VIII.	Differences Between the Elements of the Matrices of Ethane and Deuteroethane, *Ab Initio* and Model Force Field	35
IX.	Isotope Effects upon the Structure of Ethane	36
III.	Conformations of Ethane Used in the Derivation of the *Ab Initio* Force Field	41

PART II

I.	Constants for the Nonbonded Potential Interaction Functions	64
II.	Parameters of MUB-2 Force Field	64
III.	Comparison of the Experimental and Calculated Structural Parameters of Tri-*t*-butyl Methane	85
IV.	Computed and Experimental Geometrical Isomerization Energies for Vibrationless Molecules.	95
V.	Experimental and Calculated Barriers to Hindered Internal Rotation	98
VI.	Major Contributors to *Gauche*-*Trans* *n*-Butane Energy Difference	102
VII.	Major Contributors to the Axial-Equatorial Methylcyclohexane Energy Difference	104
VIII.	Major Contributors to the *trans*-*cis* 1,3 Dimethylcyclohexane Energy Difference	104
A1.	Parameters of MUB-2'	114
A2.	Experimental and Calculated Normal Mode Frequencies of Methane	115
A3.	Experimental and Calculated Normal Mode Frequencies of Ethane	115
A4.	Computed and Experimental Zero-Point Energy Differences	119

PART III

I.	Distances, Amplitudes, and Shrinkages Adopted for the *n*-Butane Structure Determination	129

LIST OF TABLES continued

II. Values of the Independent Parameters for n-Butane 130
III. Correlation Matrix for the Independent Parameters 131
IV. Experimental Conditions Under Which Diffraction Patterns of n-Hexadecane were Recorded. 143
V. Distances, Shrinkages, and Additive Amplitude Constants Adopted for n-Hexadecane 150
VI. Values of the Independent Parameters for n-Hexadecane 156
VII. Values of the Fixed Amplitudes for n-Hexadecane 156
VIII. Correlation Matrix for the Independent Parameters of n-Hexadecane 158

LIST OF FIGURES

PART I

1. Notation for Ethane Interaction Constants. . 22

PART II

1. Comparison Between $H_2...H_2$ Interaction Energies 60
2. Comparison of experimental and calculated C-C bond lengths 75
3. Comparison of experimental and calculated C-H bond lengths 77
4. Comparison of experimental and calculated CCC angles 79
5. Comparison of experimental and calculated HCC angles 81
6. Nonbonded force curves 106

PART III

1. Molecular Model Used for n-Butane 122
2. Experimental and Calculated Molecular Intensity Functions for n-Butane 132
3. Experimental Radial Distribution Function for n-Butane 133
4. Standard Deviation of the Intensity as a Function of the trans Fraction for n-Butane. 135
5. Experimental and Calculated Molecular Intensity Functions for n-Hexadecane 160
6. Experimental Radial Distribution Function for n-Hexadecane 162
7. Standard Deviation of the Intensity as a Function of ΔG° (gauche-trans) for n-Hexadecane 164

LIST OF APPENDICES

PART II

I. MUB-2': A Variant of MUB-2 Designed to Fit Vibrational Frequencies 111

PART III

I. Experimental Levelled Intensity and Background Intensity Functions for n-Butane 183

II. Experimental Levelled Intensity and Background Intensity Functions for n-Hexadecane 188

I. A FORCE FIELD FOR ETHANE: INVESTIGATION OF *AB INITIO* AND MODEL CONSTANTS, AND CALCULATION OF SECONDARY ISOTOPE EFFECTS UPON MOLECULAR STRUCTURE

A. Derivation and Description of the Force Field

1. Introduction

It is difficult to derive all quadratic and cubic force constants for even simple molecules from experimental data. Methane and ethane may be considered to be fairly simple molecules; yet some of the methane cubic constants are not known[1] and even the complete set of quadratic constants of the ethane force field is not known accurately. Experiment offers no simple way to gauge the importance of several interactions in contributing to an accurate representation of the ethane potential surface. Further information on both quadratic and higher-order interactions would be useful in improving so-called model force fields, which are used to calculate a variety of structural, vibrational, and thermochemical data. In addition, certain cubic force constants may be used to calculate the secondary isotope effect upon the carbon-carbon bond length in ethane, a piece of information which would be of interest to structural chemists and which has proven difficult to determine experimentally.[2]

One approach to determining a complete force field for ethane is the use of *ab initio* calculations of the energies of various molecular conformations. A number of

molecular force fields have been determined using single-determinant self-consistent field calculations[3]; such fields are not completely satisfactory, as the quadratic constants tend to be too high and the cubic constants too low. However, it is possible to use ab initio methods to compute the energy contribution of any component of the force field, some of which information has been inaccessible experimentally to date. While some computed force constants may be only semiquantitatively correct, they provide at least rough guidelines for determining the importance of certain interactions.

The ability to assess the importance of a given interaction will probably become of prime importance in improving existing model force fields. These are intended to be simplified representations of the generalized potential surface of a given class of molecules (e.g., hydrocarbons, amines, etc.) which may be used to calculate various pieces of information about molecules belonging to the given class. Intensive research into molecular mechanics over the past few years has led to the formulation of a number of hydrocarbon force fields[4]; all of these reproduce a large body of information to within the order of magnitude of the experimental accuracy, but the calculated values of some items of interest are poor. So far, no field has shown itself to be clearly superior to the others. There are a number of different schools of thought on the best way to construct a model force field; however,

one idea that is held by all is that, ideally, the set of model force field constants must be completely transferable within the given class of molecules. This implies that the components of the model force field must be physically reasonable separately if the field is to be more than a mathematical interpolation scheme, valid only for reproducing those pieces of data which were used in its optimization. However, the parameters of many model force fields tend to be highly correlated, which leaves the physical significance of the individual parameters somewhat questionable. In addition, the high parameter correlation can obscure the possible importance of certain interactions which have been left out of the force field. The ab initio force constants may be used both to evaluate the physical plausibility of certain models embodied in model force fields and to determine the importance of various interactions, as shown below.

One of the major reasons for computing the ab initio force field of ethane is to investigate the validity of including anharmonic repulsive atom-atom terms for 1..3 (geminal) interactions in a hydrocarbon model force field. Almost all model force fields neglect these; those that do not (see ref. 4a; also Part II of this thesis) have not been shown to be clearly superior or inferior to the other fields in reproducing observed data. Because certain quadratic interaction constants are formally equivalent to combinations of first and second derivatives of the

geminal nonbonded potential functions, comparison of the *ab initio* interaction constants with the corresponding constants evaluated from the nonbonded potential functions can indicate whether the nonbonded functions provide the proper balance of forces. If it is possible for a well-balanced set of nonbonded interaction potentials to provide proper values for a number of quadratic interaction constants, then a modified Urey-Bradley model force field may perform as well as a general valence-type model force field and be more economical of parameters, which is to be desired. In addition, a modified Urey-Bradley model force field may formally include some anharmonic interactions which are not usually included in general valence-type model force fields: if the *ab initio* values of at least some anharmonic constants are not negligible and if a well-balanced set of nonbonded interaction potentials can reproduce the values of these constants, the modified Urey-Bradley functional form is to be preferred over the general valence-type functional form commonly used for model force fields. Pulay and Meyer have computed the quadratic force constants of ethane from *ab initio* data[3b]; however, they derived no values for anharmonic constants, although the deformations that they used are large enough to show some effects of anharmonicity (Pulay has subsequently extracted some cubic constants from the energy data used in ref. 3b; these have approximately the same magnitude as those determined previously in the course of

this research[3c]). Because of this, and because of the fact that Pulay and Meyer used a slightly different basis set than the one used in this research, it was necessary to recompute the quadratic constants of the force field.

2. Calculations

The method used to determine the force constants may be briefly summarized as follows: the value of the energy at a number of points on the ethane potential surface was determined *via* an *ab initio* method, a form for the force field was assumed, and the best fit of the force constants to the energy data was obtained using least squares methods. While this is less efficient than Pulay's method,[3a] there was a ready supply of energy data and the least squares processing required neither vast amounts of computer time nor great effort to set up. The energies of appropriate conformations which were supplied by this laboratory were calculated by Dr. Warren J. Hehre of the University of California at Irvine using his computer program GAUSSIAN 70[5].

Molecular electronic energies were calculated for a number of deformations along various symmetry coordinates. The energies were calculated using single determinant *ab initio* molecular orbital theory at the split valence shell, 4-31G level. Deformation energies, designated below as V, were obtained for each conformation by subtracting the

electronic energy of the minimum energy structure from the electronic energy of each conformation. The force field was then defined by

$$V = 1/2 \sum_{ij}\sum F_{ij}S_iS_j + \sum_i F_{iii}S_i^3 + \sum_{i\neq j} F_{iij}S_i^2S_j \ . \ . \qquad (1)$$

where the F_{ij}, F_{iii}, and F_{iij} are the force constants and the S_i are the symmetry coordinates, which are defined in Table I. Since the equilibrium structure of ethane is not known with great precision, the S_i were evaluated relative to the equilibrium structure suggested by the ab initio calculations themselves. The approximate equilibrium structure which had been derived from the calculations was r_{CH} = 1.083 A, r_{CC} = 1.529 A, and angle HCC = 107.70°. The derived C-H bond length is a bit shorter than the equilibrium bond length in methane, estimated to be 1.085 A by Kuchitsu and Bartell[6] and computed to be 1.091 A by Meyer.[3b] Electron diffraction studies[6,2c] imply that the C-H bond length in methane is 0.003 A shorter than that in ethane, while 4-31G calculations make the difference 0.002 A. The derived C-C bond length is slightly greater than the estimated equilibrium length of 1.526 A, which was derived from the electron diffraction r_g value.[2c] The derived HCH angle is also slightly larger than its experimental counterpart: the thermal (0° K) average (r_z) HCH angle is estimated to be 107.4°.[7] The equilibrium structure derived from the force field after the constants had

Table I. Symmetry coordinates for ethane[a]

A_{1g}:

$$S_1 = 6^{-1/2}\Sigma_i(\Delta r_i + \Delta r_{i'})$$

$$S_2 = 12^{-1/2}[A\Sigma_i(\Delta\theta_i + \Delta\theta_{i'}) - B\Sigma_i(\Delta\psi_i + \Delta\psi_{i'})]$$

$$S_3 = \Delta R_{cc}$$

A_{1u}:

$$S_4 = \tau$$

A_{2u}:

$$S_5 = 6^{-1/2}\Sigma_i(\Delta r_i - \Delta r_{i'})$$

$$S_6 = 12^{-1/2}[A\Sigma_i(\Delta\theta_i - \Delta\theta_{i'}) - B\Sigma_i(\Delta\psi_i - \Delta\psi_{i'})]$$

E_u:

$$S_7 = 12^{-1/2}[(2\Delta r_1 - \Delta r_2 - \Delta r_3) - (2\Delta r_{1'} - \Delta r_{2'} - \Delta r_{3'})]$$

$$S_8 = 12^{-1/2}[(2\Delta\theta_1 - \Delta\theta_2 - \Delta\theta_3) - (2\Delta\theta_{1'} - \Delta\theta_{2'} - \Delta\theta_{3'})]$$

$$S_9 = 12^{-1/2}[2\Delta\psi_1 - \Delta\psi_2 - \Delta\psi_3) - (2\Delta\psi_{1'} - \Delta\psi_{2'} - \Delta\psi_{3'})]$$

E_g:

$$S_{10} = 12^{-1/2}[2\Delta r_1 - \Delta r_2 - \Delta r_3) + (2\Delta r_{1'} - \Delta r_{2'} - \Delta r_{3'})]$$

$$S_{11} = 12^{-1/2}[(2\Delta\theta_1 - \Delta\theta_2 - \Delta\theta_3) + (2\Delta\theta_{1'} - \Delta\theta_{2'} - \Delta\theta_{3'})]$$

$$S_{12} = 12^{-1/2}[(2\Delta\psi_1 - \Delta\psi_2 - \Delta\psi_3) + (2\Delta\psi_{1'} - \Delta\psi_{2'} - \Delta\psi_{3'})]$$

[a] $A = [2\gamma/(1+\gamma)]^{1/2}$, $B = [2/(1+\gamma)]^{1/2}$, $\gamma = 12\cos^2\psi_e/(4-3\sin^2\psi_e)$, ψ_e = equilibrium ∠HCC. At $\psi_e = 109.4712°$, $\gamma = A = B = 1$.

been fitted to the energy points was only negligibly different from the assumed equilibrium structure: the new structural parameters were r_{CH} = 1.0834 A, r_{CC} = 1.5289 A, and angle HCH = 107.7258°. Schwendeman has recommended[8] that theoretical force constants be calculated from experimental rather than theoretical equilibrium structures so that the effects of anharmonicity upon the quadratic force constants will be minimized. The quadratic force constants are equal to the second derivatives of the potential energy with respect to the given coordinates; for a bond stretch, the second derivative of the Morse curve is $k(1 - 3ax + \ldots)$, where $x = r - r_e$. Since a is around 2 A^{-1} for many bonds, a shift of the derived r_e from the true r_e of 0.01 A may alter a force constant by about 6%. Bending force constants are less sensitive to the precise values used for the equilibrium structure. While an error of 6% certainly is not negligible, it is tolerable for the purposes for which the force field is designed to be used. Also, since the ab initio equilibrium structure is quite close to the experimental equilibrium structure (as far as the latter is known), it would seem probable that the errors in the stretching force constants arising from the use of the ab initio equilibrium structure are less than 6% (this estimate includes only the error expected to arise from an incorrect choice of the equilibrium structure). In view of the well-known shortcomings of ab initio force fields (alluded to in the Introduction), uncertainties of such

magnitude are not a cause of undue concern. In any event, even if the uncertainties in the interaction constants were greater than 6%, the ab initio results would still be more precise than those available from experiment.

The deformations for which molecular energies were calculated ranged up to 0.056 A for C-H stretches, 0.04 A for the C-C stretch, and 7° for the bends, which magnitudes were large enough to show sizeable effects arising from anharmonicity. The final scheme adopted for the extraction of the force field from the array of potential energies was as follows: first, the diagonal force constants F_{ii} and F_{iii} (and, for A_{1g}, F_i) were derived by least squares analyses of the data for deformations along pure symmetry coordinates. An attempt was made to compensate for the effects of quartic contributions (which were small) to the A_{1g} deformation energies by including diagonal quartic terms, with the values of the F_{iiii} determined by giving the ratios F_{iiii}/F_{iii} their Morse curve values. Once the diagonal constants were derived, the interaction constants were determined from the energies for mixed deformations. In the case of important quadratic interaction constants, which were expected to have good-sized magnitudes and about which several potential energies contained information, the energy contribution arising from the diagonal terms was subtracted from each of the relevant energy points and the interaction constants were derived by least squares analyses of the energy remainders.

Table II. Ab Initio Symmetry Force Constants for Ethane with Estimated Errors due to Round-Off.[a]

Energy in Mdyne-A.

Symmetry Class	Quadratic	Anharmonic
A_{1g}	F_{11} = 5.861(4)	F_{111} = -2.086(10)
	F_{22} = 0.754(1)	F_{222} = 0.081(2)
	F_{33} = 4.877(50)	F_{333} = -3.909(2)
	F_{12} = 0.150(4)	F_{113} = 0.1446(3)
	F_{13} = 0.204(6)	F_{223} = -0.262(1)
	F_{23} = -0.581(1)	F_{133} = -1.48(15)
		F_{233} = 0.45(2)
		F_{1133} = 10.9(30)
A_{1g} linear coefficients:		
F_1 = -0.0114(3), F_2 = -0.0027(1), F_3 = 0.0025(4)		
A_{2u}	F_{55} = 5.868(6)	
	F_{66} = 0.689(1)	
	F_{56} = 0.186(1)	
E_u	F_{77} = 5.762(6)	F_{8888} = 0.4(3)
	F_{88} = 0.687(1)	F_{9999} = 0.83(15)
	F_{99} = 0.605(12)	
	F_{78} = -0.195(1)	
	F_{79} = 0.093(1)	
	F_{89} = 0.018(8)	
E_g	$F_{10,10}$ = 5.675(6)	$F_{10,10,10}$=-1.513(30)
	$F_{11,11}$ = 0.724(3)	$F_{11,11,11}$=-0.007(5)
	$F_{12,12}$ = 1.001(12)	$F_{12,12,12}$=-0.071(20)
	$F_{10,11}$ = -0.199(40)	
	$F_{10,12}$ = 0.196(40)	
	$F_{11,12}$ = -0.029(20)	

Table II continued.

Symmetry Class	Quadratic	Anharmonic
Mixed		$F_{553} = 0.144(30)$
		$F_{773} = 0.132(30)$
		$F_{10,10,3}=0.160(30)$
		$F_{663} = -0.172(6)$
		$F_{883} = 0.014(30)$
		$F_{993} = -0.466(6)$
		$F_{11,11,3}=0.043(30)$
		$F_{12,12,3}=-0.456(6)$
		$F_{443} = -0.165(5)$
		$F_{266} = 0.282(50)$
		$F_{288} = -0.173(10)$
		$F_{299} = 0.089(20)$
		$F_{2,11,11}=-0.175(10)$
		$F_{2,12,12}=0.132(18)$

[a] Last figure in parentheses corresponds to last decimal in listed value.

Cubic interaction constants and small quadratic interaction constants about which few of the calculated potential energies contained information were obtained from sets of pairs of molecular deformations for which the sums (or differences) of energies would cancel contributions from most interactions, isolating the contribution from the interaction of interest. Differences between the original energies and those calculated from the derived force constants were, for the most part, of the order of the round-off errors in the former values. The derived force constants, along with their estimated uncertainties (see below), are given in Table II. Table III lists the molecular configurations used in the computations, along with the associated energies and residuals.

There were no immediately available ab initio data from which the stretch-torsion-torsion constant, F_{344}, could be evaluated directly. However, since a number of ab initio calculations[9,10] indicate that there is an appreciable change in the C-C bond length when ethane moves from its staggered to its eclipsed conformation, it may be assumed that F_{344} is not negligible. When 4-31G methods were used, the difference δR between minimum energy C-C bond lengths for eclipsed and staggered ethane (no other internal coordinates were allowed to relax) was computed to be 0.015 A. It was assumed that the C-C bond length varies with the torsional angle τ as

$$R - R_e = (1 - \cos 3\tau)\delta R/2 \tag{2}$$

or, if τ is small,

$$R - R_e = 9\tau^2 \delta R/4 \tag{3}$$

The important associated terms in the potential energy are, for $S_3 \equiv R - R_e$ and $S_4 \equiv \tau$,

$$V(S_3,S_4) = \cdots + 1/2\ F_{33}S_3^{\,2} + F_{344}S_3S_4^{\,2} + \cdots \tag{4}$$

from which

$$\begin{aligned} \partial V/\partial S_3 &= F_{33}S_3 + F_{344}S_4^{\,2} \\ &= 0 \quad \text{at minimum V} \end{aligned} \tag{5}$$

which implies

$$(S_3)_{min} = -F_{344}S_4^{\,2}/F_{33} \tag{6}$$

Comparing equations (3) and (6) one finds that

$$F_{344} = -9F_{33}\delta R/4 \tag{7}$$

The computed value of F_{344} is given in Table II.

It is not immediately obvious that the method described above is the best way to derive the force field from the available data. However, a number of different schemes were tried, and the one described above gave the smallest residuals and lowest uncertainties overall. One definite advantage of deriving the force constants using a series of least squares analyses of subsets of the data,

as opposed to fitting all of the force constants to all of the data simultaneously, was that interaction constants which initially had been assumed to be negligible but which were not could be spotted fairly easily. Therefore, the derived values of the force constants cannot be very heavily influenced by cubic and higher-order interactions which were erroneously assumed to be unimportant. It was observed that the values of the bulk of the force constants seemed independent of the scheme used to extract them from the molecular energy information. Therefore, it may be assumed that the force field provides a good representation of the potential surface as described by the ab initio energy data.

Because of the method by which the force constants were derived, the proper way to determine the uncertainties in the derived values was not obvious. The processes of fitting the force constants to the energy data using a number of different schemes gave rough indications of the degrees of uncertainty in some of the force constants. In order to get more information on the magnitudes of the uncertainties, an error analysis was done assuming that (1) all of the constants had been fitted to all of the data simultaneously, and (2) the residuals were random. Though these conditions were not fulfilled by the fit of the force field to the data, it was assumed that the analysis would yield results which could be used along with the indications of the uncertainties in the force constants

from the various fitting schemes to give reasonable uncertainty estimates. For the most part, the uncertainties obtained from the error analysis paralleled those which would have been estimated from the variation of the force constants over the various fitting schemes. The estimated uncertainties are given along with the force constants in Table II.

3. Results

As stated before, the force constants are tabulated in Table II. Table IV compares the force field derived in the course of this research with that of Pulay and Meyer,[3b] the experimental force fields of Hansen and Dennison[11] and Duncan,[12] and force constants derived from two model force fields which were formulated prior to the determination of the ab initio force field. Table V compares selected cubic constants with the corresponding quantities computed from nonbonded interaction potentials used in a modified Urey-Bradley model force field (see Part II of this thesis).

The model force fields with which certain ab initio force constants are compared in Tables IV and V represent two rather different approaches to the formulation of model force fields. The first is the recent "consistent force field" of Ermer and Lifson,[13] while the second is the modified Urey-Bradley field described in Part II of this

Table IV. General Valence Force Constants for C_2H_6, energy in mdÅ.

Constant	Calculated			Experimental	
	ab initio MO[a]	CFF Model[b]	Steric Model[c]	H&D[d]	JLD[e]
k_r	5.767	4.735	- -	5.35	4.810
k_R	4.877	4.483	- -	4.57	4.450
k_{rr}	0.049	0	0.327	-0.02	0.045
k_{kR}	0.083	0	0.447	0.0	(0)
$k_{rr'}$	-0.030	0	0	0.08	-0.036
$k_{rr'\beta}$	0.013	0	0	-0.04	0.015
$k_{r\theta} - k_{r\theta\beta}$	-0.197	0	-0.161	-0.11	-0.076
$k_{r\psi} - k_{r\psi\beta}$	0.145	0	0.234	-0.04	(0.076)[f]
$Ak_{r\theta\beta} - Bk_{r\psi\beta}$	0.194	0	0.165	-0.52	0.074
$Ak_{R\theta} - Bk_{R\psi}$	-0.335	-0.267	-0.359	-0.33	-0.282
$k_{r\theta'} - k_{r\theta'\beta}$	-0.002	≈0	0	-0.02	(0)
$k_{r\psi'} - k_{r\psi'\beta}$	0.052	≈0	0	-0.17	(0)
$Ak_{r\theta'\beta} - Bk_{r\psi'\beta}$	0.009	≈0	0	-0.10	(0)
$k_\theta - k_{\theta\theta}$	0.706	0.549	- -	0.62	0.560
$k_\psi - k_{\psi\psi}$	0.803	0.672	- -	0.75	0.682
$k_{\theta\psi} - k_{\theta\psi\beta}$	-0.006	0	0	-0.04	0.008
$\frac{2}{[A^2k_{\theta\theta} + B^2k_{\psi\psi} - AB(k_{\theta\psi} + k_{\theta\psi\beta})]}$	-0.018	-0.055	0	0.06	-0.012
$k_{\theta\theta'} - k_{\theta\theta'\beta}$	0.019	≈0	0	-0.02	-0.006
$k_{\psi\psi'} - k_{\psi\psi'\beta}$	0.198	0.104	0	0.13	0.139
$k_{\theta\psi'} - k_{\theta\psi'\beta}$	-0.024	0	0	0.09	0.005
$\frac{2}{[A^2k_{\theta\theta'\beta}+B^2k_{\psi\psi'\beta} - AB(k_{\theta\psi'}+k_{\theta\psi'\beta})]}$	-0.039	-0.035	0	-0.09	-0.024

[a] This work. [b] Reference 13. [c] Based solely on geminal interactions. [d] Reference 11. [e] Reference 12. [f] Constrained to be the negative of the previous value.

Table V. Selected Anharmonic Force Constants for Ethane with Estimated Errors due to Round-Off. Energy in mdÅ

Force Constant	ab initio MO	geminal steric model
Diagonal Stretch		
F_{111}	-2.086 (10)	- -
F_{333}	-3.909 (2)	- -
$F_{10,10,10}$	-1.513 (30)	- -
Diagonal Bend		
F_{222}	0.081 (2)	0.050 (0.069) [a]
$F_{11,11,11}$	-0.007 (5)	-0.014
$F_{12,12,12}$	-0.071 (20)	-0.070
Coupling F_{iij}		
i=stretch,j=3		
F_{113}	0.1446 (3)	-0.578
F_{553}	0.144 (30)	-0.578
F_{773}	0.132 (30)	-0.578
$F_{10,10,3}$	0.160 (30)	-0.578
i=bend,j=3		
F_{223}	-0.262 (1)	-0.335
F_{663}	-0.172 (6)	-0.335
F_{883}	0.014 (30)	0
F_{993}	-0.466 (6)	-0.611
$F_{11,11,3}$	0.043 (30)	0
$F_{12,12,3}$	-0.456 (6)	-0.611
i=torsion,j-3		
F_{443}	-0.165 (5)	0

Table V. Continued.

Force Constant	ab initio MO	geminal steric model
i=bend,j=2		
F_{222}	0.081 (2)	0.050
F_{266}	0.282 (50)	0.149
F_{288}	-0.173 (10)	-0.218
F_{299}	0.089 (20)	0.174
$F_{2,11,11}$	-0.175 (10)	-0.218
$F_{2,12,12}$	0.132 (18)	0.174
Miscellaneous		
F_{122}	- -	-0.14
F_{133}	-1.48 (15)	-1.92
$F_{1,11,11}$	- -	-0.10
F_{233}	0.45 (2)	0.94
F_{1133}	10.9 (30)	2.3
F_{8888}	0.4 (3)	- -
F_{9999}	0.83 (15)	- -

[a] This constant also includes vicinal gauche H...H interactions.

thesis. A "consistent force field," or CFF, is derived by assuming a functional form for the model force field and then deriving the parameters by a least squares analysis of a variety of vibrational, conformational, structural, and thermochemical data. The form of the CFF examined in this research is that of a valence force field with added interactions; no geminal (1..3) nonbonded interactions are considered explicitly, but terms which might be considered to arise from geminal nonbonded interactions are included in the force field. The modified Urey-Bradley field, on the other hand, was constructed by combining components which were separately physically reasonable in order to approximate the aliphatic hydrocarbon potential surface described by the force fields of Schachtschneider and Snyder.[14] This model field has been fairly successful in reproducing experimental data (as has been the CFF). As implied by the name, the form of the modified Urey-Bradley field is closely akin to that of the "classical" Urey-Bradley force field; geminal nonbonded interactions are included explicitly, using the same nonbonded interaction potential functions as are used for the 1..4 and more distant interactions.

The model force field "force constants" displayed in Tables IV and V were obtained by taking the second and third derivatives of the model potential surfaces with respect to the given symmetry coordinates. For all but one constant, which is noted, only the contributions from the derivatives of the geminal nonbonded energies were

considered. The geminal nonbonded contribution to F_{ij} from interaction kl is $\partial^2 V_{kl}/\partial S_i \partial S_j$, while that to F_{iij} is $\partial^3 V_{kl}/\partial S_i^2 \partial S_j$. These derivatives were evaluated numerically and, in some cases, checked analytically. The comparison of the quadratic force constants is given in terms of those for a general valence force field

$$2V = \sum_{ij}\sum k_{ij} R_i R_j \qquad (8)$$

Interactions are identified in Figure 1. The relations governing the transformation of the F_{ij} into the k_{ij} are given in Table VI. Geminal nonbonded components of the k_{ij} were derived from Shimanouchi's Urey-Bradley equations[15] by identifying the Urey-Bradley F'_{kl} and F_{kl} with $r_{kl}\partial V_{kl}/\partial r_{kl}$ and $\frac{\partial^2 V_{kl}}{\partial r_{kl}^2}$, respectively.

4. Discussion

a. Quadratic Force Constants

Due to the lack of experimental values with which the ab initio force constants may be properly compared, it is difficult to judge how well the force field represents the true ethane potential surface. Some differences between the force constants derived in this research and those determined by Pulay and Meyer were to be expected: different basis sets were used, there were slight differences in the reference structures adopted, and the deformations from which Pulay and Meyer derived their quadratic

Table VI. Transformation of symmetry force constants to valence force constants[a]

$$k_r = 1/6(F_{11} + F_{55} + 2F_{77} + 2F_{10,10})$$

$$k_r = F_{33}$$

$$k_{rr} = 1/6(F_{11} + F_{55} - F_{77} - F_{10,10})$$

$$k_{rR} = 6^{-1/2}F_{13}$$

$$k_{rr'} = 1/6(F_{11} - F_{55} - 2F_{77} + 2F_{10,10})$$

$$k_{rr'\beta} = 1/6(F_{11} - F_{55} + F_{77} - F_{10,10})$$

$$k_{r\theta} - k_{r\theta\beta} = 1/2(F_{78} + F_{10,11})$$

$$k_{r\psi} - k_{r\psi\beta} = 1/2(F_{79} + F_{10,12})$$

$$Ak_{r\theta_\beta} - Bk_{r\psi_\beta} = 1/6[2^{1/2}(F_{12}+F_{56}) - A(F_{78}+F_{10,11}) + B(F_{79}+F_{10,12})]$$

$$Ak_{R\theta} - Bk_{R\psi} = 3^{-1/2}F_{23}$$

$$k_{r\theta'} - k_{r\theta'\beta} = 1/2(-F_{78} + F_{10,11})$$

$$k_{r\psi'} - k_{r\psi'\beta} = 1/2(-F_{79} + F_{10,12})$$

$$Ak_{r\theta'_\beta} - Bk_{r\psi'_\beta} = 1/6[2^{1/2}(F_{12}-F_{56}) + A(F_{78}-F_{10,11}) - B(F_{79}-F_{10,12})]$$

$$k_\theta - k_{\theta\theta} = 1/2(F_{88} + F_{11,11})$$

$$k_\psi - k_{\psi\psi} = 1/2(F_{99} + F_{12,12})$$

$$k_{\theta\psi} - k_{\theta\psi_\beta} = 1/2(F_{89} + F_{11,12})$$

$$A^2k_{\theta\theta} + B^2k_{\psi\psi} - AB(k_{\theta\psi} + k_{\theta\psi_\beta}) =$$
$$1/6[2(F_{22}+F_{66}) - A^2(F_{88}+F_{11,11}) - B^2(F_{99}+F_{12,12}) - AB(F_{89}+F_{11,12})]$$

$$k_{\theta\theta'} - k_{\theta\theta'_\beta} = 1/2(-F_{88} + F_{11,11})$$

$$k_{\psi\psi'} - k_{\psi\psi'_\beta} = 1/2(-F_{99} + F_{12,12})$$

$$k_{\theta\psi'} - k_{\theta\psi'_\beta} = 1/2(-F_{89} + F_{11,12})$$

$$A^2k_{\theta\theta'_\beta} + B^2k_{\psi\psi'_\beta} - AB(k_{\theta\psi'} + k_{\theta\psi'_\beta}) =$$
$$1/6[2(F_{22}-F_{66}) + A^2(F_{88}-F_{11,11}) + B^2(F_{99}-F_{12,12}) + AB(F_{89}-F_{11,12})]$$

[a] $A = [2\gamma/(1+\gamma)]^{1/2}$, $B = [2/(1+\gamma)]^{1/2}$, $\gamma = 12\cos^2\psi_e/-(4-3\sin^2\psi_e)$.

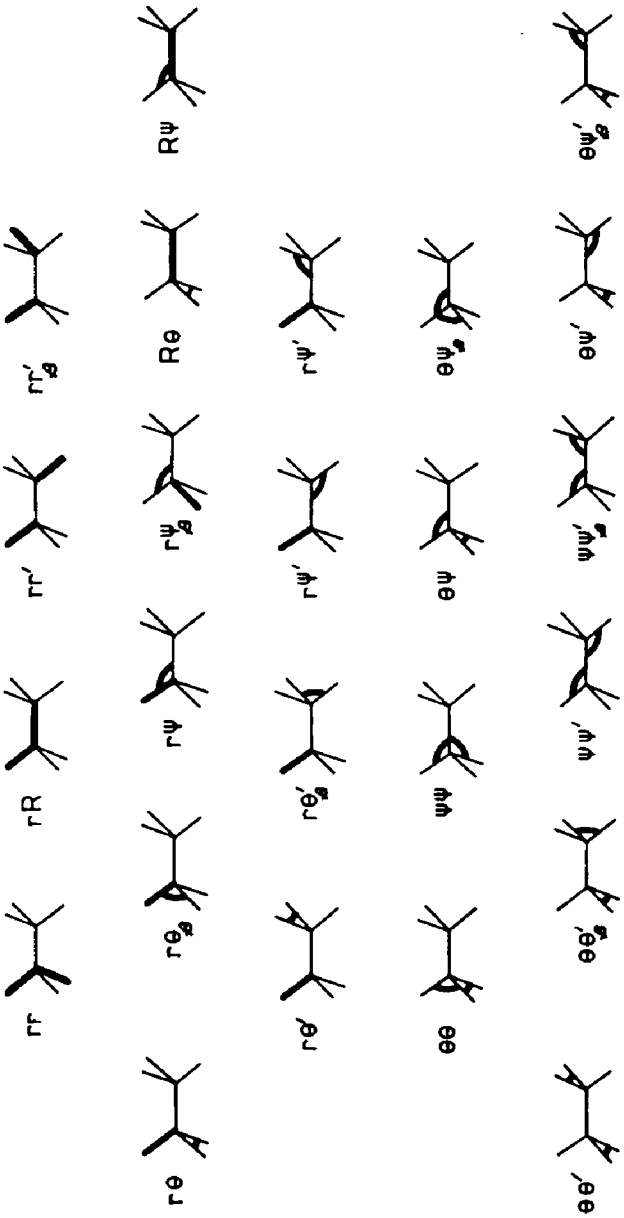


Figure 1. Notation for Ethane Interaction Constants.

force constants were comparable in magnitude to those from which quadratic and cubic (and in some cases even quartic) force constants were derived in the course of the present research. However, these differences, as may be seen in Table IV, are quite minor. Certainly the two ab initio force fields are in closer agreement than are the ab initio force fields detailed in Table II and the experimental force fields. As was to be expected, the diagonal quadratic ab initio force constants agree better with the force constants of Hansen and Dennison than with those of Duncan, since Hansen and Dennison made approximate corrections to the normal mode frequencies in order to remove the effects of anharmonicity while Duncan did not. The discrepancies between the ab initio and the experimental force constants are not too disturbing, since each of the experimental force fields has its flaws. Very few constraints were placed on Hansen and Dennison's least squares fit of the potential constants to their corrected frequencies; consequently, the interaction constants contain a fair amount of scatter. Duncan avoided this problem by imposing a larger number of constraints, but the zero values assumed for some constants influenced the values derived for others. In addition, his constants are contaminated by anharmonicity effects.

In view of the stated purpose of using the ab initio force constants to assess various model force fields, the comparisons of ab initio and model interaction constants

listed in Table IV are particularly interesting. As can be seen, those interaction constants which are included in the CFF agree in sign and in approximate magnitude with the ab initio constants (those constants listed as "≈0" do not include the effects of nongeminal H..H interactions, but according to the CFF, these should be small). However, the CFF assumes zero values for a number of stretch-bend constants for which the ab initio values are not negligible. Turning to the results from the modified Urey-Bradley model field, one sees that while it seems to provide a fairly good representation of the ab initio stretch-bend constants, it implies stretch-stretch constants which are several times as high as the corresponding ab initio constants. Here, too, one non-negligible ab initio interaction constant ($k_{\psi\psi'} - k_{\psi\psi'_\beta}$) is assumed to be zero in the modified Urey-Bradley field.

Possible reasons for the poor performance of the modified Urey-Bradley model field in reproducing the ab initio values of the stretch-stretch constants may relate to some observations which have been made in different contexts. Urey-Bradley analyses[16] have indicated that while halogen-halogen intramolecular repulsions seem to follow "normal" classical nonbonded force laws, H...H geminal interactions, as represented by the Urey-Bradley interaction $F_{H...H}$-$(\Delta r_{H...H})^2$, seem to have anomalously low energies (see the discussion in the Appendix to Part II of this thesis). A possible explanation for this observation is suggested by

examination of the general valence force field-type interactions which are contained in the term $F_{H...H}(\Delta r_{H...H})^2$. One of these is the stretch-stretch interaction term, $\Delta r_{CH_1}\Delta r_{CH_2}$. It has been suggested[17] that geminal nonbonded interactions are not the only source of the C-H stretch-stretch interaction energy, but that another interaction, designated $G\Delta r_i\Delta r_j$, also contributes to the energy and indeed makes the dominant contribution for large positive or negative displacements. It has been speculated[17] that one function of the G interaction is to correct for the tendency of hydrogens to lose their identity as they approach the nucleus, forming a pseudo-united atom. Hence, the geminal nonbonded interaction model implies an increase in the stretch-stretch interaction energy as the protons move toward the nucleus, while the G interaction model implies that the same deformation will cause a decrease in the stretch-stretch interaction energy. Considering the functional form of the Urey-Bradley force field, where the interaction $\Delta r_i\Delta r_j$ enters the potential entirely as a function of the nonbonded interactions, a good-sized H...H force opposed by a fairly large $G\Delta r_i\Delta r_j$ force could easily produce an $F_{H...H}$ which would be anomalously small. A G interaction has been suggested for the Urey-Bradley force field of methane.[17] The importance of the G interaction is also suggested by model force field calculations. An interaction $G\Delta r_i\Delta r_j$ was introduced into the modified Urey-Bradley model force field in an attempt to improve the

calculated C-H stretching frequencies (see the Appendix to Part II of this thesis). The magnitude of G was determined by varying the constant so that the splitting of the experimental C-H stretching frequencies was reproduced; the final value obtained for G was -0.28 mdyne/A. When this G constant value is taken into account, the value of k_{rr} implied by the modified Urey-Bradley model force field is 0.047 mdyne/A, quite close to the ab initio value of 0.049 mdyne/A. This result indicates that the large discrepancy between the ab initio k_{rR} and the modified Urey-Bradley k_{rR} supports the inclusion of a $G\Delta r_i \Delta R$ interaction in the modified Urey-Bradley model force field.

b. Cubic Force Constants

All ethane cubic constants may be determined from ab initio calculations. During the course of this research only the F_{iii} (which are nonzero only for g symmetry coordinates) and the F_{iij} for which j is an A_{1g} coordinate were determined. The F_{iii} were determined along with the other diagonal force constants. The F_{iij} were determined so that they could be used in determining the secondary isotope effect upon the C-C bond length. However, comparison of these ab initio constants with the corresponding quantities determined from the modified Urey-Bradley model force field can offer further insight into possible deficiencies in the Urey-Bradley model force field.

The C-H and C-C anharmonic terms were of particular

interest in that they contained some indication as to whether bonds in polyatomic molecules follow the Morse-like pattern characterizing diatomic and at least some triatomic molecules. As has been mentioned before, a Morse curve can be written as $(k/2)(x^2 - ax^3 + \ldots)$ where $\underline{a}$ is on the order of 2 A^{-1} for many diatomics. The $\underline{a}$ values implied by the values derived for F_{111} and F_{333} are 1.8 A^{-1} and 1.7 A^{-1}, respectively. As has been mentioned earlier, it is widely believed that quadratic force constants from self-consistent field wavefunctions tend to be high while cubic constants tend to be low. This would seem to be borne out by the present research. The calculated $\underline{a}$ values are roughly what would be expected for Morse-like bonds, but $\underline{a}$ for the C-H bonds is a little lower than estimated in some previous work: an $\underline{a}$ value of 1.90 A^{-1} has been calculated[18] from Meyer's methane force field,[19] which includes effects of electron correlation, while Kuchitsu and Bartell[6] estimated an $\underline{a}$ value of 2.00 A^{-1} from spectroscopic and bond energy data.

No established rules for estimating the magnitude of bending anharmonicities exist. There is evidence that these are small[20]; therefore, while the structural parameters r_g and r_e are measurably different from each other, the difference being attributable to bond stretching anharmonicity, α_e and $\langle\alpha\rangle$ are usually taken to be identical, consistent with the assumption of small bending anharmonicities. The <u>ab initio</u> force field also supports this idea,

for the computed F_{222} is small (see Table II) and of the magnitude given by the modified Urey-Bradley field (see Table V). In extracting F_{222} from the model force field, the contribution from the gauche 1..4 H...H interactions was computed as well as those from the geminal H...H and C...H interactions. These were found to be 0.019, - 0.014, and 0.064 mdyne-A/rad^2, respectively. Contributions from 1..4 interactions should be smaller for other cubic constants listed.

Examination of the model force field F_{iij} shows that these seem to follow the same pattern as did the model F_{ij} constants: semi-quantitatively, the agreement between the model and ab initio stretch-bend-bend (and pure bend) F_{iij} is good, but the model force field provides a poor representation of the pure stretching ab initio F_{iij}. In view of the improvements induced in the model field by the introduction of the interaction $G\Delta r_i \Delta r_j$, it seems possible that the model field would be further improved by the addition of a stretch-stretch-stretch interaction constant. However, even though the sign is wrong, the model stretch-stretch-stretch constants do mimic the corresponding ab initio constants in that each shows a lack of dependence upon i. This is consistent with a model in which the interaction of a given C-H bond with the C-C bond is independent of the other C-H bonds. The same lack of i-dependence is shown by both sets of F_{ii3} and F_{ii2} constants (for the ab initio constants, this is obscured somewhat

by normalization artifacts and the effects that would be expected from the extraction scheme used). Therefore, the general stretch-stretch-stretch interaction model built into the modified Urey-Bradley model force field shows some similarity to that implied by the ab initio force field, despite the lack of agreement between the interaction constant values from the two different sources.

In assessing the balance of the nonbonded interaction forces, it is instructive to examine F_{222} and F_{266}. These are the only cubic constants in Table V which depend upon both C...H and H...H forces. The quantitative agreement of the model F_{222} and F_{266} with the ab initio constants is rather poor. This would seem to imply that there is room for improvement in the balance between the H...H and C...H interaction potentials used in the model force field.

B. The Secondary Isotope Effect upon the C-C Bond Length in Ethane

1. Introduction

Primary isotope effects upon molecular structure are well understood, and the magnitude of such effects is well documented. The apparent increase in the length of a bond when one atom is replaced by a lighter isotope is generally understood to be caused by the greater amplitude of vibration of the lighter isotope in the Morse-like anharmonic potential well. Secondary isotope effects, in

which isotopic substitution has an effect upon an adjacent bond, are less well understood. A number of years ago, it was predicted[2a,b] that deuterium substitution into a C-H bond could cause a decrease in the length of an adjacent C-X bond because, owing to its smaller amplitude of vibration, the deuterium atom is "smaller" than the hydrogen atom and therefore repels the X atom less than does the hydrogen atom. One reason why such an effect might be important is its influence on molecular structures derived from spectroscopic data. It turns out that derived parameters can be very sensitive to assumptions about changes in the bond lengths upon isotopic substitution. Theoretically, structural parameters of great precision may be obtained from microwave moments of inertia; therefore, a firm estimate of the magnitude of the secondary effect is needed in order that spectroscopists may avoid injecting a major source of uncertainty into their structural determinations.

Three previous attempts to determine the approximate magnitude of the secondary isotope effect have been made. It has proven to be a quantity which is difficult to derive from experiment. Electron diffraction structure determinations showed that the C-C bond length in C_2D_6 is seemingly shorter than that in C_2H_6, but the difference determined (0.0016 A) was of the same order of magnitude as the uncertainties in the parameters.[2c] Microwave studies of CH_3X and CD_3X show an apparent decrease (on the order of 0.001 A)

of the C-X bond length in the deuterated species, but the structural parameters obtained from microwave studies are difficult to interpret physically. An estimate[2a] of 0.003 A for the decrease in the C-C bond length in deuteroethane was made using crude estimates[21] of nonbonded interaction potential functions and the deuterium isotope effect upon the nonbonded C...H amplitude of vibration in ethane. All of these measurements and calculations suggest a structural secondary isotope effect of roughly the same order of magnitude, but the validity of each is open to question. Therefore, the cubic constants of the ab initio force field were used to obtain another estimate of the secondary isotope effect.

2. Theory

If the force field is represented as

$$V = 1/2 \sum_{ij}\sum F_{ij}S_iS_j + \sum_{i\le j\le k}\sum\sum F_{ijk}S_iS_jS_k + \cdots, \qquad (9)$$

then the effects of molecular vibrations on the mean displacements $\langle S_i \rangle$ may be derived by setting $\langle -\partial V/\partial S_i \rangle$ equal to zero.[22] The result, through cubic constants, may be written as

$$\underline{F}\langle \underline{S} \rangle = \underline{\Theta}, \qquad (10)$$

where $\underline{F}$ is the force constant matrix, $\langle \underline{S} \rangle$ is the column matrix whose elements are the displacements of the totally

symmetric symmetry coordinates from the equilibrium structure, and $\underline{\mathfrak{H}}$ is the column matrix whose elements are

$$\mathfrak{H}_i = -3F_{iii}\langle S_i^2\rangle - 2\sum_{i\neq j} F_{iij}\langle S_i S_j\rangle - \sum_{i\neq j} F_{ijj}\langle S_j^2\rangle. \quad (11)$$

Equations (10) and (11) can be used along with the isotopic shifts in the mean-square amplitudes to determine the isotope effect upon a given symmetry coordinate, $\Delta\langle S_i\rangle$. $\Delta\langle S_3\rangle$ is expressed as

$$\Delta\langle S_3\rangle = \Delta[\mathfrak{H}_3 - F_{13}\langle S_1\rangle - F_{23}\langle S_2\rangle]/F_{33} \quad (12a)$$

or

$$\Delta\langle S_3\rangle = (F^{-1})_{31}\Delta\mathfrak{H}_1 + (F^{-1})_{32}\Delta\mathfrak{H}_2 + (F^{-1})_{33}\Delta\mathfrak{H}_3. \quad (12b)$$

The force constants needed have been calculated as discussed earlier. The other quantities needed could have been calculated from the ab initio force field, but a number of simplifications were made which relate to the determination of the $\Delta\langle S_i S_j\rangle$ and $\Delta\langle S_i^2\rangle$. These were calculated as follows: the $\Delta\langle Q_i^2\rangle$ (the Q_i are the normal coordinates), which may be related to the quantities in question, were obtained from the ethane and deuteroethane normal mode frequencies[12] using the following equation:

$$\langle Q_i^2\rangle = (h/8\pi^2\nu_i)\coth(h\nu_i/2kT). \quad (13)$$

The Q_i are related to the S_i via the $\underline{L}$ matrix. Rather than deriving the $\underline{L}$ matrix from the ab initio force field,

Duncan's L matrix was used, since the Duncan field and the ab initio field do not differ enough to make the difference in L matrices a significant source of error. Values of $\Delta\langle S_i^2\rangle$ and $\Delta\langle S_i S_j\rangle$ could be obtained from the values of $\langle S_i^2\rangle$ and $\langle S_i S_j\rangle$ computed for ethane and deuteroethane.

3. Calculations and Results

Values of the $\Delta\langle S_i S_j\rangle$, calculated as described above, are listed in Table VII. Values of $\Delta\Phi_1$, $\Delta\Phi_2$, and $\Delta\Phi_3$ are given in Table VIII. The two sets of values given here are the one obtained from the ab initio cubic constants and the one obtained from the modified Urey-Bradley model force field cubic constants. As may be seen, all of the ab initio constants necessary for the evaluation of $\Delta\Phi_1$ and $\Delta\Phi_2$ were not available; fortunately, the model force field components (obtained as described above) suggest that neglect of the interactions for which ab initio constants were not available causes only minor errors in the computed values. The isotope effects on the structure of ethane calculated using the ab initio force field are given in Table IX.

4. Discussion

The computed values of the secondary isotope effect on the C-C bond length, 0.0015 A at 0° K and 0.0011 A at 298° K, are of the same order of magnitude as previous

Table VII. Differences Between the Mean-Square Amplitudes of the Symmetry Coordinates of Protiated and Deuterated Ethane[a]

Symmetry		i,j	$10^3 \times \Delta\langle S_i S_j \rangle$ 0°K	298°K	
A_{1g}					
	CH	1,1	1.67	1.67	A^2
	CCH	2,2	5.88	5.70	rad^2
	CC	3,3	0.06	0.05	A^2
	...	1,2	-0.28	-0.30	A-rad
	...	1,3	0.03	0.03	A^2
	...	2,3	-0.16	-0.08	A-rad
A_{1u}					
	τ	4,4	10.0	3.8	rad^2
A_{2u}					
	CH	5,5	1.73	1.73	A^2
	CCH	6,6	5.84	5.70	rad^2
E_u					
	CH	7,7	1.64	1.64	A^2
	HCH	8,8	7.17	7.00	rad^2
	CCH	9,9	4.33	3.60	rad^2
E_g					
	CH	10,10	1.66	1.66	A^2
	HCH	11,11	7.36	7.29	rad^2
	CCH	12,12	3.55	3.43	rad^2

[a] All values except for $\Delta\langle S_4^2 \rangle$ are computed from the L matrices in reference 10. More figures are listed than are significant.

Table VIII. Differences Between the Elements of the $\mathcal{F}$ Matrices of Ethane and Deuteroethane, Ab Initio and Model Force Field

	$\Delta\mathcal{F}_1$ (mdyn) x10^3		$\Delta\mathcal{F}_2$ (mdyne-A/rad) x10^3		$\Delta\mathcal{F}_3$ (mdyne) x10^3	
	0°K	298°K	0°K	298°K	0°K	298°K
Ab Initio						
HCC bend	...	...[a]	-4.8	-4.5	9.8	9.0
HCH bend[b]	...	...[a]	5.1	5.0	-0.8	-0.8
CH stretch	62.6	62.6	...	...[a]	-1.5	-1.5
Torsion	...	...[a]	...	...[a]	1.7	0.6
Misc.[c]	0.1	0.1	-0.1	-0.1	0.9	0.8
Total	62.7	62.7	0.2[d]	0.2[d]	10.1	8.1
Model Force Field						
HCC bend	1.6	1.6	-4.5	-4.1	13.6	12.4
HCH bend[b]	2.8	2.8	6.3	6.2	0	0
CH stretch	...	...[e]	-0.4	-0.4	5.8	5.9
Torsion	0	0	0	0	0	0
Misc.	0.2	0.2	-0.1	0.0	0.7	0.5
Total	...	...	1.4	1.7	20.1	18.8

[a] Neglected.

[b] Via S_8, S_{11}.

[c] Crossterms and C-C stretch.

[d] Neglects CH stretch.

[e] Not embodied in model.

Table IX. Isotope Effects upon the Structure of Ethane. Quantities Listed are for Protiated Minus Deuterated Calculated from Ab Initio Cubic Constants

	Quantity x 10^3		
	0°K	298°K	Units
$\Delta\langle S_1\rangle$	10.1	10.1	A
$\Delta\langle S_2\rangle$[a]	-0.7	-0.8	rad
$\Delta\langle S_3\rangle$	1.5	1.1	A
$\Delta\langle r_{CH}\rangle$	4.4	4.4	A
$\Delta\langle\Delta\psi_{CCH}\rangle$[b]	1.6	0.2	deg

[a] Neglects effects of C-H stretch and torsion.

[b] $\Delta\langle\Delta\psi\rangle \simeq (\partial\psi/\partial S_2)_o\Delta\langle S_2\rangle + 1/2(\partial^2\psi/\partial S_2^2)_o\Delta\langle S_2^2\rangle$.

measurements and estimates of the effect. This would reinforce the impression that the magnitude of the secondary isotope effect on the C-C bond length in ethane is on the order of 0.002 A. There is some question as to the reliability of the value calculated for the effect from the ab initio force constants: the fit of the constants to the energy data was not perfect, leaving some cubic constants with rather large associated uncertainties, and then there is the larger question of how good force constants calculated from ab initio data really are. However, a comparison of the primary isotope effect upon the C-H bond length as calculated from the ab initio constants and as determined by electron diffraction[2c] provides some basis for belief in the reliability of parameters calculated from the ab initio field. The ab initio value for $\Delta\langle r_{CH}\rangle$ is 0.0044 A, while electron diffraction suggests a value ($\pm\sigma$) of 0.0050 ± 0.0006 A, which is similar to the value used for the deuterium primary isotope effect in microwave structure determinations. Therefore, while none of the existing determinations of the secondary isotope effect are unequivocably reliable, the approximate magnitude of the effect for ethane is probably pretty well fixed at 0.002 A. Given the precision attainable in structural parameters obtained from microwave data, some provision for including secondary isotope effects should be made in microwave studies.

Because part of the impetus for extracting the ab

initio ethane force field was the hope that such a field might provide information which would be helpful in formulating model force fields, it is instructive to compare the modified Urey-Bradley model field's and the *ab initio* field's predictions of various quantities used in calculating the secondary isotope effect. Such a comparison can aid in an assessment of the simple physical reason for the secondary isotope effect given at the beginning of this section, *i.e.* the "smaller size" of the deuterium atoms relative to the hydrogen atoms. It is encouraging to see that the *ab initio* and model results are, for the most part, in at least semiquantitative agreement. The lone exception to this is the contribution to $\mathcal{F}_3$ from the interaction of the C-H stretch with the C-C stretch. The shortcomings of the model field have been commented upon above; the poor agreement here is probably another manifestation of an interaction wich has been left out of the model field. The agreement between all of the other model and *ab initio* contributions is quite good, all things considered. Due to the model used, the secondary isotope effect as predicted by the model force field has a steric origin. The agreement between the various model and *ab initio* quantities suggests that the *ab initio* calculations support the steric explanation of the secondary isotope effect.

C. Final Remarks

This research has generated information which may

be used to evaluate and improve model force fields. A comparison of results from two model force fields and the ab initio field pointed out deficiencies in both model fields. As is shown in the Appendix to Part II, adjusting the modified Urey-Bradley field in the direction indicated by the ab initio results has improved the field's ability to reproduce experimental quantities. Therefore, there is reason to believe that the ab initio force field could be used to advantage in systematically improving model force fields. The semiquantitative agreement of many of the quantities calculated using the modified Urey-Bradley model force field with the corresponding quantities calculated using the ab initio force field is of more than passing interest: it provides strong support for the intramolecular interaction model embodied in the model force field. It may be said that a model which includes anharmonic terms for geminal interactions may provide at least a qualitative representation of the true ethane potential surface, insofar as the ab initio surface represents the true surface. This provides some vindication of a seldom-used potential form, and may possibly stimulate further research into modified Urey-Bradley model force fields.

Other information also came out of this research. The approximate magnitude of the secondary isotope effect is now established; as indicated above, this information will be important in determining molecular structures from microwave data and in assessing structures so determined.

The indications that the effect may have a simple steric origin are of interest; they may aid in explanations of other isotope effects. The good overall agreement of the ab initio force field and quantities calculated from it with the corresponding experimental quantities augers well for the future use of ab initio calculations in providing information which is difficult to obtain from experiment. Perhaps one of the most important things to come out of this research is further evidence that ab initio methods may be used to supplement experimental ones.

Table III. Conformations of Ethane Used in the Derivation of the Ab Initio Force Field

Residual[a,b]	Energy[a]	$S_1, {}^cS_2, {}^dS_3$[c]	$S_5, {}^cS_6$[d]	$S_7, {}^cS_8, {}^dS_9$[d]	$S_{10}, {}^cS_{11}, {}^dS_{12}$[d]
-4.89859×10^{-6}	2.57580×10^{-4}				
		1.0×10^{-2}			
-2.04785×10^{-5}	2.55520×10^{-4}				
		-1.0×10^{-2}			
-1.38570×10^{-5}	9.83490×10^{-4}				
		2.0×10^{-2}			
-5.59205×10^{-6}	9.86850×10^{-4}				
		-2.0×10^{-2}			
-2.23863×10^{-5}	2.14979×10^{-3}				
		3.0×10^{-2}			
-2.07074×10^{-5}	2.28281×10^{-3}				
		-3.0×10^{-2}			
-9.22130×10^{-6}	1.59657×10^{-3}	2.44949×10^{-2}			
-8.80695×10^{-7}	1.92888×10^{-3}	-2.44949×10^{-2}			
-2.03721×10^{-5}	6.53194×10^{-3}	4.89898×10^{-2}			

Table III continued

Residual[a,b]	Energy[a]	S_1, [c]S_2, [d]S_3 [c]	S_5, [c]S_6 [d]	S_7, [c]S_8, [d]S_9 [d]	S_{10}, [c]S_{11}, [d]S_{12} [d]
-2.67092×10^{-5}	7.59107×10^{-3}	-4.89898×10^{-2}			
-6.17785×10^{-6}	2.56809×10^{-2}	9.79796×10^{-2}			
6.81325×10^{-6}	3.02796×10^{-2}	-9.79796×10^{-2}			
1.64982×10^{-5}	1.53884×10^{-3}	-6.28644×10^{-2}			
-1.91159×10^{-5}	1.35643×10^{-3}	6.17991×10^{-2}			
-5.27500×10^{-5}	6.01430×10^{-3}	-1.26751×10^{-1}			
-5.90650×10^{-5}	5.58267×10^{-3}	1.22481×10^{-1}			
-7.83515×10^{-6}	3.74008×10^{-2}	-3.24081×10^{-1}			
-1.13313×10^{-5}	3.51536×10^{-2}	2.97331×10^{-1}			

Table III continued

Residual[a,b]	Energy[a]	S_1, [c]S_2, [d]S_3 [c]	S_5, [c]S_6 [d]	S_7, [c]S_8, [d]S_9 [d]	S_{10}, [c]S_{11}, [d]S_{12} [d]
-1.80508×10^{-5}	4.42262×10^{-2}	-3.24081×10^{-1} 3.0×10^{-2}			
-1.98899×10^{-5}	4.34204×10^{-2}	2.97331×10^{-1} -3.0×10^{-2}			
2.24254×10^{-5}	2.13745×10^{-3}	-6.28644×10^{-2} 1.0×10^{-2}			
3.01161×10^{-5}	1.95214×10^{-3}	6.17991×10^{-2} -1.0×10^{-2}			
5.15005×10^{-6}	2.91617×10^{-3}	2.44949×10^{-2} -6.28644×10^{-2}			
5.23560×10^{-6}	3.07233×10^{-3}	-2.44949×10^{-2} 6.17991×10^{-2}			
2.86525×10^{-7}	2.84180×10^{-2}	9.79796×10^{-2} 3.0×10^{-2}			
-2.12245×10^{-7}	3.37804×10^{-2}	-9.79796×10^{-2} -3.0×10^{-2}			
-1.33453×10^{-5}	1.90113×10^{-3}	2.44949×10^{-2} 1.0×10^{-2}			

Table III continued

Residual[a,b]	Energy[a]	S_1, [c] S_2, [d] S_3 [c]	S_5, [c] S_6 [d]	S_7, [c] S_8, [d] S_9 [d]	S_{10}, [c] S_{11}, [d] S_{12} [d]
6.02600×10^{-6}	2.21205×10^{-3}	-2.44949×10^{-2}			
		-1.0×10^{-2}			
-1.64926×10^{-5}	3.47215×10^{-2}				
		-3.24081×10^{-1}			
		-3.0×10^{-2}			
-1.79358×10^{-5}	3.15321×10^{-2}				
		2.97331×10^{-1}			
		3.0×10^{-2}			
-2.16401×10^{-7}	2.72733×10^{-2}	9.79796×10^{-2}			
		-3.0×10^{-2}			
-3.11936×10^{-7}	3.25325×10^{-2}	-9.79796×10^{-2}			
		3.0×10^{-2}			
3.49995×10^{-6}	1.33498×10^{-3}		-6.23343×10^{-2}		
8.84975×10^{-6}	2.80642×10^{-3}		2.44949×10^{-2}		
			-6.23343×10^{-2}		
8.80565×10^{-6}	3.37363×10^{-3}		-2.44949×10^{-2}		
			-6.23343×10^{-2}		
1.59441×10^{-5}	3.44121×10^{-3}			3.46410×10^{-2}	

Table III continued

Residual[a,b]	Energy[a]	$S_1, {}^cS_2, {}^dS_3{}^c$	$S_5, {}^cS_6{}^d$	$S_7, {}^cS_8, {}^dS_9{}^d$	$S_{10}, {}^cS_{11}, {}^dS_{12}{}^d$
5.57000×10^{-6}	1.60267×10^{-3}			6.04590×10^{-2} 3.20942×10^{-2}	
8.31950×10^{-7}	1.50414×10^{-3}			3.20670×10^{-2} 6.04408×10^{-2}	
-3.62076×10^{-5}	4.73870×10^{-3}			3.46410×10^{-2} 6.04620×10^{-2} 3.20942×10^{-2}	
2.07612×10^{-5}	5.35083×10^{-3}			-3.46410×10^{-2} 6.04620×10^{-2} 3.20942×10^{-2}	
1.85111×10^{-5}	4.92225×10^{-3}			3.46410×10^{-2} 3.20791×10^{-2} 6.04620×10^{-2}	
1.85085×10^{-5}	4.96715×10^{-3}			-3.46410×10^{-2} 3.20791×10^{-2} 6.04620×10^{-2}	
3.50119×10^{-6}	6.22147×10^{-4}			4.53440×10^{-2}	
6.96680×10^{-6}	3.33527×10^{-3}				3.46410×10^{-2}
3.29442×10^{-6}	3.47129×10^{-3}				-3.46410×10^{-2}

Table III continued

Residual[a,b]	Energy[a]	S_1, [c]S_2, [d]S_3 [c]	S_5, [c]S_6 [d]	S_7, [c]S_8, [d]S_9 [d]	S_{10}, [c]S_{11}, [d]S_{12} [d]
6.34295×10^{-6}	1.79799×10^{-3}				6.04580×10^{-2} 3.25275×10^{-2}
2.01228×10^{-6}	1.77096×10^{-3}				-6.04580×10^{-2} -3.16589×10^{-2}
-9.14895×10^{-6}	2.12411×10^{-3}				3.14049×10^{-2} 6.04660×10^{-2}
1.31248×10^{-5}	2.16204×10^{-3}				-3.27512×10^{-2} -6.04559×10^{-2}
3.91438×10^{-6}	4.53858×10^{-4}				-3.01316×10^{-2}
5.58315×10^{-5}	4.93184×10^{-3}				3.46410×10^{-2} 6.04680×10^{-2} 3.25315×10^{-2}
-4.95505×10^{-5}	5.04301×10^{-3}				-3.46410×10^{-2} -6.04741×10^{-2} -3.16568×10^{-2}
1.00743×10^{-5}	5.64946×10^{-3}				-3.46410×10^{-2} -3.27532×10^{-2} -6.04640×10^{-2}
-6.43630×10^{-6}	5.82735×10^{-3}				3.46410×10^{-2} 3.13989×10^{-2} 6.04680×10^{-2}

Table III continued

Residual[a,b]	Energy[a]	S_1, [c]S_2, [d]S_3 [c]	S_5, [c]S_6 [d]	S_7, [c]S_8, [d]S_9 [d]	S_{10}, [c]S_{11}, [d]S_{12} [d]
2.14172×10^{-5}	2.70825×10^{-2}			9.69945×10^{-2}	
3.33273×10^{-5}	2.52823×10^{-2}				9.69945×10^{-2}
3.37495×10^{-7}	3.19236×10^{-2}	4.0×10^{-2}	9.79796×10^{-2}		
3.57485×10^{-7}	3.22112×10^{-2}	-4.0×10^{-2}	9.79796×10^{-2}		
-1.04135×10^{-5}	3.08668×10^{-2}	4.0×10^{-2}		9.69949×10^{-2}	
-1.04339×10^{-5}	3.11659×10^{-2}	-4.0×10^{-2}		9.69949×10^{-2}	
-4.84321×10^{-7}	2.90790×10^{-2}	4.0×10^{-2}			9.69949×10^{-2}
-4.84408×10^{-7}	2.93572×10^{-2}	-4.0×10^{-2}			9.69949×10^{-2}
1.26987×10^{-6}	3.62930×10^{-2}	4.0×10^{-2}	3.10706×10^{-1}		

Table III continued

Residual[a,b]	Energy[a]	S_1, [c] S_2, [d] S_3 [c]	S_5, [c] S_6 [d]	S_7, [c] S_8, [d] S_9 [d]	S_{10}, [c] S_{11}, [d] S_{12} [d]
1.68066×10^{-6}	3.80176×10^{-2}	-4.0×10^{-2}	3.10706×10^{-1}		
1.60909×10^{-5}	1.76596×10^{-2}	4.0×10^{-2}		-2.08928×10^{-1}	
1.60568×10^{-5}	1.96848×10^{-2}	-4.0×10^{-2}		-2.08928×10^{-1}	
4.14406×10^{-7}	2.53976×10^{-2}	4.0×10^{-2}			-2.08928×10^{-1}
4.33758×10^{-7}	2.73881×10^{-2}	-4.0×10^{-2}			-2.08928×10^{-1}
1.60901×10^{-5}	3.686445×10^{-3}	4.0×10^{-2}			
1.45871×10^{-5}	4.08643×10^{-3}	-4.0×10^{-2}			
-1.745002×10^{-8}	2.49126×10^{-2}	-4.0×10^{-2}		2.3834×10^{-1}	
-3.57063×10^{-8}	2.45764×10^{-2}	4.0×10^{-2}		2.3834×10^{-1}	

Table III continued

Residual[a,b]	Energy[a]	S_1,[c] S_2,[d] S_3[c]	S_5,[c] S_6[d]	S_7,[c] S_8,[d] S_9[d]	S_{10},[c] S_{11},[d] S_{12}[d]
2.01928×10^{-7}	2.39045×10^{-2}				2.34903×10^{-1}
		-4.0×10^{-2}			
1.87107×10^{-7}	2.36979×10^{-2}				2.34903×10^{-1}
		4.0×10^{-2}			

[a] All energies and residuals are in mdyne-Å.

[b] "Residual" = $E_{calc}-E_{"exp"}$.

[c] Units of S_1, S_3, S_5, S_7, S_{10}: Å.

[d] Units of S_2, S_6, S_8, S_9, S_{11}, S_{12}: rad.

REFERENCES

1. a. V. G. Trofimenko and V. P. Morozov, Opt. Spektrosk., 25, 190 (1968);
b. B. L. Sadullaev and M. M. Sushchinskii, Opt. Spektrosk., 23, 46 (1967).

2. See, for example,
a. L. S. Bartell, Iowa State J. Sci., 36, 137 (1961);
b. L. S. Bartell, J. Chem. Phys., 36, 3495 (1962);
c. L. S. Bartell and H. K. Higginbotham, J. Chem. Phys., 42, 851 (1965);
d. R. H. Schwendeman and J. D. Kelley, J. Chem. Phys., 42, 1132 (1965).

3. See, for example,
a. P. Pulay, Mol. Phys., 17, 197 (1969);
b. P. Pulay and W. Meyer, Mol. Phys., 27, 473 ( );
c. P. Pulay, private communication.

4. See, for example,
a. E. J. Jacob, H. B. Thompson, and L. S. Bartell, J. Chem. Phys., 47, 3736 (1967);
b. S. Lifson and A. Warshel, J. Chem. Phys., 49, 5116 (1968); A. Warshel and S. Lifson, J. Chem. Phys., 53, 582 (1970);
c. R. H. Boyd, J. Chem. Phys., 49, 2574 (1968); R. H. Boyd et al., J. Phys. Chem., 75, 1264 (1971);
d. E. M. Engler, J. D. Andose, and P. von R. Schleyer, J. Amer. Chem. Soc., 95, 8005 (1973).

5. GAUSSIAN 70 may be obtained from Quantum Chemistry Program Exchange, Bloomington, Indiana. I wish to thank Dr. Hehre for making the computed energies available to me.

6. K. Kuchitsu and L. S. Bartell, J. Chem. Phys., 36, 2470 (1962).

7. K. Kuchitsu, J. Chem. Phys., 49, 4456 (1968).

8. R. H. Schwendeman, J. Chem. Phys., 44, 2115 (1966).

9. R. M. Stevens, J. Chem. Phys., 52, 1397 (1970).

10. A. Veillard, Theor. Chim. Acta, 18, 21 (1970).

11. G. H. Hansen and D. M. Dennison, J. Chem. Phys., 20, 313 (1952).

12. J. L. Duncan, Spectrochim. Acta, 20, 1197 (1964).

13. O. Ermer and S. Lifson, J. Amer. Chem. Soc., 95, 4121 (1973).

14. J. H. Schachtschneider and R. G. Snyder, Spectrochim. Acta, 19, 117 (1963).

15. T. Shimanouchi, J. Chem. Phys., 17, 96 (1949).

16. T. Shimanouchi, Pure Appl. Chem., 7, 131 (1963).

17. L. S. Bartell and K. Kuchitsu, J. Chem. Phys., 37, 691 (1962).

18. L. S. Bartell, private communication.

19. W. Meyer, J. Chem. Phys., 58, 1017 (1973).

20. a. K. Kuchitsu and Y. Morino, Bull. Chem. Soc. Japan, 38, 805, 814 (1965);
b. K. Kuchitsu and Y. Morino, Spectrochim. Acta, 22, 33 (1966);
c. Y. Morino, Pure Appl. Chem., 18, 323 (1969).

21. L. S. Bartell, J. Chem. Phys., 32, 827 (1960).

22. L. S. Bartell, J. Chem. Phys., 38, 1827 (1963).

II. FORMULATION AND TESTING OF A MODIFIED UREY-BRADLEY MODEL FORCE FIELD AND AN INVESTIGATION OF THE "GAUCHE HYDROGEN EFFECT"

A. Introduction

Intensive work over the past few years in the field of "molecular mechanics" has led to the formulation of a number of model force fields which reproduce experimental structural information, conformational information, thermochemical data, and (in some cases) vibrational normal mode frequencies quite well.[1] However, although most of the force fields in use at the present time give similar values for many quantities of interest, the details of parameterization and even the functional forms of the different fields are quite dissimilar. Also, different researchers formulate model force fields using different approaches. Despite the numerous schemes explored to date, no generally accepted "correct" way to formulate a model force field has yet evolved: no field which is clearly superior to the others has emerged.

Few researchers base force fields upon the Urey-Bradley force field functional form. Geminal nonbonded interactions are rarely considered explicitly, but their effects may be lumped in with the diagonal force and interaction constants, as in the general valence force field functional form. One modified Urey-Bradley field[1a] (hereafter referred to as MUB-1) has enjoyed a fair amount of

success, especially with regard to the calculation of structural parameters and geometrical isomerization energies. Consideration of the fact that MUB-1 was almost totally unoptimized and yet was still fairly successful in reproducing experimental quantities prompted further research into model force fields based on the Urey-Bradley potential model. This research led to the formulation of a new force field (hereafter referred to as MUB-2), which will be described in the following sections.

There are a number of ways in which the parameters of a model force field can be optimized once the functional form of the field has been chosen. However, blind optimization of parameters can result in a force field which is little more than an interpolation scheme, with the physical significance of the parameters being uncertain at best. One way to formulate a physically meaningful model force field is to construct the field from quantities which have physical significance apart from the field. The goal of this research was to devise a model force field whose components meet this criterion. Of course, lack of information on many interactions prevents a definitive assessment of the physical reasonability of the representation of these interactions by a model force field. Faithful representations of other interactions may be so complex that introducing them into a model force field would produce a field so complicated that it would not be generally useful. The model force field discussed below is a compro-

mise which strives to retain simplicity while taking advantage of current knowledge. Computations done using this force field will give some indication of how well certain simplified representations of intramolecular interactions can function in a model force field. Then, computations done with a force field built from separately significant components may point out those interactions which are left out of a given model force field but which will improve the field if included. It is possible that the "missing" interactions discovered will be transferable to some extent, and thus information which can improve one model force field can be used to improve others.

It must be emphasized that the field being reported on here is only a second approximation to a fully defined and optimized modified Urey-Bradley model force field. The results which were obtained using this field have suggested some changes which may improve the field, as have the ab initio ethane force field calculations reported on in part I of this thesis. A preliminary study on incorporating one of these changes (see Appendix) has shown that the force field's ability to reproduce certain experimental quantities can be improved, and other changes will be tested in the future. Therefore, the utility of the field described below must be regarded as somewhat transient. However, MUB-2 reproduces many experimental parameters and trends satisfactorily, so it is not anticipated that future changes in the modified Urey-Bradley model force field will

produce drastic changes in the force field or its behavior. It is unlikely that the computed values of most of the quantities which will be reported here will change significantly as new modifications are introduced into the force field.

While a force field may be constructed from elements which are physically reasonable, attaching physical significance to interpretations which are made from calculations done using the force field should be done cautiously, if at all. As has been noted, a variety of force fields with very different details of parameterization give pretty much the same values for structural parameters, energy differences, etc. for a limited class of compounds, and contributions to the final value obtained may not come from the same source when different force fields are used. Therefore, basing a physical explanation upon the mathematical pecularities of one or two force fields is a risky proposition, especially if the parameters of the fields were chosen by trial and error. Only when an interpretation is supported by several force fields with different details of parameterization is it safe to draw tentative conclusions.

Recently, Allinger and Wertz[2] have made the intriguing suggestion that the instability of a gauche methyl or methylene conformation relative to the trans conformation is caused by gauche interactions between the vicinal (1...4) 2,3 hydrogens rather than by the gauche interactions

between methyl or methylene groups, as has long been assumed. This viewpoint affords a simple explanation for several puzzling observations. However, the explanation of the relative instability of the gauche methyl conformation in terms of gauche hydrogen interactions is based upon calculations done with only one force field (which was parameterized by trial and error), the details of which are given in the literature.[18] Allinger and Wertz stated that they believed that investigations of n-butane and methylcyclohexane done with any of the current force fields, except possibly one of Lifson's,[1b] would confirm their hypothesis. Accordingly, trans and gauche n-butane were investigated using MUB-1. It was found that the gauche hydrogen interactions contributed only slightly to the gauche-trans energy difference. In order to test the plausibility of the "gauche hydrogen effect" hypothesis further, n-butane and methylcyclohexane were investigated using MUB-2. The results of this investigation are given below, following the description of the model force field and the results calculated using it.

B. Formulation of MUB-2

1. General Considerations

As stated above, the potential form of MUB-2 was based upon that of the Urey-Bradley force field. There were some modifications and additions made. The expression

adopted for the potential energy is

$$V_{total} = \sum_n V^n_{nb}(r_n) + 1/2\sum_\ell k_\ell(\phi_\ell - \phi^o_\ell)^2 + 1/2\sum_\ell k_\ell a_\ell(\phi_\ell - \phi^g_\ell)^3$$

$$+ 1/2\sum_q V^q_{tor}(1 + \cos 3\beta_q) + 1/2\sum_i V^i_{st}(\tau, r^i_{CC}), \qquad (1)$$

where $V^n_{nb}(r_n)$ is the nonbonded potential energy coores-ponding to the nth nonbonded distance, r_n; ϕ_ℓ is the lth internal coordinate (bond length or bond angle), where the superscript o denotes the reference value of ϕ_ℓ and the superscript g indicates the "unstrained" value of ϕ_ℓ; k_l is the force constant for the lth deformation, and a_l is the Morse asymmetry constant for the lth deformation. V^q_{tor} is the appropriate barrier to the hindered internal rotation described by the dihedral angle β_q. $V^i_{st}(\tau, r_i)$ is the potential energy from the stretch-torsion interaction; the stretch-torsion functional form is

$$V^i_{st}(\tau, r^i_{CC}) = K_{st}(r^i_{CC} - r^g_{CC})(1 - \cos 3\tau), \qquad (2)$$

where K_{st} is the stretch-torsion constant, r^i_{CC} is the ith carbon-carbon bond length, and τ is the mean displacement of the anti dihedral angles around bond i from 180°.

MUB-2 was, in a sense, built around the nonbonded potential functions. Much attention was paid to making these physically reasonable. Strictly speaking, pairwise additive functions of the type used in MUB-2 are incapable

of giving a proper representation of interatomic forces. However, they have done a pretty good job in model force fields to date, and they use few adjustable parameters. Therefore, pairwise additive nonbonded functions were retained.

There is more information available for the formulation of the H...H potential function than there is for the C...H or C...C functions, so the H...H interaction function is probably the best determined of the nonbonded potentials. The principal source of information used was Kochanski's treatment of the $H_2...H_2$ system[3] by the perturbative procedure of Musher and Amos. The $H_2...H_2$ interaction energies were computed at four orientations of one molecule relative to the other and at close intervals over a range from 4 to 10 a.u. Kochanski tabulates a weighted average of the energies at the different orientations. The $H_2...H_2$ mean interaction energy curve thus generated agrees well with the results of recent molecular beam studies of the $H_2...H_2$ system.[4,5] For the purposes of the present investigation, it was assumed that the Kochanski interaction energies could be approximated by pairwise interactions between nonbonded hydrogens, where the interaction function took the form of the Buckingham potential:

$$V_{HH} = A\exp(-\alpha r) - Br^{-6}. \qquad (3)$$

The hydrogens were "foreshortened," as suggested by Williams,[6] so that the interaction centers in bond to hydrogen

atoms are moved a distance Δ toward the bond center, away from the protons. Reasonable values of A, α, B, and Δ were found by trial and error, the greatest emphasis being placed on fitting the energies from Kochanski's orientations I and IV.

Figure 1 compares Kochanski's calculated interaction energies with those given by the H...H Buckingham function finally obtained. It is obvious that the interatomic forces cannot be completely accounted for by the model used; they depend too strongly upon bond orientations. Values of A, α, B, and Δ which reproduce the Kochanski energies for orientations I and IV and those for orientations II and III at 2 A separations make the atoms far too repulsive for orientations II and II at 3 A. Also, no model of the sort proposed can account for the increased dispersion forces for orientation III. However, the model of H...H interactions provided by the simple Buckingham function may be satisfactory for use in model force fields, and the function itself is probably an improvement over H...H interaction functions currently in use.

There was no source of information comparable to Kochanski's calculations from which C...H and C...C interaction functions could be extracted. However, information exists which can be used to set rough bounds on the values of A, α, and B for the functions: Pitzer and Catalano have estimated values for the B parameter for both C...H and C...C,[7] Williams has extracted a set of intermolecular

Figure 1. Comparison Between $H_2 \ldots H_2$ Interaction Energies as Calculated at Four Orientations by E. Kochanski and as Represented by the MUB-2 Pairwise Additive Buckingham Potential Functions. The Right-hand Lobes of the Curves Correspond to Negative Values of V(r).

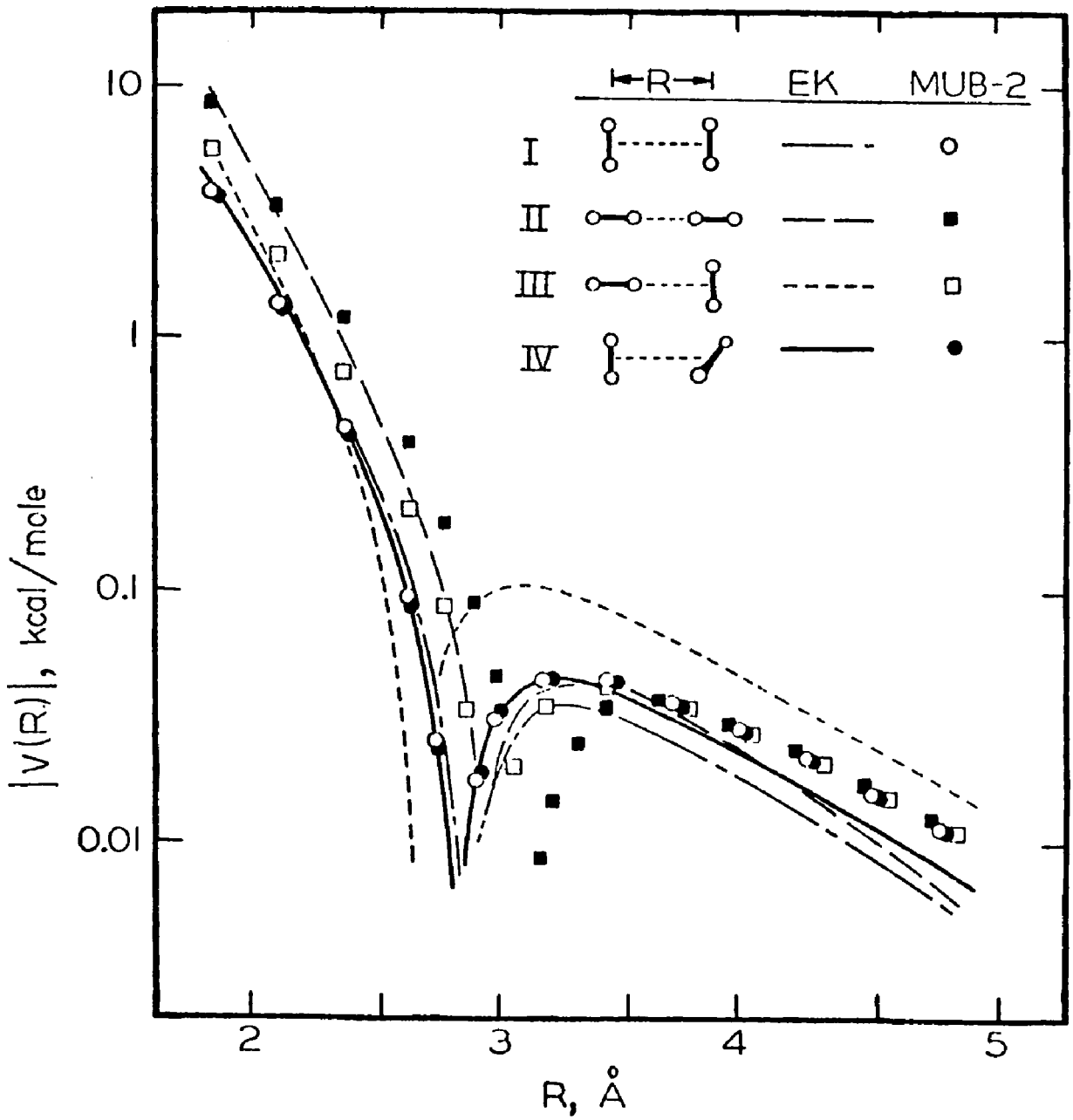


Figure 1.

potential functions from various crystal data,[8] Schachtschneider and Snyder's,[9] Lifson and Warshel's,[10] and Shimanouchi's[11] values of the F constant are formally equivalent to $(\partial^2 V(r)/\partial r^2)_r$. A preliminary set of k_1 and ϕ^o_ℓ constants was established, providing a framework within which the A's, α's, and B's could be varied by trial and error, within the limits suggested by the data listed above, to reproduce the experimental values of the CCC angle in n-alkanes and the n-butane to isobutane isomerization energy. The values of A, α, and B obtained are listed in Table I, along with the A, α, B, and Δ derived for H...H.

Once the final values of the adjustable parameters of the nonbonded potential functions were obtained, a set of Urey-Bradley diagonal force constants was derived from Schachtschneider and Snyder's Urey-Bradley force field,[9] using the transformations given in reference 9 (slightly modified so as to be consistent with the molecular geometries used and to include the actual F', not -.1F) and setting the Urey-Bradley nonbonded force constants equal to the second derivatives of the nonbonded potential functions. This procedure was followed so that the model force field obtained would be as good a representation of the Schachtschneider and Snyder hydrocarbon potential surface as possible, given the constraints placed on the model. The a parameters for bond stretches were set equal to 2.0 A^{-1}, which value is supported by a number of experiments on diatomic molecules and which is often used for bond

anharmonicities. The a parameters for bond angle deformations were set equal to zero. V_{tor}, the barrier to hindered internal rotation, was set equal to 3.1 kcal/mol, in order that the observed eclipsed-staggered energy difference of 3.0 kcal would be reproduced by the force field (eclipsed ethane relaxes so that its energy is 0.1 kcal lower than that of staggered ethane when the barrier to hindered internal rotation is not considered). There was no experimental information which could be used to determine K_{st}, since the only indication of the importance of this interaction came from ab initio calculations.[12,13] In lieu of anything better, K_{st} was adjusted to reproduce the approximate magnitude of the C-C bond length difference for eclipsed and staggered ethane predicted by the ab initio calculations. Values of all force constants used in MUB-2 are given in Table II.

All ϕ_ℓ^o for angular coordinates were fixed at the tetrahedral angle. The value of ϕ_ℓ^o for the C-H bond length was fixed by requiring that the force field reproduce the experimental structure of methane[14]; once r_{CH}^o was fixed, a value for r_{CC}^o was obtained by varying the parameter so that the force field reproduced the experimental structure of ethane[15] as well as possible. The values of r_{CH}^g and r_{CC}^g were set equal to the experimental C-H bond length in methane and the experimental C-C bond length in ethane, respectively. Because anharmonicity of bond angles was not considered (except as introduced by the nonbonded

Table I. Constants for the Nonbonded Potential Interaction Functions of the Form $V = A \exp(-\alpha r) - Br^{-6}$ (energies yielded in mdyne-A)

Interaction	A	α	B	Foreshortening (Δ)[a]
H...H	14.72	3.4	0.3333	0.117
C...H	135.4	3.75	1.076	0.117
C...C	502.2	3.75	2.779	- -

[a] The hydrogens are foreshortened by a distance Δ as explained in the text. The potential functions are for the foreshortened distances.

Table II. Parameters of MUB-2 Force Field.[a]

Bond Stretching: $V(r) = 1/2K(r-r^\circ)^2 - 1/2Ka(r-r^g)^3$

Bond	K	r°	a	r^g
C-H	3.85	1.0203	2.0	1.1068
C-C	2.34	1.166	2.0	1.534

Angle Bending: $V(\underline{\theta}) = 1/2H(\underline{\theta}-\underline{\theta}^\circ)^2$

Angle	H	θ° (radians)
C-C-C	0.629	1.91063
C-C-H	0.322	1.91063
H-C-H	0.350	1.91063

Torsional:[b] $V(\underline{\tau}) = 1/2 \sum_{i=1}^{9} V_3 (1+\cos 3\underline{\tau}_i)$

$V_3 = (2.154 \times 10^{-2})/9$ mdyne - Å for any dihedral angle

Stretch-Torsion: $V(r,\underline{\tau}) = 1/2K_{st}(r-r^g)(1+\cos 3\underline{\tau})$

$K_{st} = -7.125 \times 10^{-2}$ mdyne $\quad r^g = 1.534$ Å

[a] All units are such that energies are in units of mdyne-Å, angles in radians, and distances in Angstrom units.

[b] The contribution to the potential energy from a torsion around a given carbon-carbon bond is taken as the sum of contributions from all nine dihedral angles across that bond.

interaction potentials), no values of ϕ_{ℓ}^{q} were defined for the angular coordinates.

2. Specific Considerations

The general guidelines used in constructing MUB-2 have been given in the preceding section. A number of details which would not have elucidated the formulation process but which may be of interest to persons who wish to use MUB-2 are given below.

a. Force Constants

One problem with trying to adjust the constants of a field with the potential form of MUB-2 to fit the Schachtschneider and Snyder potential surface is that the description of the surface to be fitted uses many more adjustable parameters than are contained in MUB-2. For example, the Schachtschneider and Snyder force fields use different force constants for methyl, methylene, and tertiary C-H stretches, while MUB-2 uses the same force constant for all C-H stretches (it is true that some differentiation in the "acting" or "valence-type" force constants is introduced by the differences in nonbonded environments for C-H bonds of different types, but no attempt to correlate this differentiation with that observed in the experimental fields has been made). Also, the experimentally derived force fields contain a number of interactions which MUB-2 does not, explicitly or hidden in nonbonded interactions. Therefore, the extent to which MUB-2 can act as

a good representation of the Schachtschneider and Snyder hydrocarbon potential surface is somewhat limited.

In practice, the force constants for MUB-2 were determined by averaging the values of the different valence force constants for a MUB-2 parameter (such as a C-H stretch), and then transforming these constants to Urey-Bradley space as described above. This process introduces a certain amount of latitude into the values of the MUB-2 constants, since the values obtained depend upon how the valence force constants are averaged. Probably the force constant values could be somewhat better optimized, but those in Table II represent a reasonable compromise. In any event, the characteristics of a modified Urey-Bradley force field seem to be largely determined by the nonbonded potential functions. Fairly large changes in the force constants make little difference in the results obtained using the force field.

b. Torsional Potential

Both the form of the torsional potential function and the magnitude of the barrier to hindered internal rotation in ethane are well established. The magnitude of V_{tor} was found by minimizing the energies of eclipsed and staggered ethane and then assuming that the energy difference between the two is 3 kcal/mol (the often-quoted value for the height of the ethane barrier). The C-C bond length of the eclipsed ethane was forced to be longer than the staggered ethane C-C bond length by the amount predicted by

ab initio calculations,[12,13] as explained below in the section on the stretch-torsion interaction. The computed energy of eclipsed ethane was 0.1 kcal/mol lower than that of staggered ethane when V_{tor} was set equal to zero; therefore, V_{tor} was set equal to 3.1 kcal/mol, providing the 3 kcal/mol eclipsed-staggered energy difference.

The proper choice of the dihedral angle which specifies the degree of rotation around a given bond is not immediately obvious. For saturated hydrocarbons, there are nine dihedral angles across each carbon-carbon bond. Reckoning the potential energy from only one of these can cause a molecule to assume a conformation which is appreciably different from the one which would be assumed if the energy were reckoned from another. The most logical way to circumvent this problem is to reckon the potential energy from all nine dihedral angles. The contribution to the energy from each dihedral angle is then

$$V(\beta_q) = (V_{tor}/18)(1 + \cos 3\beta_q), \qquad (4)$$

where a factor of 1/9 has been inserted to compensate for the summation over the nine angles.

Many of the calculations which will be reported here were done using this so-called nine-torsional model. However, the computer programs used (see below) precluded the use of the nine-torsional model on some of the molecules which were studied. A three-torsional model (potential reckoned from three carefully chosen dihedral angles) was

used for some of those molecules which could not be done nine-torsionally; a one-torsional model was used on those which exhibited only modest deviations from "zero-point" (60°, 180°, or 300°) dihedral angles.

c. Stretch-Torsion Interaction

As stated above, a number of ab initio calculations on the barrier to internal rotation in ethane have indicated that the C-C bond lengthens appreciably (0.01-0.02 A) when the molecule assumes an eclipsed conformation. This degree of lengthening is ten times that which would be induced by the MUB-2 H...H nonbonded repulsions when internal rotation occurs. Therefore, the bond lengthening must be caused by a different type of interaction. The interaction is necessarily anharmonic and dependent upon both the C-C bond length and the average dihedral angle across that bond. Given these conditions, the simplest form for the interaction is that of equation (2). As stated above, the value of K_{st} was obtained by adjusting the constant to reproduce the magnitude of the C-C bond lengthening predicted by the ab initio calculations. Since the different ab initio calculations predicted different values for the bond length difference, a compromise value of 0.017 A was used. The value of K_{st} which reproduced this change was -7.125×10^{-2} mdyne. This value may be compared with the value calculated from the ab initio constant F_{344} determined in part I of this thesis, which was -7.316×10^{-2} mdyne.

d. Reference Values

The choice of the tetrahedral angle for the reference value of all angles was a logical first approximation; as may be seen from Figures 4 and 5, the nonbonded forces were of the proper magnitude to reproduce experimental angle values without optimizing the reference angles. As stated above, the reference values for the bond lengths were derived by requiring that MUB-2 reproduce the experimental methane and ethane structures as well as possible. Mathematical considerations dictate that it is possible to adjust r^o_{CH} so that the experimental methane structure is reproduced exactly: the symmetry of the molecule dictates the tetrahedral angle, and the one remaining experimental parameter, the bond length, can be fitted to absolute accuracy with one adjustable parameter of the force field, r^o_{CH}. However, it is impossible to fit the experimental ethane structure exactly, because there are three experimental parameters (r_{CH}, r_{CC}, and α_{HCC}) to be fitted, but only one force field parameter to be varied (r^o_{CC}). The degree of success which the force field has in fitting the experimental ethane structure provides a measure of the balance of the forces. The structure of ethane as given by MUB-2 is r_{CH} = 1.1111 A, r_{CC} = 1.5338 A, and α_{HCC} = 111.5116°, while the experimental electron diffraction structure is r_{CH} = 1.1122 ± 0.0012 A, r_{CC} = 1.5340 ± 0.0011 A, and α_{HCC} = 111.5 ± 0.3°.[15,16] The agreement here is good, indicating that the forces are fairly well balanced.

The so-called unstrained parameters, r^g_{CH} and r^g_{CC}, were set equal to the methane C-H bond length and the ethane C-C bond length, respectively. This ensures that the effects of the bond stretching anharmonicity constants will be important only for those compounds whose bond lengths depart appreciably from "normal" values. There are some preliminary indications that this method of including the anharmonicity causes the proper range of splittings in the calculated C-H stretching frequencies of tri-t-butylmethane.

C. Computer Programs Used

The computer programs used for potential energy minimization were modifications of DIPSY VI and MOLBD2, both of which have been described in the literature.[1] A few of the minimizations and all of the frequency calculations were done using a modification of R. L. Hilderbrandt's combination potential minimization and frequency calculation program.[17] The versions of the programs used were written during the course of this research; the modifications made were not complex, but were tedious to implement in some cases. All programs used were extensively checked, individually and against each other. The Hilderbrandt program was essentially a vastly improved version of MOLBD2, but was not developed until most of the research being reported on here had been completed. In the context of this section, any remarks made about MOLBD2 may be taken as applying also to the Hilderbrandt program.

Each program has its advantages, which originate from the choice of the set of parameters which are varied as the potential energy is minimized. MOLBD2 varies the Cartesian coordinates of the atoms which compose the molecule, while DIPSY VI varies a user-specified set of "independent parameters" which provide a complete, geometrically consistent description of the molecular structure. MOLBD2 has the advantages of being able to accommodate a nine-torsional model of hindered internal rotation and of being able to minimize the energies of cyclic structures. However, it is costly to operate, and no constraints may be placed upon the minimization. While DIPSY VI is much cheaper to run and has provisions whereby a number of constraints may be placed upon the molecule, it cannot accommodate a nine-torsional model of hindered internal rotation or minimize the potential energy of a cyclic structure. Between DIPSY VI and MOLBD2 it was possible to investigate all of the molecules which were of interest in this research while imposing all desired constraints.

D. Evaluation of MUB-2

MUB-2 must be evaluated on the basis of the accuracy with which it reproduces experimental results. Although the field was not optimized to reproduce a large number of experimental data (all those which were used to devise the field have been mentioned above), it seems reasonable to

expect it to do a good job of predicting structures and isomerization energies, since MUB-1 was fairly successful in predicting these quantities. However, it was not expected that MUB-2 would reproduce vibrational frequencies very well. Schachtschneider and Snyder[9] have found that it is necessary to add a number of interactions to a simple Urey-Bradley force field if the field is to reproduce the experimental frequencies accurately. No attempt has been made to include these interactions in MUB-2, and, in addition, the site-to-site variations of the K's for a given interaction have not been explicitly included, as discussed above. Therefore, no comparison between observed and calculated normal mode frequencies will be given here (however, experimental and calculated frequencies of methane and ethane are compared in the Appendix). Comparisons of experimental and calculated structural parameters, isomerization energies, and rotational barriers are given below.

1. Structural Trends

a. Interpretation of Derived Structures

The bond length reference point parameters were derived by requiring that the force field fit observed electron diffraction r_g structures. Structural parameters are determined and reported on a number of different bases; the most common of these involve equilibrium lengths (r_e), thermal average lengths (r_g), distances between thermal average positions (r_α), and "spectroscopic" lengths (r_o or

r_s). Equilibrium structures are appealing, for their physical meaning is easy to understand: an equilibrium structure represents the minimum in the potential energy surface. Unfortunately, equilibrium structures have been determined for relatively few molecules, and nearly all of these are diatomics (the remainder are triatomics). Gas-phase electron diffraction yields r_g structures directly and with a precision of a few thousandths of an Angstrom unit. An r_g structure has the advantage that the bond lengths may be related to the equilibrium bond lengths to a good approximation <u>via</u>

$$r_g - r_e = (3a/2)\ell_g^2, \qquad (5)$$

where <u>a</u> is the anharmonicity parameter derived earlier and l_g is the amplitude of vibration of the bond, which is available from a number of sources, electron diffraction data among them. So-called r_α structures may be determined from electron or X-ray diffraction (though an electron diffraction r_α structure is slightly different from an X-ray diffraction r_α structure); the precision of the structural parameters obtained is often competitive with the precision of r_g parameters. However, the relationship between r_α and r_e is not as simple as equation (5), particularly for X-ray diffraction lengths, though generally r_α lengths are somewhat shorter than r_g lengths. The values determined for "spectroscopic" structural parameters are often more precise than are those determined from diffrac-

tion data, but the lengths involved are complex averages whose physical meaning is unclear. Values of "spectroscopic" bond lengths can range from less than the r_e to more than the r_g values.

The above considerations suggest that, while molecular mechanics structures are minimum energy structures, they are most conveniently keyed to and compared with r_g structures. The lengths can be converted readily to equilibrium lengths, since l_g and $\underline{a}$ are quite constant for a given bond type and l_g is not very temperature dependent at ordinary temperatures. Experimental r_g structures are available for a variety of hydrocarbons; therefore, a given model force field may be extensively tested against experimental data. Most recent force fields are parameterized so that their minimum-energy structures correspond to r_g structures.

b. Comparison of Calculated and Experimental Structures

As may be seen, MUB-2 reproduces a variety of structures well. The comparison between calculated and experimental structural parameters is summarized in Figures 2-5. Structural parameters calculated using other force fields[1d,18,19] are included so that comparisons between different fields may be made. MUB-2 seems to be superior to the others (force fields of Schleyer, Allinger, and Warshel) in predicting structural parameters. Almost all of the MUB-2 calculated structural parameters are within

Figure 2. Comparison of experimental and calculated C-C bond lengths. The vertical error bars correspond to ± σ. Points which represent fits of the same bond length by different force fields are joined by dotted lines. The numbers refer to the following molecules: (1) Ethane. (2) n-Butane. (3) Isobutane. (4) Cyclopentane. (5) Tri-t-butylmethane (C2-C5). (6) Tri-t-butylmethane (C1-C2). (7) Hexamethylethane (end bond). (8) Tetramethylethane (central bond). (9) Tetramethylethane (end bond). (1) Methylcyclohexane. (11) Adamantane. (12) Hexamethylethane (central bond).

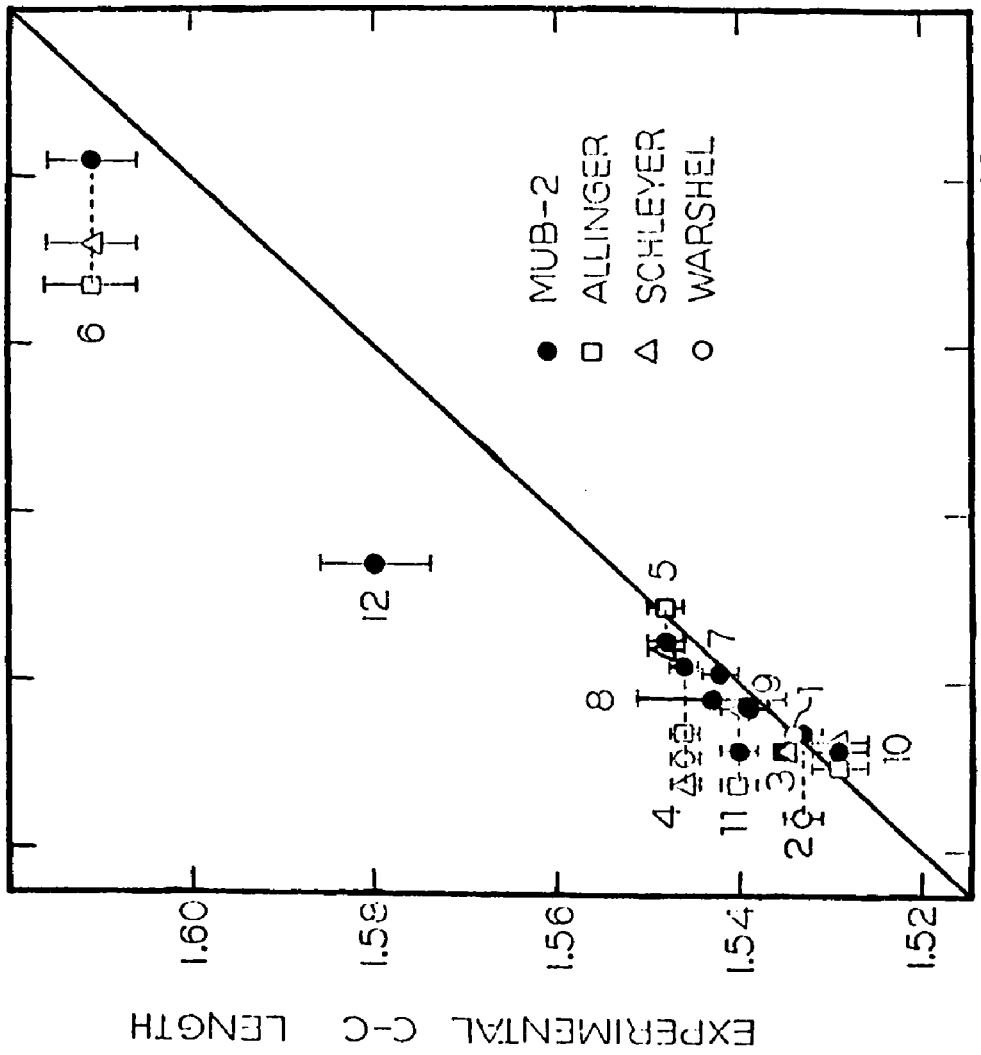

MUB-2
ALLINGER
SCHLEYER
WARSHEL
EXPERIMENTAL C-C LENGTH
CALCULATED C-C LENGTH
1.52
1.54
1.56
1.58
1.60

Figure 2.

Figure 3. Comparison of experimental and calculated C-H bond lengths. The vertical error bars correspond to ± σ. Points which represent fits of the same bond length by different force fields are joined by dotted lines. The numbers refer to the following molecules: (1) Methane. (2) Ethane. (3) n-Butane. (4) Isobutane (methyl), tetramethylethane (methyl). (5) Isobutane (tertiary). (6) Cyclopentane. (7) Tri-t-butylmethane. (8) Hexamethylethane. (9) Tetramethylethane (tertiary).

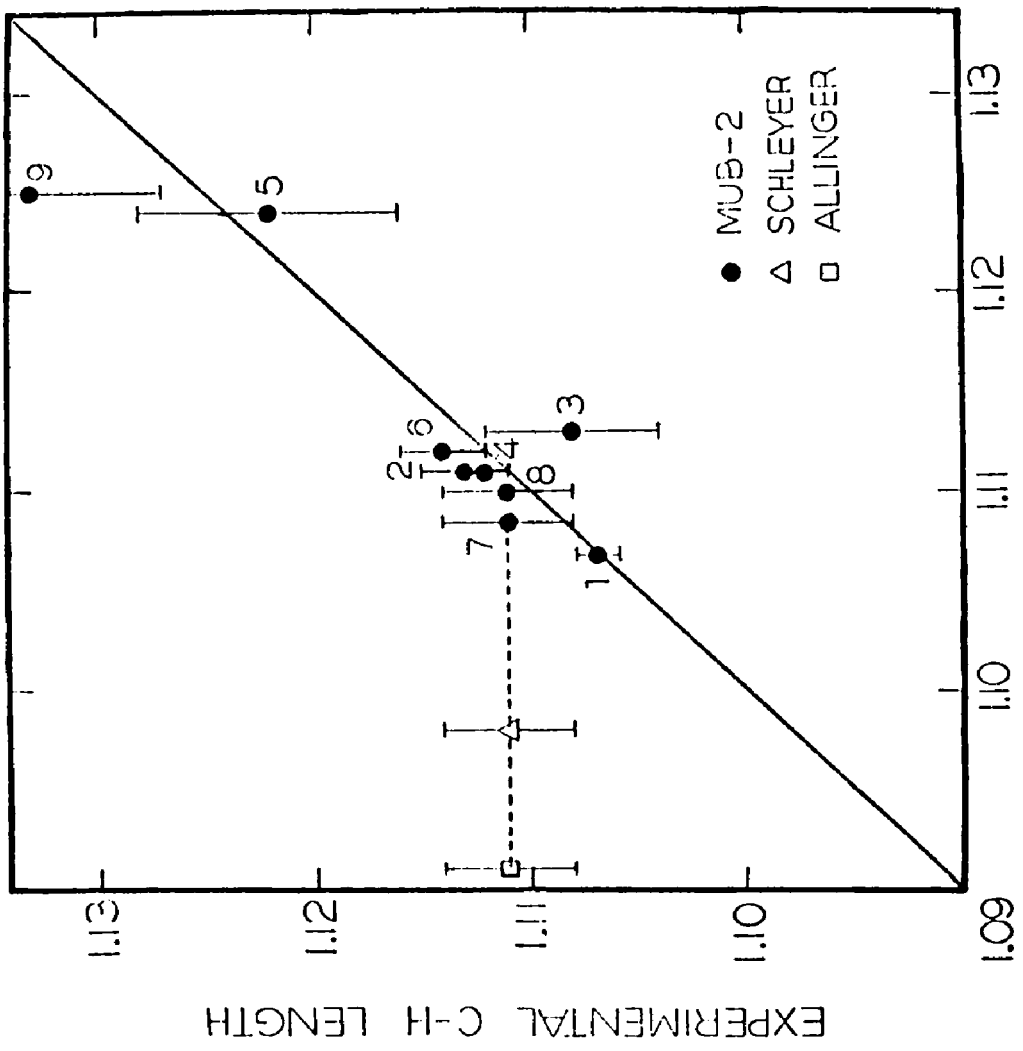

MUB-2
SCHLEYER
ALLINGER
1.09
1.10
1.11
1.12
1.13
EXPERIMENTAL C-H LENGTH
CALCULATED C-H LENGTH

Figure 3.

Figure 4. Comparison of experimental and calculated CCC angles. The vertical error bars correspond to ± σ. Points which represent fits of the same angle by different force fields are joined by dotted lines. The numbers refer to the following molecules: (1) n-Butane. (2) Isobutane. (3) Tetramethylethane (Me-C-Me). (4) Tetramethylethane (C-C-Me). (5) Hexamethylethane (C-C-Me). (6) Hexamethylethane (Me-C-Me). (7) Tri-t-butylmethane (Ct-C-Me). (8) Tri-t-butylmethane (C-Ct-C). (9) Tri-t-butylmethane (Me-C-Me). (10) Di-t-butylmethane (C2-C-C2'). (11) Di-t-butylmethane (C-C2-C3). (12) Di-t-butylmethane (C-C2-C4). (13) Di-t-butylmethane (C-C2-C5). (14) Adamantane (Ct-Cs-Ct). (15) Adamantane (Cs-Ct-Cs).

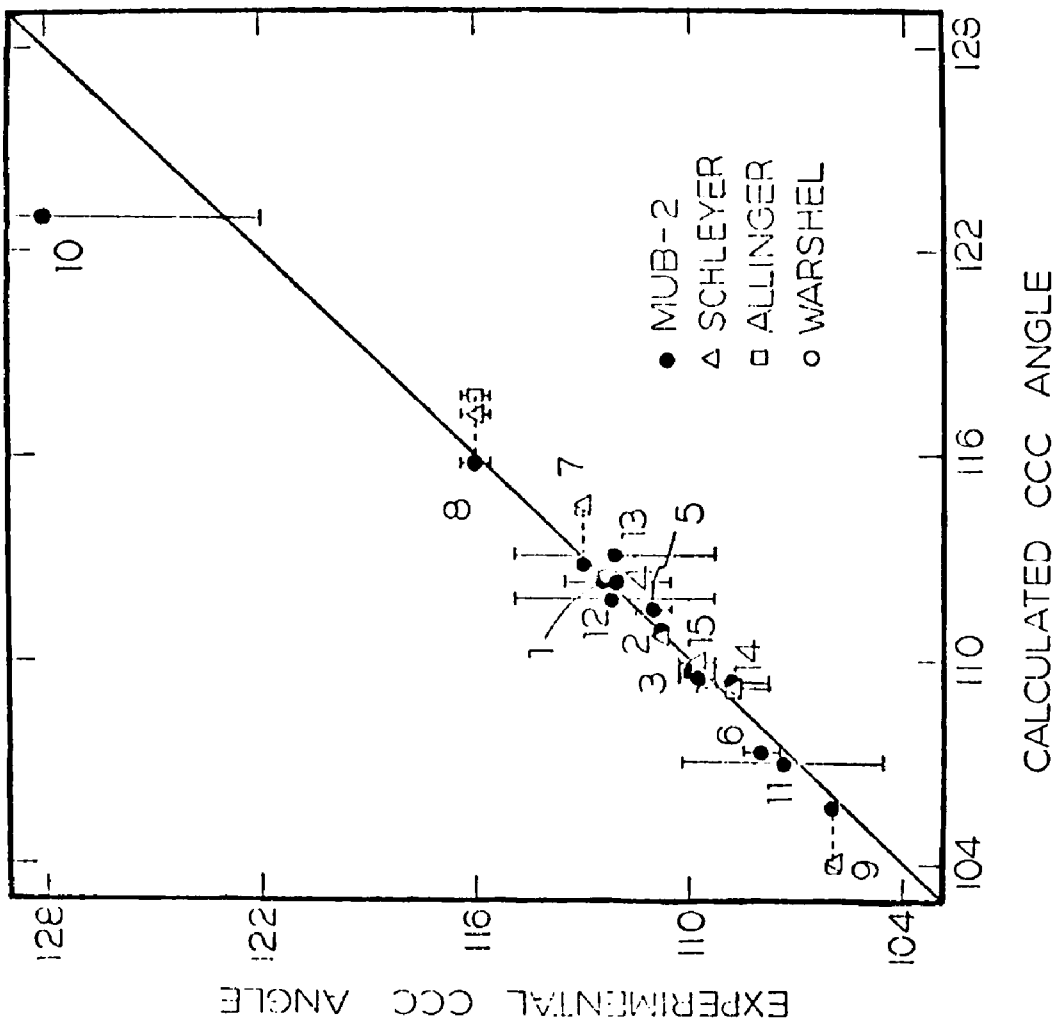

EXPERIMENTAL CCC ANGLE
CALCULATED CCC ANGLE
104
110
116
122
128
125
MUB-2
SCHLEYER
ALLINGER
WARSHEL

Figure 4.

Figure 5. Comparison of experimental and calculated HCC angles. The vertical error bars correspond to ± σ. Points which represent fits of the same angle by different force fields are joined by dotted lines. The numbers refer to the following molecules: (1) Ethane. (2) n-Butane. (3) Di-t-butylmethane. (4) Hexamethylethane. (5) Tetramethylethane. (6) Cyclopentane. (7) Methylcyclohexane. (8) Tri-t-butylmethane. (9) Adamantane.

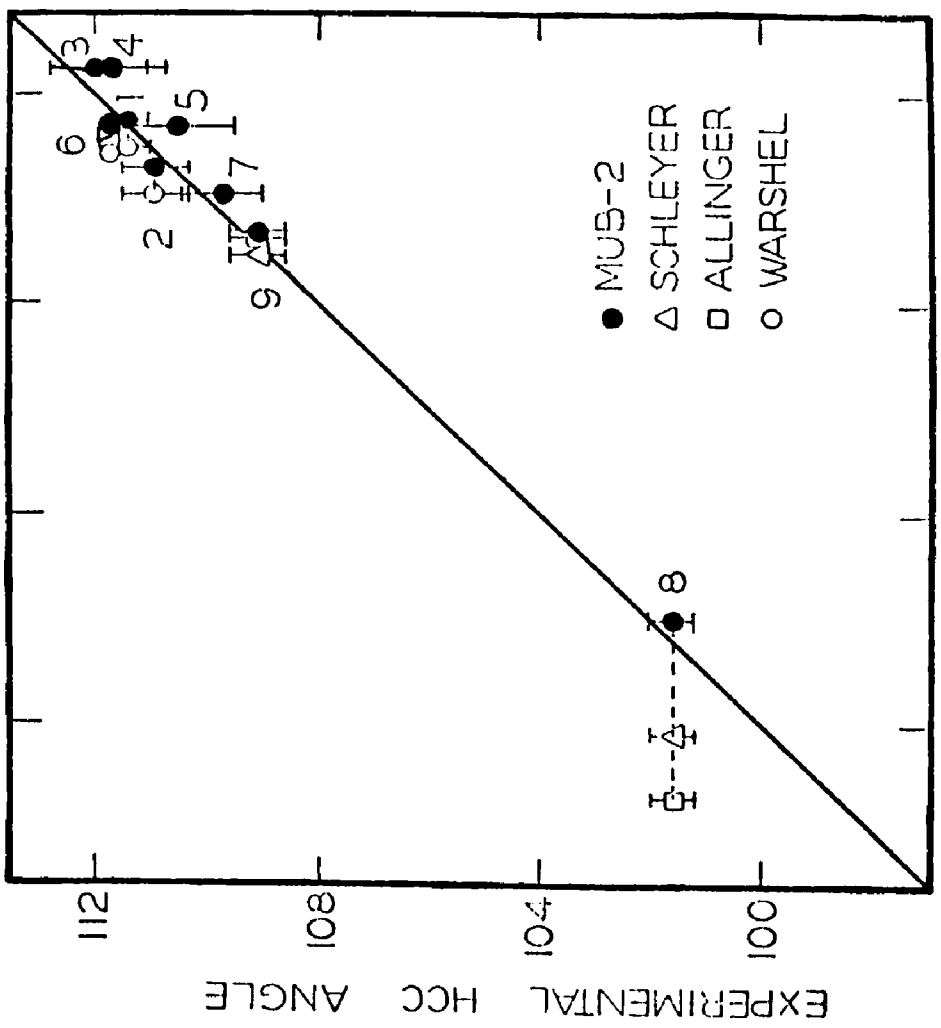

EXPERIMENTAL HCC ANGLE
CALCULATED HCC ANGLE
100
104
108
112
MUS-2
SCHLEYER
ALLINGER
WARSHEL

Figure 5.

2σ of the experimental structural parameters. The most conspicuous exception is the central bond length in hexamethylethane, which is calculated to be 1.554 A but for which experiment gives a value (±σ) of 1.580 ± 0.006 A.[20] The discrepancy between the MUB-2 and experimental values here is neither alarming nor a compelling indication of inadequacy in MUB-2, since the field gives fairly good values for the carbon-carbon bond lengths in tri-t-butylmethane, which is more strained than is hexamethylethane. Considering the difficulty in determining small differences in bond lengths from electron diffraction data and the state of the art of error analysis of electron diffraction determinations of molecular structures, it is possible that a realistic standard deviation of the hexamethylethane central bond length is larger than the one reported.

It is difficult to evaluate MUB-2's performance in predicting the puckering amplitude of cyclopentane. When a general procedure proposed by Pople and Cremer[21] is used to calculate the puckering amplitude from the MUB-2 Cartesian coordinates of the carbons, a puckering amplitude of 0.356 is obtained. This may be compared with the electron diffraction value (calculated on the same basis) of 0.416.[22] However, the molecular model assumed in determining the experimental structure was subject to several constraints which were not imposed upon the model used in the force field calculations. Therefore, there is some question as to the significance of a comparison between the two values

of the puckering amplitude, as the value obtained is dependant to a certain extent upon the molecular model assumed. The average C-C bond length calculated using MUB-2 is a bit shorter than the experimental bond length, which was determined using a model in which all C-C bond lengths were constrained to be equal. The average C...C nonbonded distance calculated using MUB-2 is longer than the electron diffraction average (2.453 A vs. 2.444 ± 0.0015 A). This would indicate that the puckering amplitude given by MUB-2 is somewhat smaller than the one which would be implied by an unconstrained electron diffraction structure, but it is difficult to say how large the discrepancy would be.

The success of MUB-2 in reproducing the structure of tri-t-butylmethane, a highly strained molecule, deserves special attention. The computed and experimental structural parameters[23] are compared in Table III. It may be noted that, save for one torsional angle, all of the computed parameters are within 2σ of the experimental parameters. Moreover, the given σ are described as "crude lower limits to be regarded with caution."[23]

The structure of another highly strained hydrocarbon, norbornane, was computed using MUB-2. Here the comparisons of calculated structural parameters with those obtained from experiment is harder to make, because two recent electron diffraction studies of norbornane[24,25] have yielded different results for the C-C bond lengths. The MUB-2 parameters are closer to the results of Yokoseki and Kuchitsu,

Table III. Comparison of the Experimental and Calculated Structural Parameters of Tri-t-butyl Methane

	Experimental[a]	Calculated
r_g(C-H)	1.111 ± 0.003 Å	1.109 Å
r_g(C2-C5)	1.548 ± 0.002 Å	1.545 Å
r(C1-C2)	1.611 ± 0.005 Å	1.602 Å
B(C1-C2-C5)	113.0 ± 0.2°	112.8°
α(H-C1-C2)	101.6 ± 0.4°	102.0°
γ(C2-C5-H8)	114.2 ± 1.0°	112.9°
Δτ(H1-C1-C2-C5)	10.8 ± 0.5°	17.2°
Δτ(Methyl groups)	18.0 ± 6°	8.1°

[a] The indicated uncertainties are the least squares standard deviations of the parameters.

which are usually considered to be the more dependable: the experimental values for the average C-C length and bridge CCC angle are 1.549 ± 0.001 A and 93.1 ± 0.6°, respectively, while the computed values are 1.550 A and 94.5°. The MUB-2 values of the individual C-C bond lengths differ from the experimental values, but the experimental values are not firm, as it is difficult to determine small differences between bond lengths from electron diffraction intensities. The error estimates of reference 25 reflect this. The bond lengths determined are 1.560 ± 0.024 A for the ring to bridging carbon-carbon bond, 1.539 ± 0.012 A for the secondary to tertiary ring carbon-carbon bond, and 1.557 ± 0.025 A for the secondary to secondary ring carbon-carbon bond. The values of these bond lengths determined using MUB-2 are 1.542 A, 1.550 A, and 1.561 A, respectively. All computed values are within the limits of error, and the agreement between the computed and experimental average C-C bond lengths is good, further illustrating the ability of MUB-2 to give correct values of structural parameters. Other force fields tend to compute values of the average norbornane C-C bond length that are either too short or too long.[26]

2. Isomerization Energies

a. Rotational Isomerization Energies

The gauche-trans energy difference was computed for several molecules which display this type of

rotational isomerism. There are some difficulties in comparing the calculated with the experimental values, for the calculated values apply to vibrationless molecules at 0° K, while the experimental values are for vibrating molecules at temperatures above 0° K. It was assumed that corrections for the temperature differences would be the same for different rotational isomers of the same compound, which seems reasonable. It was further assumed that the zero-point energy differences for rotational isomers are small. In order to test this assumption, the normal mode vibrational frequencies of rotational isomers of selected molecules were computed using MUB-2. As stated above, MUB-2 does not reproduce experimental frequencies very well; calculated values for normal coordinates composed largely of angle deformations were in error by as much as 200 cm^{-1}. However, it may be assumed that the gross errors in the computed frequencies will cancel for rotational isomers of the same molecule, and therefore that the small differences in the computed frequencies for different rotational isomers arise from the structural differences. For this reason, the computed zero-point energy differences are assumed to be significant. This assumption is reinforced by the fact that the computed zero-point energy differences are small (less than 100 calories) and have the same direction (<u>trans</u> lower than <u>gauche</u>) and approximate magnitude for those molecules which were investigated. Hence, the results of the frequency calculations support

the original assumption that the zero-point energy differences do not make major contributions to the experimental energy differences for rotational isomers.

Values of the thermodynamic functions may be calculated from the vibrational frequencies and other information, but here there is no reason to assume that the errors caused by the systematic deviation of the computed frequencies from the experimental frequencies will cancel for different rotational isomers of the same molecule. Hence, differences in the vibrational contributions to the thermodynamic values computed for rotational isomers were not assumed to be significant.

n-Butane is the simplest molecule which exhibits gauche-trans rotational isomerism. Electron diffraction gives a gas-phase value of 630 ± 200 cal/mol for ΔG° (gauche-trans n-butane),[27] while liquid Raman studies yield a value of 770 ± 70 cal/mol for ΔH° (gauche-trans).[28] MUB-2 gives a gauche-trans energy difference of 540 cal/mol for vibrationless n-butane. The MUB-2 zero-point energy difference is 90 cal/mol; therefore, the computed value for the vibrating gauche-trans n-butane energy difference is 630 cal/mol. The comparison between the computed and experimental values is good.

Other n-alkanes show similar values for the gauche-trans energy difference. Liquid Raman studies on n-pentane and n-hexane indicate that ΔH° (gauche-trans) for one gauche conformation is around 500 cal/mol[28]; electron dif-

fraction yields a value of ΔG° (gauche-trans) of around 600 cal/mol for gas-phase n-pentane, n-hexane, and n-heptane.[27] Calculations done using MUB-2 give a 600 cal/mol gauche-trans energy difference for vibrationless n-pentane. It would seem, therefore, that MUB-2 may be expected to be fairly successful in reproducing the rotational isomerization energies of n-alkanes.

The rotational isomerization energies of two branched molecules, 2-methylbutane and 2,3 dimethylbutane, were computed using MUB-2. Raman studies on liquid 2,3 dimethylbutane (tetramethylethane) have indicated that the energy difference (ΔH°) between the two isomers is less than 200 cal/mol.[29] Electron diffraction results imply a ΔG° (gauche-trans) of 170 ± 200 cal/mol,[20] but the associated uncertainties are fairly large. The energy difference between vibrationless gauche and trans tetramethylethane computed using MUB-2 is 277 cal/mol, the trans isomer having the higher energy. The computed zero-point energy difference is zero. In view of the uncertainties in the experimental data, it is hard to evaluate the success of the force field in this instance. For 2-methylbutane, Raman studies on the liquid have indicated an energy difference of less than 200 cal/mol,[29] while calculations using MUB-2 give a gauche-trans energy difference of 489 cal/mol for the vibrationless molecule (the zero-point energy difference was not calculated). Here the calculated result seems high, but the value of a comparison between

experimental and computed results is diminished by the fact that the experimental studies were done on the liquid, while the calculated value is approximate for the hypothetical gas-phase species at 0° K.

When the geometries of 2-methylbutane and tetramethylethane are considered, the computed energy differences can be rationalized qualitatively. Gauche tetramethylethane has three gauche methyl-methyl interactions, while trans tetramethylethane has only two; however, the gauche isomer can relieve two of its gauche interactions at the expense of the third by a rotation around the central C-C bond, while the trans isomer cannot relieve either of its gauche interactions by such a rotation. Hence, a destabilization of the gauche sites in the trans isomer relative to those in the gauche isomer is to be expected. The opposite situation is present in 2-methylbutane. Gauche-gauche 2-methylbutane has two gauche methyl-methyl interactions, while the gauche-trans isomer has one. Here, however, the GG isomer can relieve neither gauche interaction via rotation around the central C-C bond, while the GT isomer can relieve its gauche interaction at the expense of its trans methyl-methyl interaction by such a rotation. Hence, one would expect that the gauche-trans energy difference for 2-methylbutane would be larger than the corresponding difference for tetramethylethane, as was found using MUB-2.

Finally, rotational isomerization energies were calculated for two cyclic molecules, methylcyclohexane and 1,3

dimethylcyclohexane. The axial-equatorial methylcyclohexane energy difference has long been of interest to workers in the field of conformational analysis, and unfortunately the early idea that the strain energy associated with gauche methyl conformations is (1) constant, and (2) additive still has some effect on the current literature pertaining to methylcyclohexane. The same is true, to a certain extent, of the literature on 1,3 dimethylcyclohexane. Therefore, it was a bit difficult to find experimental results for these molecules which could be used to evaluate the energies computed using MUB-2. One recent nuclear magnetic resonance study which appears to be relatively free from bias indicates that the axial-equatorial energy difference is 1.78 ± 0.15 kcal/mol.[30] Computations made using MUB-2 give an axial-equatorial energy difference of 0.954 kcal/mol for the vibrationless molecule. The zero-point energy difference is 0.08 kcal/mol, which implies a total computed (axial-equatorial) energy difference of 1.03 kcal/mol, which looks rather low. Axial-equatorial type energy differences are available for other cyclic molecules, and one of these, 1,3 dimethylcyclohexane, was investigated using MUB-2. The experimental energy difference was obtained fairly directly and without recourse to preconceived notions about conformational energy differences. The heats of isomerization of gaseous cis 1,3 dimethylcyclohexane and the trans isomer relative to ethylcyclohexane have been obtained from the experimentally

measured heats of formation. The derived values are -3.11 ± 0.22 kcal/mol for the cis isomer and -1.15 ± 0.21 kcal/mol for the trans isomer,[31] which implies a trans-cis energy difference of 1.96 ± 0.30 kcal/mol. As the measured "axial-equatorial type" energy differences for 1,2 and 1,4 dimethylcyclohexane are also very close to 1.9 kcal/mol, the uncertainty in the value for 1,3 dimethylcyclohexane is probably less than 0.30 kcal/mol. The calculated trans-cis energy difference for vibrationless 1,3 dimethylcyclohexane is 1.03 kcal/mol, and the zero-point energy difference is 0.06 kcal/mol; therefore, the total calculated energy difference is 1.09 kcal/mol. Judging from the results on the two substituted cyclohexanes, it seems that MUB-2 may systematically yield values of axial-equatorial methyl energy differences which are lower than the observed values.

Summarizing the results of this section, it would seem that while MUB-2 can be used to compute fairly accurate values for the rotational isomerization energies of the n-alkanes, the rotational isomerization energy values computed for branched and cyclic compounds may not be quantitatively correct, although the trends in the computed values seem to be in accord with the observed trends insofar as the few computed values allow one to judge. As stated above, the computed rotational isomerization energies for substituted cyclohexanes are probably systematically low. It is a bit harder to assess the deficiencies

in the computed values for the branched compounds, as the experimental values were imprecise and, for the most part, were not obtained from measurements on gas-phase species. The failures of MUB-2 in computing quantitatively correct rotational isomerization energies do not point toward any one simple deficiency in the force field, but would seem to be the results of slight imbalances in the forces and possibly the neglect of some interactions.

b. Geometrical Isomerization Energies

Geometrical isomerization energies were calculated for a few molecules during the course of the investigation of MUB-2. Owing to considerations discussed in the section above on rotational isomerization energies, the computed geometrical isomerization energies are most suitably compared to differences in ΔH_f^o extrapolated to 0° K and corrected for zero-point energy differences. Corrections of the experimental values of ΔH_f^o (t° K) to 0°K are based on Pitzer's calculation methods for hydrocarbons.[32] These methods embody a number of simplifying assumptions concerning barrier heights and interactions of vibrations, as well as the seemingly ubiquitous assumption of the constancy and additivity of gauche methyl interactions, which are somewhat questionable. In addition, errors in the experimental measurements of the heats of formation must be considered. Pitzer estimates[32] uncertainties of ± 0.3 kcal/mol for the n-alkanes and ± 0.7 - ± 1.0 (± 2.0 for

tetramethylethane) kcal/mol for the branched alkanes. In view of the sources of uncertainty discussed above, the estimate of ± 0.3 kcal/mol for the uncertainty in the n-alkane ΔH_f° (0° K) seems a bit low; the uncertainty estimates for the branched compounds seem reasonable.

Since the observed isomerization energy of isobutane was one of the pieces of information used in the derivation of the nonbonded potential functions, it is not surprising that MUB-2 reproduces this value fairly well. The computed isomerization energy is 1.30 kcal/mol, as compared with the corrected experimental value of 1.39 ± 0.7 kcal/mol. The other computed isomerization energies are compared with the experimental values in Table IV. Some values of isomerization energies computed with Schleyer's[1d] and Allinger's[18] force fields are included for purposes of comparison. It must be pointed out here that the complete Schleyer and Allinger force fields were not used to calculate the isomerization energies shown in Table IV. Both Schleyer and Allinger are concerned with reproducing experimental heats of formation at 298° K, which include contributions from thermal effects and zero-point energies. Their force fields include bond or group increments which are added to the so-called "steric" energies (which apply to vibrationless molecules at 0°K) to obtain heats of formation for the gaseous species at 298° K. The bond or group increments of the Allinger and Schleyer fields are designed to account for differences in so-called "chemical binding

Table IV. Computed and Experimental Geometrical Isomerization Energies[a] for Vibrationless Molecules.[a]

	Experimental Isomerization Energy[b,i]	MUB-2 Isomerization Energy	Allinger Isomerization Energy	Schleyer Isomerization Energy	Experimental Zero-Point Energy
n-butane	0.0···	0.0···	0.0···	0.0···	80.62[c]
isobutane	1.39 ± 0.7	1.30	2.32	0.28	80.38[c]
n-pentane	0.0···	0.0···	0.0···	0.0···	98.32[c]
isopentane	0.63[d] ± 0.7	0.44	0.76	-0.88	97.61[c]
neopentane	3.49[d] ± 1.0	3.73	4.80	0.79	97.30[c]
n-hexane	0.0···	0.0···	0.0···	0.0···	116.02[e]
2,2 dimethylbutane	2.91 ± 1.0	1.78	3.02	1.59	115.19[f]
tetramethylethane	(1.0) ± 2.0	-0.21[j]	1.06	0.29	(115.2)[g]
ethylcyclohexane	0.0···	0.0···			
cis 1,3 dimethyl-cyclohexane	2.38[h] ± 0.7	2.70			
trans 1,3 dimethyl-cyclohexane	0.42[h] ± 0.7	1.67			

[a] All energies are in kcal/mole. The Allinger and Schleyer values are taken out of context (see text). Heats of formation at 0°K were, except where noted, taken from F. D. Rossini, K. S. Pitzer, R. L. Arnett, R. M. Braun, and G. C. Pimentel, Selected Values of Physical and Thermodynamic Properties of Hydrocarbons and Related Compounds, w tables. All energy differences listed are energy (n-alkane)--energy (isomer).

[b] The experimental isomerization energies listed have been corrected for zero-point energy differences.

Table IV continued.

---

[c] Reference 7.

[d] New experimental ΔH_f° for n-pentane, isopentane, and neopentane given by G. Pilcher and J. D. M. Chadwick, Trans. Faraday Soc., 63, 2357 (1967). The Pitzer corrections to 0°K were used.

[e] Calculated from zero-point energy of n-pentane on the basis of the increment per CH_2 unit of 17.7 kcal/mole given in Reference 7.

[f] T. L. Allen, J. Chem. Phys., 31, 1039 (1959).

[g] Zero-point energy of tetramethylethane ≈ zero-point energy of 2,2 dimethylbutane.

[h] Experimental energies (corrected to 0°K) from E. J. Prosen, W. H. Johnson, and F. D. Rossini, J. Res. Nat. Bur. Stds., 39, 173 (1947) minus 0.700 kcal, approximate zero-point energy difference for n-pentane--isopentane, n-hexane--isohexane, etc. (this seemed appropriate given the difference in the two structures).

[i] The uncertainties given may be regarded as lower limits, as they are Pitzer's estimates for the ΔH_f° (0°K) for the branched compounds and do not reflect the uncertainties in ΔH_f° (0°K) for the n-alkanes.

[j] Energy (n-hexane) - Energy (trans tetramethylethane).

[k] Energy (n-hexane) - Energy (gauche tetramethylethane).

energies" as well as zero-point energy differences. Hence, the steric energy differences calculated using the Allinger or Schleyer fields do not reflect the effects of an extra correction term which each field contains. However, it is perhaps worth noting that MUB-2, which contains no such correction term, does a better job than the "uncorrected" Allinger and Schleyer force fields of computing geometrical isomerization energies.

All but two of the MUB-2 energies are within the given uncertainties of the experimental quantities. The values of the uncertainties shown in Table IV are lower limits, for these are taken from Pitzer's estimates of the uncertainties in the branched compound values and do not reflect the effects of uncertainties in the n-alkane values of ΔH_f° (0° K). The poorest agreement between the computed and experimental values is for 2,2 dimethylbutane and tetramethylethane; however, the experimental measurements on these compounds are quite old, and Pitzer estimated[32] fairly high uncertainties in his ΔH_f° (0° K) values. The poor agreement between observed and calculated values for trans 1,3 dimethylcyclohexane shows the low axial-equatorial methyl energy difference given by MUB-2.

3. Rotational Barriers

While the value of the "intrinsic portion" of the MUB-2 rotational barrier was adjusted so that the observed

Table V. Experimental and Calculated Barriers to Hindered Internal Rotation[a]

	Experimental	MUB-2	Allinger	Schleyer[b]
ethane	2.93 ± 0.03[c]	(3.0)	- -	(2.8)
propane	3.33 ± 0.02[d]	3.60	- -	2.9
n-butane (H ecl. Me)	3.72[e], 4.2 ± 0.4[f]	4.03	2.94	- -
n-butane (Me ecl. Me)	6.10[e], 6.7 ± 0.4[f]	6.10	4.55	5.8
neopentane	4.3[g]	4.15	- -	- -

[a] All energies are in kcal/mole and are the differences between the energies of the eclipsed and staggered forms of the molecule.

[b] The Schleyer force field contains special barrier parameters to distinguish between the end atoms of τ_{ijkl}. The Allinger force field and MUB-2 do not.

[c] S. Weiss and G. E. Leroi, J. Chem. Phys., 48, 962 (1968) (from torsional frequencies).

[d] E. Hirota, C. Matsumura, Y. Morino, Bull. Chem. Soc. Japan, 40, 1124 (1967) (from microwave data).

[e] K. Ito, J. Amer. Chem. Soc., 75, 2430 (1953) (estimates from thermodynamic data).

[f] J. E. Piercy and M. G. S. Rao, J. Chem. Phys., 46, 3951 (1967) (from ultrasonic data).

[g] K. S. Pitzer and J. E. Kilpatrick, Chem. Rev., 39, 435 (1946) (from entropy calculation).

3.0 kcal/mol difference between eclipsed and staggered ethane would be reproduced by the force field, this does not guarantee that MUB-2 will reproduce the values of rotational barriers in other molecules. The values which are computed for various rotational barriers using a given force field provide some measure of the balance of the forces within the field and of the validity of the way in which hindered internal rotation is modelled into the force field.

The barriers to hindered internal rotation for a few simple molecules have been calculated using MUB-2. The calculated values are compared to the experimental ones and values calculated using other force fields in Table V. As may be seen, MUB-2 does a fairly good job of reproducing the experimental barrier values, in spite of the simple way in which the torsions are modelled into the field.

E. Investigation of the Gauche Hydrogen Hypothesis

The accepted explanation of why trans n-butane has a lower energy than gauche n-butane is that the gauche Me...Me interaction, in particular the close 1...6 methyl hydrogen interaction, destabilizes the gauche conformer. Allinger's hypothesis[2] is that it is gauche n-butane's extra gauche 1...4 H...H interaction (gauche n-butane has three of these interactions while the trans isomer has only two) which is the principal cause of the destabilization of

the gauche isomer. Support for the gauche hydrogen hypothesis comes from dissections of the energy difference between gauche and trans n-butane (see reference 2) computed using the force field of reference 18. However, the hypothesis was not supported by similar dissections of energies computed using MUB-1, so Allinger's assertion that the gauche hydrogen effect will appear in almost all popular hydrocarbon force fields is somewhat suspect. The gauche-trans n-butane energy difference given by MUB-2 was examined to see what support, if any, calculations done using MUB-2 lend to the gauche hydrogen hypothesis.

The dissection of the MUB-2 n-butane energy difference is shown in Table VI. The gauche 1...4 H...H interaction energy is not shown, because doing so could be somewhat misleading: the gauche 1...4 H...H interaction energy might be large individually, but if it is balanced by large gauche H...Me and Me...Me interactions there is no reason why it would be a destabilizing force. If, on the other hand, the gauche hydrogen hypothesis is correct and the gauche 1...4 H...H interaction does contribute heavily to the destabilization of gauche n-butane relative to trans, the difference in the sum of all gauche interactions should contribute a sizeable portion of the gauche-trans energy difference. As can be seen in Table VI, the gauche interaction energy difference is a small part of the total energy difference. The difference between the bonded energies is by far the largest contributor, followed by the

difference in the energies arising from the geminal non-bonded interactions. These may be totalled to give a "valence deformation" energy difference of 0.56 kcal/mol, which is comparable to Allinger's value of 0.43 kcal/mol for the same quantity. However, the valence deformations cannot be considered the primary cause of the gauche destabilization. The gauche isomer relaxes its structure from that of the trans isomer to relieve interactions which destabilize gauche: these interactions may be regarded as the true "cause" of the gauche destabilization. The interactions which cause the relaxation cannot be identified using Table VI; perhaps the easiest way to determine them is to compare the energies of trans and unrelaxed gauche n-butane. The unrelaxed gauche isomer was generated by changing the CCCC dihedral angle of the trans isomer to 60° without varying any other parameters. The energies of the gauche and trans H...H, H...Me, and Me...Me interactions across the central C-C bond are shown in Table VIA for both isomers. It is true that the gauche 1...4 H...H interaction energy is higher for the gauche isomer than for the trans; the gauche isomer has an extra gauche 1...4 H...H interaction. However, the largest contributor to the energy difference is the Me...Me interaction, as is popularly supposed. The gauche Me...Me interaction may be relieved by opening the dihedral angle out to greater than 60°, among other relaxation motions; the gauche 1...4 H...H interactions cannot be relieved by small rotations

Table VI. Major Contributors to the Gauche-Trans n-Butane Energy Difference

Energy Source	Energy (kcal/mol)
Bonded	0.4304
Geminal Nonbonded	0.1263
Gauche Nonbonded	0.0558
Trans Nonbonded	0.0730

[a] All differences are gauche isomer-trans isomer.

Table VIA. Energies of Interactions Across Central C-C Bond of n-Butane (kcal/mol)

Trans Isomer		Gauche Isomer	
Gauche Interactions		Gauche Interactions	
4 H...Me	1.8489	1 Me...Me	1.7383
2H...H	0.6081	2H...Me	0.7728
		3 H...H	1.0342
Trans Interactions		Trans Interactions	
1 Me...Me	-0.2494	1 H...H	0.0281
2 H...H	0.0558	2 H...Me	-0.1490

around the central C-C bond. The information given in Table VIA indicates that the Me...Me interaction is the primary cause of the relaxation of the gauche isomer. Therefore, computations done with MUB-2 support the traditional explanation of the relative instability of gauche n-butane rather than that offered by the gauche hydrogen hypothesis.

As further support for the gauche hydrogen hypothesis, Allinger cited[2] the case of methylcyclohexane. Apparently, computations done using the Allinger field showed that a large part of the axial-equatorial methylcyclohexane energy difference comes from the increase in the steric energy of the equatorial hydrogen relative to the axial hydrogen. In order to provide a fuller evaluation of the gauche hydrogen hypothesis, the MUB-2 axial-equatorial energy differences for methylcyclohexane and 1,3 dimethylcyclohexane were examined. Although the axial-equatorial methyl energy differences calculated using MUB-2 seem to be low systematically, it is to be expected that some indication of the gauche hydrogen effect will show up in the energy dissections if the effect is operative in MUB-2. However, as Tables VII and VIII show, the steric interactions involving the tertiary isomer actually stabilize the axial isomer. For both substituted cyclohexanes, the steric interactions of the methyl hydrogens at first glance appear to be a significant factor in the stabilization of the equatorial isomer, but for 1,3 dimethylcyclohexane the stabilizing

Table VII. Major Contributors to the Axial-Equatorial Methylcyclohexane Energy Difference

Energy Source	Energy (kcal/mol)[a]
Bonded	0.87
Geminal Nonbonded	0.19
Methyl Carbon Nonbonded	-0.11
Methyl Hydrogen Nonbonded	0.32
Tertiary Hydrogen Nonbonded	-0.01
Other 1...4 C...C	-0.05
Other 1...4 C...H	-0.14
Other 1...4 H...H	-0.03

[a] All differences are axial isomer-equatorial isomer.

Table VIII. Major Contributors to the trans-cis 1,3 Dimethylcyclohexane Energy Difference

	Energy (kcal)[a]
Bonded	0.96
Geminal Nonbonded	0.13
1-Methyl Carbon Nonbonded	-0.10
1-Methyl Hydrogen Nonbonded	0.32
1-Tertiary Hydrogen Nonbonded	-0.14
Other 1...4 C...C	-0.04
Other 1...4 C...H	-0.06
Other 1...4 H...H	-0.02

[a] All differences are trans isomer-cis isomer.

influence of the methyl hydrogens is largely balanced by the destabilizing influences of the methyl carbon and tertiary hydrogen interactions. As was true for n-butane, the valence deformations contribute the bulk of the energy difference. Here again it may be said that the axial isomer relaxes to relieve certain nonbonded interactions, and Tables VII and VIII indicate that the primary cause of the relaxation is the methyl group-ring interactions.

It is clear, therefore, that calculations done using MUB-2 do not support the gauche hydrogen hypothesis. As was pointed out in the Introduction, it is risky to assume that an interpretation made from calculations done with only one force field (and that one parameterized by trial and error) corresponds to a physical effect. Certainly much stronger evidence than is now available would be needed to establish the gauche hydrogen effect hypothesis. The MUB-1 and MUB-2 results suggest that the effect is an artifact of the Allinger force field. An examination of the nonbonded interaction forces used in various force fields lends some support to this view. Forces derived from nonbonded interaction potentials used in various force fields are shown in Figure 6. While the Allinger C...H force is close to the consensus value, his H...H and C...C forces are displaced much less from the C...H force than are the corresponding forces from other force fields. It is evident that Allinger's "fat" hydrogens and "skinny" carbons could lead to the kind of effect that is observed.

Figure 6. Nonbonded force curves, $-\partial V(r)/\partial r$, corresponding to various nonbonded potential energy functions.

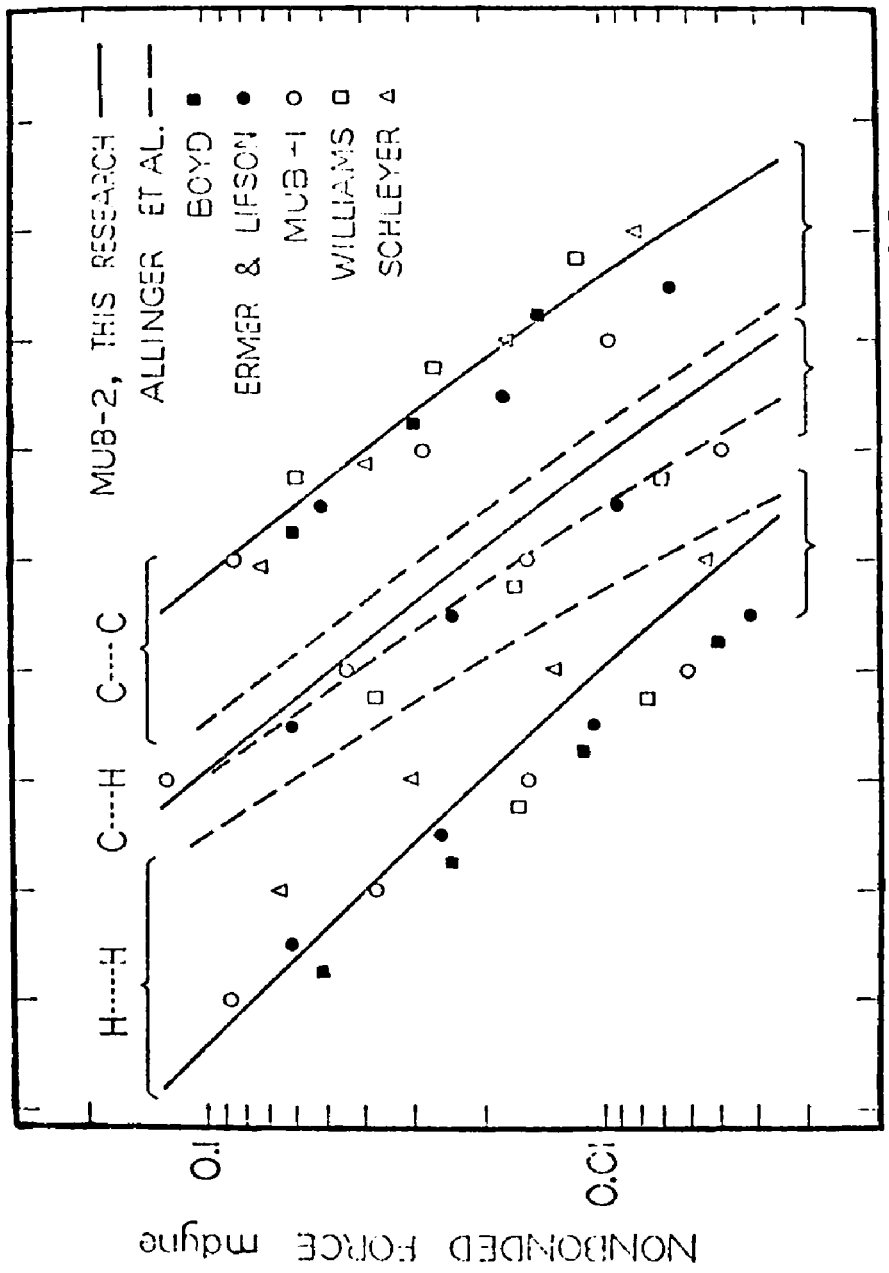

MUB-2, THIS RESEARCH
ALLINGER ET AL.
BOYD
ERMER & LIFSON
MUB-1
WILLIAMS
SCHLEYER
H----H
C---H
C---C
NONBONDED FORCE mdyne
0.1
0.01
1.6
2.0
2.4
2.8
3.2
r, Å

Figure 6.

The difference between the Allinger H...H and C...C forces and those derived from the nonbonded potentials shown in Figure 6 may be related to the fact that Allinger's nonbonded functions are derived from Hill's rare-gas atom-atom interaction potentials, while the other potential functions shown are derived from information on hydrogen and hydrocarbons. These facts indicate that Allinger's H...H and C...C potentials may be less physically reasonable than the others shown in Figure 6.

REFERENCES

1. See, for example,
   a. E. J. Jacob, H. B. Thompson, and L. S. Bartell, J. Chem. Phys., 47, 3736 (1967);
   b. R. H. Boyd, J. Chem. Phys., 49, 2574 (1968);
   c. A. Warshel and S. Lifson, J. Chem. Phys., 53, 582 (1970);
   d. E. M. Engler, J. D. Andose, and P. von R. Schleyer, J. Amer. Chem. Soc., 95, 8005 (1973).

2. N. L. Allinger and D. H. Wertz, Tetrahedron, 30, 1579 (1974).

3. E. Kochanski, J. Chem. Phys., 58, 5823 (1973).

4. J. M. Farrar and Y.T. Lee, J. Chem. Phys., 57, 5492 (1972).

5. M. G. Dondi, U. Valbusa, and G. Scoles, Chem. Phys. Let., 17, 137 (1972).

6. D. Williams, J. Chem. Phys., 43, 4424 (1965).

7. K. S. Pitzer and E. Catalano, J. Amer. Chem. Soc., 78, 4844 (1956).

8. D. E. Williams, J. Chem. Phys., 45, 3770 (1966).

9. J. H. Schachtschneider and R. G. Snyder, Spectrochimica Acta, 19, 117 (1961).

10. S. Lifson and A. Warshal, J. Chem. Phys., 49, 5116 (1968).

11. T. Shimanouchi in Physical Chemistry, An Advanced Treatise, H. Eyring, D. Henderson, and W. Jost, Eds., Academic Press, New York, N.Y., 1970, Volume 4, Ch. 6.

12. R. M. Stevens, J. Chem. Phys., 52, 1397 (1970).

13. A. Veillard, Theor. Chim. Acta, 18, 21 (1970).

14. L. S. Bartell, K. Kuchitsu, and R. J. DeNeui, J. Chem. Phys., 33, 1254 (1960).

15. L. S. Bartell and H. K. Higginbotham, J. Chem. Phys., 42, 851 (1965).

16. K. Kuchitsu, J. Chem. Phys., 49, 4456 (1968).

17. My thanks to R. L. Hilderbrandt for making this program available to me.

18. N. L. Allinger et al., J. Amer. Chem. Soc., 93, 1637 (1971).

19. A. Warshel, private communication.

20. T. L. Boates, Thesis, Iowa State University, 1966.

21. J. A. Pople and D. H. Cremer, to be published.

22. W. J. Adams, H. J. Geise, and L. S. Bartell, J. Amer. Chem. Soc., 92, 5013 (1970).

23. H. B. Burgi and L. S. Bartell, J. Amer. Chem. Soc., 94, 5236 (1972).

24. J. F. Chiang, C. F. Wilcox, Jr., and S. H. Bauer, J. Amer. Chem. Soc., 90, 3149 (1968).

25. A. Yokoseki and K. Kuchitsu, Bull. Chem. Soc. Japan, 44, 2356 (1971).

26. O. Ermer, Tetrahedron, 30, 3103 (1974).

27. L. S. Bartell and D. A. Kohl, J. Chem. Phys., 39, 3097 (1963).

28. N. Sheppard and G. J. Szasz, J. Chem. Phys., 17, 86 (1949).

29. G. J. Gzasz and N. Sheppard, J. Chem. Phys., 17, 93 (1949).

30. F. A. Anet, private communication.

31. E. J. Prosen, W. H. Johnson, and F. D. Rossini, J. Res. Nat. Bur. Stds., 39, 173 (1947).

32. K. S. Pitzer, Chem. Rev., 27, 39 (1940).

33. R. S. Mulliken, J. Amer. Chem. Soc., 72, 4493 (1950); 77, 887 (1955).

34. P. Pulay, Mol. Phys., 17, 197 (1969).

35. S. Weiss and G. E. Leroi, J. Chem. Phys., 48, 962 (1968).

36. H. J. Monkhorst, Chem. Phys. Let., 3, 289 (1969).

Appendix. MUB-2': A Variant of MUB-2 Designed to Fit Vibrational Frequencies

Although MUB-2 was not designed to reproduce vibrational frequencies with a high degree of accuracy, the constants were chosen to give a fair representation of the Schachtschneider and Snyder hydrocarbon potential surface.[9] Therefore, the fact that MUB-2 reproduced vibrational frequencies rather poorly was a disappointment. An effort to change MUB-2 in order to improve its fit of observed vibrational frequencies produced the variant MUB-2'. In deriving MUB-2', the areas of MUB-2 which were to be changed and the size of the changes made were limited, as major changes in the structures and energies calculated by the two force fields were not desired. It has been observed that, for a MUB force field, moderate changes in the force constants used cause only minor changes in computed structures and energies; the nonbonded potential functions seem to have the major influence on both computed structures and energies. Therefore, the nonbonded potential functions were not changed. Instead, the contributions to the MUB-2 representation of the Schachtschneider and Snyder potential surface made by the force constants were examined so that this portion of the force field could be altered to compute normal mode frequencies closer to those observed.

As has been noted in Section B above, a number of simplifications were made in the Schachtschneider and

Snyder force field when it was used to derive the MUB-2 force constants. The most noteworthy of these were (1) the neglect of certain interactions explicitly added to the Schachtschneider and Snyder Urey-Bradley field to improve the frequency fit, and (2) the averaging of the diagonal force constants for specific bond types. It was to be expected that these simplifications would cause some inaccuracies in the frequencies computed using MUB-2; the concern in this phase of the research was to minimize the inaccuracies without sacrificing simplicity.

While it is probably not necessary to include all interactions neglected in MUB-2 to get a satisfactory fit of the frequencies, some of them must be included. For instance, it has been shown that the addition of a term $G\Delta r_i \Delta r_j$ improves the Urey-Bradley force field of methane. Turning to the Schachtschneider and Snyder Urey-Bradley force field, it may be seen that $F_{H...H}$ is much smaller than the second derivative of the MUB-2 $V_{H...H}$, to which it is formally equivalent. It has been noted before that reasonable estimates of H...H interaction potentials[33] yield second derivatives which are much larger than Urey-Bradley $F_{H...H}$ constants. Because the MUB-2 $V_{H...H}$ has been constructed to be physically reasonable, it seems likely that the low Urey-Bradley $F_{H...H}$ value may be the result of $(\partial^2 V_{HH}/\partial r_{HH}^2)_r$ and G cancelling each other. If this is the case, MUB-2 has one obvious deficiency which will affect the computed frequency values. In order to

remedy this problem, the term $G\Delta r_i \Delta r_j$ (for C-H stretches) was added to the force field. The value of G was determined by varying the constant so that the magnitude of the splitting of the C-H stretching frequencies in methane was approximately reproduced. The value of G thus obtained was -0.28 mdyne/A. This may be compared with the value of -0.27 mdyne/A given by Pulay's ab initio methane force field,[32] and the value of -0.28 mdyne/A (methyl C-H) derived from the Schachtschneider and Snyder Urey-Bradley force field.[9]

No other additions to the force field were made. The force constants were varied to produce as good a fit of the calculated to the experimental frequencies as was possible. The C-H stretching force constant was varied so that the center of gravity of the calculated methane C-H stretching frequencies was approximately equal to the center of gravity of the experimental C-H stretching frequencies. The HCH bending constant was varied similarly to reproduce the experimental center of gravity of the methane HCH bending frequencies. Next, ethane was examined: the C-C stretching constant was varied to reproduce the experimental C-C stretching frequency. Fitting the centers of gravity of the ethane HCC bending frequencies proved to be somewhat more difficult; this could not be done (for the upper frequencies) without making the HCC bending constant ridiculously low. The poor fit of the calculated HCC bending frequencies to the experimental ones is probably a conse-

Table A1. Parameters of MUB-2'.[a]

Bond Stretching: $V(r) = 1/2K(r-r^\circ)^2 - 1/2Ka(r-r^g)^3$

Bond	K	r°	a	r^g
C-H	4.356	1.0303	2.0	1.1068
C-C	1.89	1.0795	2.0	1.534

Angle Bending: $V(\underline{\theta}) = 1/2H(\underline{\theta}-\underline{\theta}^\circ)^2$

Angle	H	θ° (radians)
C-C-C	0.589	1.91063
C-C-H	0.30	1.91063
H-C-H	0.34	1.91063

Torsional:[b] $V(\underline{\tau}) = 1/2 \sum_{i=1}^{9} V_3 (1+\cos 3\underline{\tau}_i)$

$V_3 = (2.154\times10^{-2})/9$ mdyne - Å for any dihedral angle

Stretch-Torsion:[b] $B(r,\underline{\tau}) = 1/2K_{st}(r-r^g)(1+\cos 3\underline{\tau})$

$K_{st} = -7.125\times10^{-2}$ mdyne $\qquad r^g = 1.534$

Stretch-Stretch: $V(r_1,r_2) = k_{rr}(r_1-r_1^g)(r_2-r_2^g)$

Bond Types	k_{rr}	r_1^g	r_2^g
C-H, C-H	-0.28	1.1068	1.1068

[a] All units are such that energies are in units of mdyne-Å, angles in radians, and distances in Angstrom units.

[b] (Same as for Table II).

Table A2. Experimental and Calculated Normal Mode Frequencies of Methane.[a]

Experimental[b]	Calculated	Description
3020	3019	F_2 C-H stretch
2914	2890	A_1 C-H stretch
1526	1462	E H-C-H bend
1306	1446	F_2 H-C-H bend

[a] All frequencies in units of cm^{-1}.

[b] G. Herzberg, Infrared and Raman Spectra of Polyatomic Molecules, 1945, p. 306.

Table A3. Experimental and Calculated Normal Mode Frequencies of Ethane.[a]

Experimental[b]	Calculated	Description
2974	3004	E_u C-H stretch
2950	2988	E_g C-H stretch
2915	2917	A_{1g} C-H stretch
2915	2899	A_{2u} C-H stretch
1370	1524	A_{2u} HCC bend
1388	1471	A_{1g} HCC bend
1469	1429	E_g HCH bend
1460	1428	E_u HCH bend
1190	1110	E_g HCC bend
995	1002	A_{1g} C-C stretch
822	952	E_u HCC bend
279	332	A_{1u} torsion

[a] All frequencies in units of cm^{-1}.

[b] Reference 9.

auence of the neglect of a "bond flexibility" interaction ($k_{\psi\psi'} - k_{\psi\psi'\beta}$ in the notation of part I). The calculated torsional frequency is high, for reasons which are outlined below. An energy difference of 3.0 kcal/mol between eclipsed and staggered ethane was assumed, which is quite close to the experimental barrier height of 2.93 kcal/mol,[35] which was determined from torsional frequencies. However, the value of the barrier height used in MUB-2' was determined by the energy difference between relaxed staggered ethane and relaxed eclipsed ethane, whereas any normal coordinate calculation in effect uses the difference between relaxed staggered ethane and unrelaxed eclipsed ethane as the barrier height. There is some indication from ab initio calculations that the relaxation energy is around 0.6 kcal/mol,[13,36] while MUB-2' calculations make the difference 0.46 kcal/mol. An increase in the barrier height of this magnitude produces a large part of the calculated-observed torsional frequency difference.

The force constants and reference lengths used in MUB-2' are listed in Table A1. The observed and calculated methane and ethane normal mode frequencies are compared in Tables A2 and A3. Some portions of the spectra are in good agreement, while others point out deficiencies in the force field.

MUB-2' was used to recalculate the energy differences between gauche and trans n-butane and axial and equatorial methylcyclohexane. As expected, the differences between

the rotational isomerization energies calculated using MUB-2 and MUB-2' were small: MUB-2 yielded 0.540 kcal/mol for the vibrationless gauche-trans n-butane energy difference, while MUB-2' gave 0.482 kcal/mol for the same quantity. The vibrationless axial-equatorial methylcyclohexane energy difference was calculated to be 0.954 kcal/mol using MUB-2, and 0.932 kcal/mol using MUB-2'. Vibrational corrections were also made. Boyd[1d] has pointed out that good values of thermodynamic functions may be calculated from computed vibrational spectra which have the correct centers of gravity for groups of frequencies but which may not show the proper splittings. Because frequencies computed using MUB-2' meet this criterion for the most part, the differences between thermodynamic quantities calculated using MUB-2' may be assumed to be significant. The vibrational corrections alluded to here are the sums of the differences in the zero-point energies and in the quantities $(\Delta H^{\circ}_{298} - \Delta H^{\circ}_{0})$. These vibrational contributions raised the gauche-trans energy difference for n-butane to 0.50 kcal/mol and the axial-equatorial energy difference for methylcyclohexane to 0.98 kcal/mol.

As was expected, differences between the structures calculated using MUB-2 and MUB-2' were minimal. The largest structural parameter differences observed were 0.001 Å for bond lengths and 0.1° for bond angles.

MUB-2' was used to calculate a series of zero-point energy differences, which are compared with the experi-

mental values in Table A4. Though the zero-point energies calculated using MUB-2' are systematically high, due to deficiencies in the model force field, the agreement of the computed with the experimental zero-point energy differences is semiquantitative.

It is to be hoped that MUB-2' will provide further insights into features which will improve future MUB force fields.

Table A4. Computed and Experimental Zero-Point Energy Differences.[a]

	Experimental[b]	Computed
n-butane	0.0•••	0.0•••
isobutane	0.24	0.24
n-pentane	0.0•••	0.0•••
isopentane	0.71	0.21
neopentane	1.02	0.72
n-hexane	0.0•••	0.0•••
2,2 dimethylbutane	0.83	0.63

[a] All energy differences are in kcal/mol, and represent the differences between the energies of the n-alkane and the isomer.

[b] The experimental zero-point energies from which the differences were obtained are listed in Table IV.

III. GAS-PHASE ELECTRON DIFFRACTION DETERMINATIONS OF THE STRUCTURES OF n-ALKANES: n-BUTANE AND n-HEXADECANE

A. Determination of the Structure of n-Butane

1. Introduction

This study was done primarily to acquaint the researcher with the procedures for determining molecular structures from electron diffraction data. n-Butane is the smallest n-alkane to exhibit gauche-trans rotational isomerism, and as such could serve as a prototype for the n-hexadecane structural determination, which is detailed in part B of this section. Many of the principles learned during the course of the n-butane study were carried over into the n-hexadecane study.

The experimental data of W. F. Bradford[1] were used. An earlier structural refinement processing these data[2] with a more or less automated computer procedure gave the value of the gauche dihedral angle as 54° and the value of the trans fraction as 40%. Though the associated uncertainties are fairly large, these results are somewhat disturbing, for they depart from the results of previous studies.[3,4] Chemical intuition suggests that the value of the gauche dihedral angle should be slightly larger than 60° (at which value the energy contribution from hindered internal rotation is generally considered to be at a minimum) in order to relieve the repulsive energy of the Me...Me interaction. The 40% value for the trans fraction,

under the conditions of the experiment,[2] suggests a value for ΔG° (gauche-trans) of 160 cal/mol, as compared with the other measured values of ΔG° for n-butane[3,4] and other n-alkanes,[6] all of which are around 600 cal/mol. Both the gauche dihedral angle and the trans fraction are parameters which can be dependent upon the way in which the intensity data are analyzed. Certain systematic discrepancies between the calculated and observed intensities were possible factors in producing the above anomalies. It was deemed desirable to see if a second analysis of the diffraction data which relied more upon operator judgement and less upon preprogrammed procedures for data analysis would yield the same results as the first.

2. Experimental

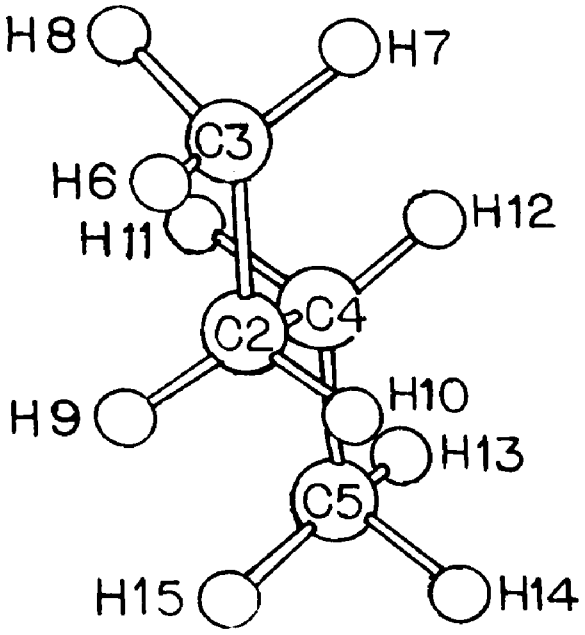
The recording of the diffraction patterns and preliminary analysis of the data are described in reference 2. The analysis described below used the three different sets of interpolated (to integral q values) experimental levelled intensities obtained by Bradford.[1]

3. Analysis of Data

a. Molecular Model Used

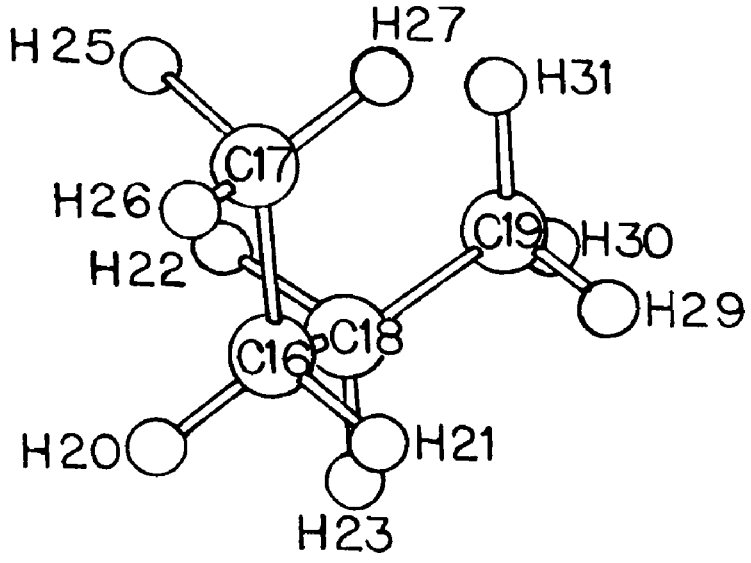
Bradford's model for n-butane was not used. A new model which consisted of a complete trans and a complete gauche isomer was devised. C_{2h} and C_2 symmetries were maintained for the trans and gauche isomers, respectively. The molecular model used is shown in Figure 1.

Figure 1. Molecular Model Used for n-Butane.



TRANS

ISOMER



GAUCHE

ISOMER

Figure 1.

All C-C bond distances and CCC bond angles were assumed to be equivalent, as were all C-H bonded distances. All HCC angles were not constrained to be equivalent: the model used gave two distinct geminal C...H distances, 4...9 and 3...9, but the values of the HCC angle which these implied differed by only a few tenths of a degree. Only one value of the HCC angle was refined. This gave four independent parameters. The gauche dihedral angle was the fifth. Following Bradford's experience,[2] which suggested that the value of the twist angle of the gauche methyl group could not be determined from the intensity data with any precision, the twist angle was not varied but was set at -2.5°, which value was suggested by MUB-2 calculations. Five amplitudes were allowed to vary: these were the bonded C-H and C-C, the geminal C...H and C...C, and the 1...4 gauche C...C. The earlier investigation had shown that the 1...4 trans and gauche amplitudes tended to be highly correlated with the trans fraction, so the 1...4 trans C...C amplitude was fixed, as were all others not mentioned above. The values of the fixed amplitudes and the shrinkages used for the various distances are given in Table I. The asymmetry constants for all internuclear distances were set equal to 2.0 A^{-1}.

The trans fraction was determined from information gained by minimizing a number of different structures with different values of the trans fraction, as described below.

b. Processing of the Intensity Data

The data consisted of a set of reduced molecular intensities, interpolated to integral q ($q = 10s/\pi$), for each of the three camera distances. Initially, the different data sets were treated separately. The two r^3 data sets were subjected to least squares analyses to derive computer-fitted backgrounds and obtain preliminary indications of the best value of the trans fraction. The computer backgrounds and the derived structural parameters were used to compute correlation backgrounds for both data sets. New backgrounds were then drawn by hand, using the criteria that a background should be smooth and should "split" the correlation background as evenly as possible. Least squares analyses were done on the data sets using the new backgrounds, and, using the indices of resolution [$R = M^{exp}(s)/M^{calc}(s)$] so determined, the r^3 data were blended, yielding a smooth molecular intensity function over the range s = 3.14 to s = 39.58 (q = 10 to q = 126). A set of structural parameters was derived from the blended intensities. The r^2 intensity data were subjected to least squares analysis with the structural parameters fixed at the values derived from the blended r^3 data so that a computer fitted background could be derived. A correlation background was computed for the r^2 data, and a new background was hand-drawn through the data, using the same criteria described earlier. A least squares analysis of the r^2 data was done, using the new background

with the structural parameters fixed at the values obtained from the blended r^3 data, in order to derive the index of resolution for use in the blending. All of the data were then blended, with care taken to ensure that the intensity data from the different camera distances joined smoothly. The resulting molecular intensity function ranged from s = 2.51 to s = 39.58 (q = 8 to q = 126). A set of structural parameters was derived from the blended data. The parameters were used to compute new correlation backgrounds, and new hand backgrounds were drawn for all data sets. The new indices of resolution were obtained, and the data were reblended, with the smoothness of the joins of intensity data from different sets having improved. The indices of resolution for the 21-cm r^2 and the 21- and 11-cm r^3 data were 0.737, 0.861, and 0.964, respectively.

The early analyses of the individual data sets done in the course of this research had indicated that the best value of the trans fraction was between 50 and 60%. Therefore, the trans fraction was set to either 50 or 60% throughout the derivation of the individual backgrounds and the determination of the indices of resolution which were used in the blending process.

Weighting proportional to s^2 was used throughout the process of background refinement and data blending. As was true of Bradford's analysis, the optimal weighting appeared to be between s and s^2, but the s-weighted residuals appeared to be more uniformly distributed than did the

$s^{1/2}$-weighted residuals, so s^2 weighting was used throughout the initial treatment of the data. It is expected that an analysis using s weighting would be more sensitive to the values of the trans fraction and the gauche dihedral angle, for most of the information about these two parameters is contained in the intensity at small s values. Hence, an s-weighted as well as an s^2-weighted analysis of the blended intensity data was performed. Results of the different least squares analyses are discussed below.

A succession of least squares analyses of the blended intensity data was performed with different values of the trans fraction. The value of the fraction had only a minor influence on the values obtained for the independent parameters. The parameters which exhibited the greatest dependence upon the trans fraction value were the gauche dihedral angle and the gauche 1...4 C...C nonbonded amplitude, but the variations of these parameters with the trans fraction were of the same order as σ for each parameter and so cannot be considered to be significant. The values obtained for $\sigma(I)$ were, of course, dependent upon the trans fraction, and this dependence was taken as the criterion for determining the best value of the trans fraction. The $\sigma(I)/\langle I \rangle$ were plotted versus the trans fraction values, and a parabola was fitted to the points. The value of the trans fraction at the vertex of the parabola was taken as the best value.

The best value of the trans fraction was obtained for

both the s- and s^2-weighted least squares analyses done using the molecular model described above. In addition, the best value of the trans fraction was determined for a slight variant of the molecular model. This model varied from the one described earlier only in that the CCC angle in the gauche isomer was fixed to be greater than the trans CCC angle by a constant increment. The value of the increment was set equal to the MUB-2 prediction of the difference between the gauche and trans n-butane CCC angles, which was 1.5°. A series of s^2-weighted least squares analyses of the blended intensity data was performed with the molecular model variant described above. The change from the original model produced only insignificant changes in the values obtained for the other independent parameters.

4. Results

The values determined for the independent parameters and the estimated uncertainties in the derived values are shown in Table II. The correlation matrix for the independent parameters is tabulated in Table III. Figure 2 shows the weighted blended molecular intensity curve. The radial distribution function is shown in Figure 3. The molecular model used for the determination of the values given in Tables II and III and the figures shown was the model without any differentiation of CCC angles. Weighting proportional to s^2 was used, and the

Table I. Distances, Amplitudes, and Shrinkages Adopted for the n-Butane Structure Determination

Atom #1	Atom #2	Amplitude	Shrinkage
2	4	a	0.
4	3	a	0.0073
19	17	a	0.0137
3	5	0.0722	0.0265
10	2	a	0.
12	2	a	0.0105
9	4	a	0.0059
27	19	0.33	-0.0194
25	18	0.18	0.0099
9	5	0.14	0.0070
21	19	0.10	0.0070
14	2	0.15	0.0099
31	16	0.17	0.0099
25	19	0.33	0.0300
20	19	0.18	0.0283
26	18	0.10	0.0366
6	4	0.10	0.0298
26	19	0.19	0.0458
8	5	0.18	0.0352
13	3	0.12	0.0469
11	12	0.13	0.0065
13	14	0.13	0.0029
20	26	0.18	0.0065
27	31	0.34	-0.1029
11	13	0.18	0.0065
20	22	0.18	0.0017
21	26	0.18	0.0149
21	27	0.13	0.0090
8	9	0.13	0.0059
20	25	0.13	0.0064
21	22	0.18	0.0008
23	25	0.28	-0.0244
10	15	0.22	-0.0291
27	29	0.47	-0.0033
20	27	0.19	0.0308
11	15	0.18	0.0203
21	25	0.19	0.0285
10	11	0.18	0.0289
9	15	0.22	0.0203
23	27	0.13	0.0308
20	29	0.27	0.0375
27	30	0.29	0.0375
21	30	0.14	0.0375
22	27	0.19	0.0375
25	29	0.42	0.0600
25	30	0.35	0.0356

Table I continued.

Atom #1	Atom #2	Amplitude	Shrinkage
22	26	0.14	0.0356
6	11	0.19	0.0375
8	14	0.20	0.0356
8	15	0.28	0.0654
8	13	0.23	0.0480
6	13	0.14	0.0779

[a] Value determined from structure analysis. See Table II.

Table II. Values of the Independent Parameters for n-Butane (q^2 weighting, trans fraction = 55%)

Parameter	Value	3σ
C-C length	1.531 Å	0.001
C-H length	1.117 Å	0.003
HCC angle	111.0°	0.5
CCC angle	113.8°	0.4
gauche CCCC torsion	64.9°	2.9
C-C bonded amplitude	0.0531 (0.051)[a]	0.0015
C-H bonded amplitude	0.0805 (0.079)[a]	0.0028
1...3 C...C amplitude	0.0700 (0.071)[a]	0.0040
1...3 C...H amplitude	0.1088 (0.109)[a]	0.0054
1...4 C...C (gauche)	0.1214 (0.172)[a]	0.0053

The 1...4 C...C trans amplitude was fixed at 0.0722, the value obtained from Bradford's normal coordinate study of n-butane.

[a] Values in parentheses are from Bradford's normal coordinate study of n-butane.

Table III. Correlation Matrix (zero-order) for the Independent Parameters (n-butane, q^2 weighting, trans fraction = 55%)

	1	2	3	4	5	6
1	1					
2	0.05	1				
3	-0.20	-0.31	1			
4	-0.39	-0.01	0.16	1		
5	0.03	0.05	-0.22	0.14	1	
6	0.07	0.13	-0.11	0.0001	0.05	1
7	0.05	0.16	-0.11	0.004	0.05	0.37
8	0.03	0.06	-0.15	-0.02	0.08	0.17
9	0.002	0.03	0.05	0.16	0.03	0.20
10	-0.01	0.002	0.05	0.01	-0.12	-0.01
11	0.07	0.20	-0.16	0.01	0.08	0.68

	7	8	9	10	11
7	1				
8	0.14	1			
9	0.16	0.004	1		
10	-0.01	-0.02	-0.0006	1	
11	0.55	0.25	0.30	-0.01	1

The order of the parameters is

1. r_g(CC)
2. r_g(CH)
3. $\angle$HCC
4. $\angle$CCC
5. τ(CCCC)
6. ℓ_α(CC)
7. ℓ_α(CH)
8. ℓ_α(1,3 C...C)
9. ℓ_α(1,3 C...H)
10. ℓ_α[1,4C...C(G)]
11. R

The zero-order standard deviations of the parameters are

1. 4.3×10^{-4}
2. 9.3×10^{-4}
3. 1.7×10^{-1}
4. 1.3×10^{-1}
5. 9.7×10^{-1}
6. 4.9×10^{-4}
7. 9.3×10^{-4}
8. 1.4×10^{-3}
9. 1.8×10^{-3}
10. 1.8×10^{-2}
11. 9.3×10^{-3}

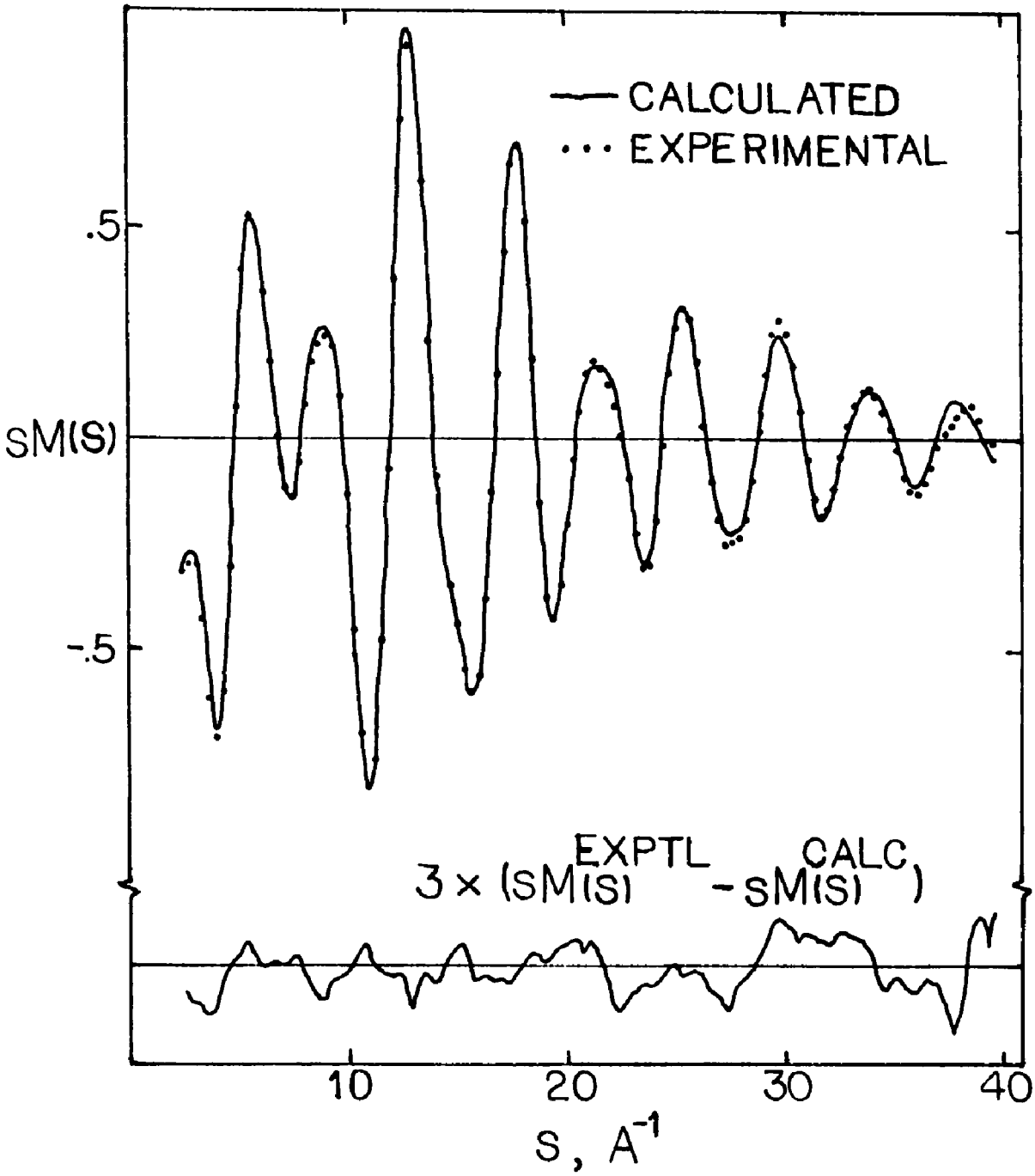


Figure 2. Experimental and Calculated Molecular Intensity Functions for n-Butane.

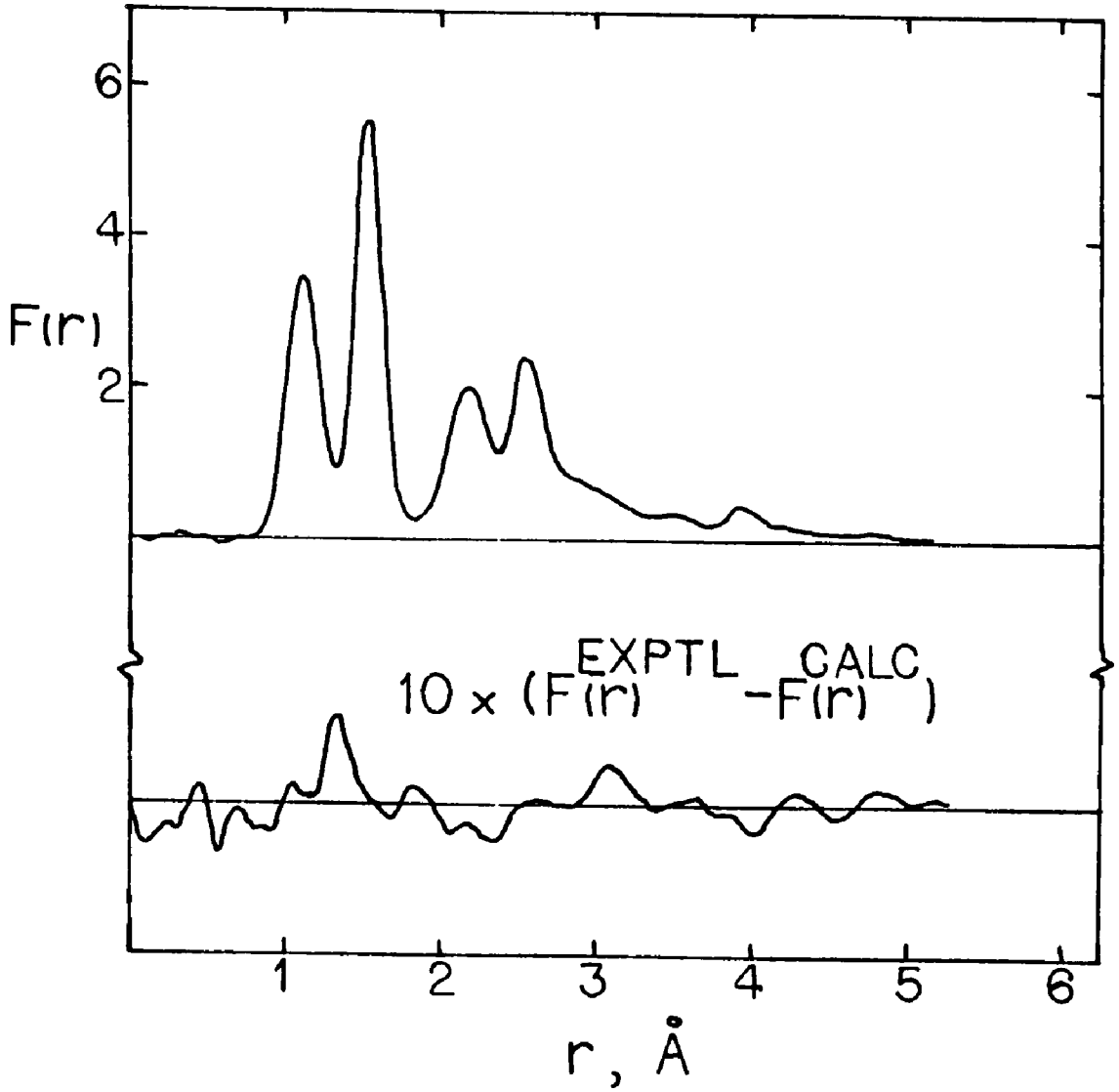


Figure 3. Experimental Radial Distribution Function for n-Butane.

trans fraction assumed was 55% (60% for the radial distribution curve).

A plot of the various values of $\sigma(I)/\langle I\rangle$ obtained from the s-weighted least squares analyses versus per cent trans is shown in Figure 4. The parabola which was fitted to the points is also shown. The vertex of the parabola is at 53.5%. Values of the trans fraction yielded by the two sets of s^2-weighted analyses were 57.0% (model without CCC angle differentiation) and 60.7% (model with CCC angle differentiation). The uncertainty in the optimum trans fraction arising from the fit of the parabolae to the $\sigma(I)/\langle I\rangle$ points was minimal (less than 0.5%) for the 53.5% and 57.0% values but was ± 4% for the 60.7% value. As will be discussed below, the value for the trans fraction was taken to be ($\pm\sigma$) 55 ± 5%.

5. Discussion

The values obtained for the structural parameters are in the range which one would expect based on other structural studies of n-alkanes.[5] The C-C bond length seems a bit short, but the difference between the value determined here and the average value of a C-C bond length in n-alkanes given in reference 5 is not significant. The gauche dihedral angle has opened out to more than 60°, in accordance with the rather simple model of hindered internal rotation given in the Introduction. The n-butane structure determined during the course of this research is

Figure 4. Standard Deviation of the Intensity as a Function of the trans Fraction for n-Butane.

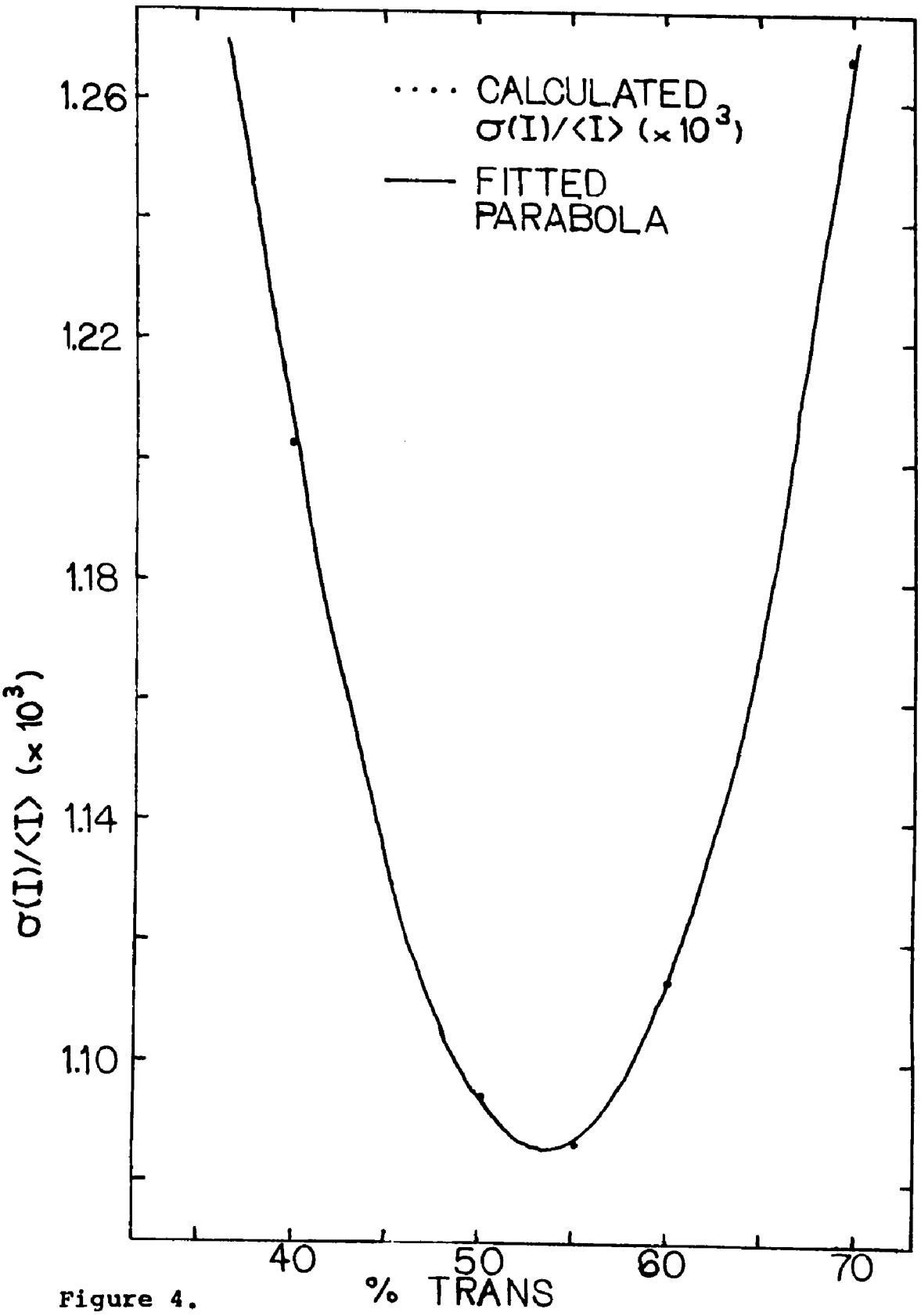

.... CALCULATED σ(I)/<I> (× 10³)
—— FITTED PARABOLA
1.26
1.22
1.18
1.14
1.10
σ(I)/<I> (× 10³)
40
50
60
70
% TRANS

Figure 4.

in fairly good agreement with one determined a number of years ago.[3]

The fact that three different values of the trans fraction were determined from the three sets of least squares analyses is not a cause for concern, for the difference between the values obtained is not statistically significant. One fact which must be remembered in assessing the different trans fraction values is that the derivation of the backgrounds and the blending of the intensity data were done using the model without CCC angle differentiation and with s^2 weighting. As is discussed below, the backgrounds used and the way in which the intensity data are blended can affect the values derived for the gauche dihedral angle and the trans fraction. Therefore, some uncertainty in the best value of the fraction arises from whatever bias the background derivation and blending processes place on the final molecular intensity function determined from the experimental data. However, the preliminary least squares analyses of the separate data sets gave values for the gauche dihedral angle and the trans fraction which were close to the final values obtained. The small differences between the values obtained for the trans fraction from the three sets of least squares analyses may be due to slight biases in the molecular intensity function.

The choice of 55% for the trans fraction represents a compromise among the different values obtained. Both sets

of s^2-weighted analyses yielded rather shallow parabolae, and the fit of the parabola to the $\sigma(I)/\langle I\rangle$ points for the differentiated CCC angle model was not good. The s-weighted analyses gave a deeper parabola, and, as is discussed above, it is expected that s-weighted analyses will be more sensitive to the value chosen for the trans fraction than will s^2-weighted analyses. However, s^2 weighting gave a more even distribution of weighted residuals than did s weighting, and, as noted above, s^2 weighting was used in the derivation of the blended molecular intensity function. The value of 55% adopted for the trans fraction is an average of the s- and s^2-weighted undifferentiated CCC angle model values. The ± 5% uncertainty was obtained from the $\sigma(I)/\langle I\rangle$ versus per cent trans curve for the s-weighted analyses as follows. The standard deviation σ_ℓ of a given parameter θ_ℓ may be found from

$$\sigma_I(\hat{\theta}_\ell + \sigma_\ell) = \sigma_I(\hat{\theta}_\ell)\{1 + [B_{\ell\ell}(B^{-1})_{\ell\ell}/(n-m)]\}, \qquad (1)$$

where $\sigma_I(\hat{\theta}_\ell)$ is the minimum value of the standard deviation of the intensity, $\sigma_I(\hat{\theta}_\ell + \sigma_\ell)$ is the standard deviation of the intensity when parameter θ_ℓ has been displaced from its least squares value $\hat{\theta}_\ell$ by one standard deviation, n is the number of intensity points, m is the number of independent parameters which are derived from the data, and B is equal to A'WA, where A is the design matrix and W is the weight matrix. Of course, the method of analysis used did not provide values of $B_{\ell\ell}$ and $(B^{-1})_{\ell\ell}$ for the trans fraction

parameter, but work in this area[7] suggests that a plausible value for $B_{\ell\ell}(B^{-1})_{\ell\ell}$, in the absence of a firmer estimate, is three. Hence, three was used for $B_{\ell\ell}(B^{-1})_{\ell\ell}$ in equation (1) above, and the value of $\sigma_I(\hat{\theta}_\ell + \sigma_\ell)$ obtained indicated that the estimated standard deviation for the trans fraction is ± 5%. A 55% trans, 45% gauche model implies a gauche-trans free energy different ($\Delta G°$) of 510 cal/mol, slightly lower than the previous estimate of 630 cal/mol,[3] but well within the uncertainty in the value. The uncertainty in $\Delta G°$ implied by the ± 5% uncertainty in the value of the trans fraction is ± 110 cal/mol. However, the value of $\Delta G°$ is dependent upon the temperature of the sample when it encounters the electron beam, which cannot be measured. Therefore, a more realistic estimate of the standard deviation of $\Delta G°$ is probably ± 130 cal/mol.

The results of the structural analysis discussed here depart from those of Bradford only for the gauche dihedral angle and the trans fraction. The values for these two parameters reported here are within 3σ of Bradford's values, and so the differences between them should not be considered to be significant. Both studies determined a value of 0.86 ppt for the minimum $\sigma(I)/\langle I\rangle$ when s^2 weighting was used. When s weighting was used, the minimum $\sigma(I)/\langle I\rangle$ determined in the course of the present study was slightly lower than that found by Bradford. It may be noted that the range of Bradford's molecular intensity function was s = 3.14 to s = 39.58 (q = 10 to q = 126), while the range of the

molecular intensity function used in this analysis was $s = 2.51$ to $s = 39.58$ ($q = 8$ to $q = 126$). The systematic discrepancies between the calculated and observed intensities corresponding to the 3.9 A distance in Bradford's study have been appreciably reduced in the present analysis. It is possible that the parameters derived by this analysis provide a "better" representation of the intensity data than do Bradford's, though the statistical criteria for judging "goodness of fit" do not suggest substantial differences between the two studies. A comparison of the results of the two studies does show that the values obtained for the gauche dihedral angle and the trans fraction depend upon the backgrounds and the way in which the separate intensity data sets are blended.

B. Determination of the Structure of n-Hexadecane

1. Introduction

n-Hexadecane is a straight-chain alkane, $C_{16}H_{34}$. The structures of a number of simpler straight-chain alkanes, n-butane, n-pentane, n-hexane, and n-heptane, have been determined using electron diffraction methods.[3-5] The values determined for the C-C bond length and the gauche-trans free energy difference[6] were the same (to within experimental error) for all of the n-alkanes named above. However, n-hexadecane is much larger than any n-alkane whose structure has been investigated by gas-

phase electron diffraction methods previously, and it is possible that the uniformity of C-C bond lengths and gauche-trans free energy differences displayed by the smaller n-alkanes may not extend to such a large molecule. Given the number of conformations which, in theory, n-hexadecane may assume, it is possible that interactions which are separated by a large number of atoms (1...7, 1...8, etc.) and whose effects upon molecular structure are generally considered to be negligible may correspond to fairly short interatomic distances and thus may have an appreciable influence upon the structure after all. Alternatively, widely separated atoms may influence each other indirectly through a series of short-range interactions. Differences between the n-hexadecane structural parameters and those of the smaller n-alkanes may provide information about the effects of so-called long-range interactions on molecular structure.

n-Hexadecane is also of interest in that it may be considered to be a "mini-polymer" having a chemical composition homologous to that of polymethylene. Therefore, it may be possible to use the derived n-hexadecane structural parameters to gain some information about the conformation of polymethylene. The characteristic ratio, which may be considered to be a measure of the extension of a polymer, may be calculated using information from the n-hexadecane structure determination and information calculated using MUB-2. Results of such calculations will be reported and

discussed below.

2. Experimental

A sample of n-hexadecane with a stated purity of 99 mole percent was obtained from Aldrich Chemical Company and was used without further purification. The sample was transferred to a heated nozzle similar to one described in the literature[8] and the air introduced during the loading process was pumped off. The nozzle was heated to 150° C to provide a sample temperature of 15 torr. Data were obtained at the 21-, 11-, and 7-cm camera distances through a radius cubed (r^3) sector and at the 21-cm camera distance through a radius squared (r^2) sector. Experimental conditions are summarized in Table IV. The diffraction patterns were recorded on 4 x 5 in Kodak electron image plates. The plates were developed in Kodak HRP developer (diluted 1:4 with 3.8 gm/gal benzotriazole added) for five minutes at 68° F with agitation provided by a one-second burst of nitrogen every six seconds. Voltages proportional to the light transmitted through the diffraction pattern were measured at 0.125 mm intervals across the full diameter of the plate with a modified Sinclair Smith recording microphotometer. The plates were spun at an integral number of revolutions per reading (3 Hz) to average over grain irregularities in the emulsions. The unusable center voltages from each plate were discarded and the remaining voltage values from the two halves of the plate were averaged.

Table IV. Experimental Conditions Under Which Diffraction Patterns of n-Hexadecane were Recorded

	I	II	III	IV
Camera Distance (cm)	21.538	21.550	10.472	6.035
Sector (radius, cm)	r^2, 3.2	r^3, 4.8	r^3, 4.8	r^3, 4.8
Sample temp (°C)	150	150	150	150
Sample pressure (torr)	15	15	15	15
Exposure time (sec)	1.5	9	40	90
Beam Currents (μA)	0.700	0.728	0.700	impossible to measure
Nozzle throat dia. (cm)	0.041	0.041	0.041	0.041
Nozzle lip to beam dist (cm)	0.100	0.18	0.17	0.18
Electron Wavelength (Å)	0.06015	0.06015	0.06015	0.06015
Number of plates	5	5	5	4

3. Analysis of Data

a. Determination of Molecular Intensities

The averaged voltage values were converted to absorbances using the relation

$$A = -\log_{10}[(V - V_0)/(V_{100} - V_0)], \qquad (2)$$

where V is the measured voltage, V_{100} is the voltage corresponding to the intensity transmitted through a clear portion of the plate, and V_0 is the voltage when no light is transmitted through the plate. The absorbances were then converted to relative intensities, E, by[2]

$$E = A(1 + 0.116A + 0.017A^2 + 0.00312A^3). \qquad (3)$$

Five apparently flawless plates were selected from those taken at the 21- and 11-cm camera distances. Four plates were selected from those taken at the 7-cm camera distance. The intensity values for each group of plates were averaged together. The resulting data set for each camera distance was interpolated to integral q values [$q = 40/\pi\sin(\theta/2)$] using a five-point-five-term Lagrangian scheme.

The experimental levelled intensities were obtained by dividing the experimental intensity values for each camera distance by the theoretical atomic intensity function. This function was determined using the partial wave elastic and inelastic scattering factors of Schafer, Yates, and Bonham.[9]

b. Molecular Model Used

n-Hexadecane is such a large molecule that a number of simplifications must be made in formulating a model which is simple enough to be used in the analysis of the intensity data. The n-hexadecane model may be considered analogous to the model used for n-butane in that it is assumed that both trans and gauche sites occur in the molecule. However, the n-hexadecane problem is complicated by the fact that the rotational configuration of a series of bonds must be considered when the molecular description is devised. For instance, two adjacent carbon-carbon bonds in the interior of an alkane chain may show a trans-trans, trans-gauche, or gauche-gauche configuration. Three interior carbon-carbon bonds in a row may exhibit any of seventeen rotational configurations, and so on. Theoretically, n-hexadecane can exist in well over a million different conformations. Then, of course, a given gauche dihedral angle will have a value which depends upon the conformation of the nearby groups, as will the trans. The lengths of the C-C and C-H bonds, as well as the values of the CCC and HCC angles, may be expected to take on slightly different values in different parts of the molecule. Therefore, there are two problems which must be made manageable when formulating a model for n-hexadecane: the proliferation of independent parameters, and the huge number of nonbonded distances which arise from the large number of conformations accessible to the molecule.

The first problem is more easily dealt with than the second. The differences in individual bond lengths and angles are not such that they can be determined from the electron diffraction intensity data, so a single parameter was adopted to represent each of the bond angles and lengths. Some preliminary work showed that the use of a large number of gauche dihedral angle parameters in the molecular description led to dihedral angle values which were extremely unstable. Therefore, one independent parameter was used to describe all gauche dihedral angles. All trans angles were fixed at 180° (shrinkage corrections were made). All methylene groups were assumed to possess local C_{2v} symmetry. It was further assumed that the energy of a configuration containing a multiple number x of gauche sites was equal to x times the energy of a single gauche site (i.e., $E_{GG} = 2E_G$, etc.). These approximations reduced the problem to the determination of two bond lengths, two bond angles, one dihedral angle, and the ratio of gauche to trans sites.

Obviously, if the n-hexadecane problem is to be tractable, all possible atom-atom distances cannot be considered. Fortunately, many possible distances are long and broad in distribution and therefore make only minor contributions to the intensity. These may be dropped from consideration. For C...C, no distance from any interaction greater than 1...7 was considered. Since the shortest 1...7 C...C distance was 5.3 A and had a low multiplicity and a large

amplitude of vibration, it seems justified to neglect distances further than 1...7. No distance from any C...H or H...H interaction farther than 1...5 was considered. Though $\sigma(I)$ would have been improved if distances arising from longer-range interactions had been considered, the improvement would have been small, judging from observations made during the course of the analysis, and of marginal benefit. The distances which were considered permitted the structural parameters of the molecule to be determined with a reasonably high precision. A model which allowed the explicit specification of all C...C distances through 1...7 and all C...H and H...H distances through 1...5 was devised. Multiplicities (the number of times an interatomic distance of a given type occurs in the molecular model assumed) of the C...C distances were obtained from assumed values of $\Delta G°$ (gauche-trans) as follows. The multiplicities of the various 1...7 distances were determined from the ratio of gauche-containing conformations to the all-trans conformation, which is dependent upon $\Delta G°$ according to the relationship.

$$\% \text{ gauche cont.}/\% \text{ all-trans} = M \exp(-n\Delta G°/RT), \quad (4)$$

where M is the number of ways in which a given gauche-containing configuration may occur in a chain (for example, the conformation TGTG may occur in eight different ways) and n is the number of gauche sites which that configuration contains. No gauche^+-gauche^- sites were considered

to occur; models show that this configuration is badly sterically hindered, and MUB-2 calculations on n-nonane indicate that a gauche$^+$-gauche$^-$ conformation lies 3 kcal above a gauche$^+$-gauche$^+$ conformation. The M values used in equation (4) for the various 1...7 distances were the multiplicities of the various heptane conformations given in reference 6. Due to the disallowance of the gauche$^+$-gauche$^-$ conformation, it was expedient to determine the multiplicities of the 1...6, 1...5, and 1...4 C...C distances from the percentages of the various 1...7 configurations rather than from the percentages of each configuration computed from equation (4), since the value of M for a certain local configuration is dependent upon the larger configuration in which the local one is situated. The C...H and H...H distance multiplicities were computed using the multiplicities of the various rotational configurations. A total of fifty-four distances was considered by the final model.

The molecular model described above may be objected to on the grounds that the exclusion of gauche$^+$-gauche$^-$ conformations means that determining the multiplicities of the 1...7 C...C distances from equation (4) is invalid. Strictly speaking, this is true: a rigorous model would have all C...C distances reckoned from the multiplicities of the 1...16 C...C configurations, which would be computed using equation (4). Needless to say, implementing such a model would be highly impractical. It is estimated that

the method of calculating the various C...C distance multiplicities which was actually used imparts an error of less than 3% in the value of the gauche fraction which is associated with a given value of ΔG°. As will be shown below, this is less than the uncertainty in the value determined for the gauche fraction. The assumption that the energy of a gauche conformation is site-independent (which MUB-2 calculations indicate is not the case) probably introduces at least as large an error into the C...C distance multiplicities as does the approximate method of calculating them which was described above.

The amplitudes of all of the distances could not be varied simultaneously. The bonded C-C, C-H amplitudes, the 1...3 C...C and C...H amplitudes, and the 1...4 gauche C...C amplitude were considered to be independent parameters which were varied along with the previously specified independent structural parameters. Seven other amplitudes were specified: 1...4 trans C...C, 1...5 and greater C...C, 1...4 and 1...5 C...H, and 1...3, 1...4, and 1...5 H...H. These amplitude parameters were not varied along with the independent parameters, but were intended to be minimum values for the amplitudes of the individual distances. A constant to be added to the minimum value parameter was specified for each distance. The first set of these constants which was used was derived from the amplitude differences used for analogous n-butane distances, while the second set used was derived from Mastryukov's

Table V. Distances, Shrinkages, and Additive Amplitude Constants Adopted for n-Hexadecane

	Distance	Shrinkage	Amplitude Constant [a]
	C-C bonded (1.541)	0.	0.
	C...C geminal (2.59)	0.0073[b]	0.
	C...C gauche (3.27)	0.0137[b]	0.
	C...C trans (3.98)	0.0400[c]	0.
	C...C TT (5.19)	0.0470[d]	0.04
	C...C GT (4.66)	0.0400[d]	0.06
	C...C GG (4.15)	0.0265[d]	0.08
	C...C TTT (6.54)	0.0610[d]	0.10
	C...C TTG (5.69)	0.0520[d]	0.08
	C...C GGT (5.29)	0.0470[d]	0.14
	C...C GTG(I) (5.03)	0.0450[d]	0.10
	C...C GTG(II) (5.69)	0.0450[d]	0.10
	C...C TGT (6.13)	0.0560[d]	0.12
	C...C GGG (5.34)	0.0470[d]	0.14
	C...C TTTT (7.78)	0.0750[d]	0.15
	C...C TTTG (7.09)	0.0670[d]	0.15
	C...C TTGT (7.09)	0.0670[d]	0.15
	C...C TTGG (6.43)	0.0580[d]	0.15
	C...C GTTG(I) (6.37)	0.0520[d]	0.14
	C...C GTTG(II) (5.79)	0.0520[d]	0.14
	C...C TGTG (6.57)	0.0610[d]	0.15
	C...C TGGT (6.37)	0.0520[d]	0.14
	C...C TGGG (6.47)	0.0470[d]	0.14
	C...C GTGG (5.23)	0.0580[d]	0.18
	C...C GGGG (6.41)	0.0470[d]	0.16
	C-H bonded (1.13)	0.	0.
	C...H geminal (2.21)	0.0059[b]	0.
	C...H 1...4 trans (2.83)	0.0100[e]	0.
(2.83)	C...H 1...4 gauche(1)	0.0100[e]	0.
(2.82)	C...H 1...4 gauche(2)	0.0100[e]	0.
(3.55)	C...H 1...4 gauche(3)	-0.0194[b]	0.12
	C...H 1...4 methyl (3.53)	0.0325[e]	0.01
(4.28)	C...H 1...5 TTT, GTT	0.0400[e]	0.14
(4.28)	C...H 1...5 TTG, GTG	0.0400[e]	0.14
(4.78)	C...H 1...5 TTG, GTG	0.0325[e]	0.15
	C...H 1...5 TGT (2.93)	0.0325[e]	0.06
	C...H 1...5 TGT (3.63)	0.0325[e]	0.08
(4.14)	C...H 1...5 GGT, GGG	0.0325[e]	0.09
(2.93)	C...H 1...5 GGT, GGG	0.0325[e]	0.06
	C...H 1...5 GGT (3.63)	0.0325[e]	0.08
	C...H 1...5 GGT (2.93)	0.0325[e]	0.06
(4.24)	C...H 1...5 methyl G	0.0400[e]	0.095
(4.76)	C...H 1...5 methyl T	0.0470[e]	0.15
	H...H geminal (1.73)	0.0065[b]	0.

Table V continued.

All H...H amplitude constants were zero. The value of 0.0070 was used for all 1...4 H...H shrinkages, while 0.0200 was used for all 1...5 H...H shrinkages.

[a] The Mastrukov amplitude constants are listed.

[b] These shrinkages were taken from Bradford's n-butane values.

[c] This shrinkage was empirically adjusted.

[d] These shrinkages were extrapolated roughly from Bradford's 300°C n-butane values, estimating the dependence of the shrinkage values on the distances and neglecting the temperature dependence.

[e] These shrinkages were averages of the n-butane shrinkages for these distances.

scheme for computing C...C and C...H amplitudes.[10] The results of the least squares analyses showed no dependence upon the difference set used. The "fixed" C...C, 1...4 C...H, and 1...3 H...H amplitudes were allowed to vary once a good structure for a given value of ΔG° had been determined, but were never varied in concert with the other independent parameters. The values of the shrinkages used for the various internuclear distances were extrapolated roughly from those determined for n-butane by Bradford.[2] Shrinkages and amplitude increments used for the distances are given in Table V. Morse asymmetry constants of 2.0 A^{-1} were used for all distances.

c. Processing of the Intensity Data

Initially, the data sets from the different camera distances were treated separately. First, before any least squares fits of the intensity were done using the model described above, a least squares fit of the 21-cm r^3 data was done using a model which contained no internuclear distances greater than 1...4. The purpose of this procedure was to get some idea of the value of the gauche percentage before doing a lot of work with the more complicated molecular model. Preliminary indications were that the gauche fraction was between 40 and 60%, and was probably close to 50%. Least squares fits of the intensity data were done using a slight variant of the more complicated model described above and a gauche fraction of 45 or

50%. As a first approximation, computer-fitted backgrounds were derived for each of the three r^3 data sets. These backgrounds and the derived structural parameters were used to compute correlation backgrounds for each data set. New backgrounds were then drawn by hand, using the criteria that a background should be smooth and should "split" the correlation background as evenly as possible. New least squares analyses were done using the newly-derived backgrounds, and the r^3 data were blended, yielding a smooth molecular intensity function over the range s = 3.14 to s = 46.81 (q = 10 to q = 149). A set of independent parameters was derived from the blended intensities. The r^2 intensity data was subjected to least squares analysis with the independent parameters fixed at the values derived from the blended r^3 data so that a preliminary background could be derived. A correlation background for the r^2 data was computed, and a new background was hand-drawn through the data, using the same criteria given earlier. All of the data were then blended, with care taken to ensure that intensity data from different camera distances joined smoothly. The resulting molecular intensity function ranged from s = 2.20 to s = 46.81 (q = 7 to q = 149). A new set of structural parameters was derived from the blended data. These parameters were used to compute new correlation backgrounds for all of the individual data sets. New backgrounds were then drawn by hand for all data sets except the 7-cm camera distance set. The data

were reblended, with the smoothness of the joins of intensity data from different sets somewhat improved. The indices of resolution, $R = M^{exp}(s)/M^{calc}(s)$, for the 21-cm r^2 and the 21-, 11-, and 7-cm r^3 data were 0.973, 0.907, 0.958, and 0.868, respectively.

A succession of least squares analyses of the blended intensity data was performed with different values of $\Delta G°$ assumed. The value chosen for $\Delta G°$ had only a minor influence upon the independent parameters. The parameters which were influenced most strongly were the gauche dihedral angle and the gauche 1...4 C...C nonbonded amplitude, but the effects were of the order of σ, and so are not significant. However, $\sigma(I)$ was dependent upon $\Delta G°$, and was used as the criterion which determined the best value of $\Delta G°$ and therefore of the gauche/trans ratio. The values of $\sigma(I)/\langle I \rangle$ obtained using the different $\Delta G°$ values were plotted versus $\Delta G°$, and a parabola was passed through the points. The value of $\Delta G°$ at the vertex was taken as the best value. This value of $\Delta G°$ was used with equation (4) to determine the relative percentages of the various 1...7 C...C distances, and the fraction of gauche sites was determined from the multiplicities of the 1...7 configurations.

Weights proportional to s were used throughout the least squares analyses. The $s^{1/2}$-weighted residuals were evenly distributed throughout the data space, indicating that a weight matrix proportional to s was the proper one

to use. The weighted residuals appeared to be somewhat less correlated than has been the case in many electron diffraction structure studies.

4. Results

The values determined for the independent parameters are shown along with their estimated uncertainties (3σ) in Table VI. The two sets of uncertainties shown correspond to the σ's determined from the zero order error matrix (the usual σ values reported) and the σ's determined from the "bona fide" error matrix as defined by Bartell and Anashkin.[11] The bona fide σ's include the effects of an approximate correction for the correlation of the weighted residuals. An autocorrelation study was done on the weighted residuals which yielded a γ value of 2.7 A. The usual value of γ seems to be around 1 A, so it appears that, formally, the weighted residuals for n-hexadecane are correlated over a shorter range of scattering angles than are many sets of weighted intensity residuals. However, examination of the least squares residuals reveals that while the residuals appear to be randomly distributed throughout some portions of $\underline{s}$ space, their distribution throughout most of $\underline{s}$ space is no more random than is the pattern of least squares residuals observed in most electron diffraction studies. Therefore, it seems likely that the high value of γ may be accidental, an artifact of the

Table VI. Values of the Independent Parameters for n-Hexadecane (ΔG° = 296 cal/mol)

Parameter	Value	3σ zero order	3σ "bona fide"
C-C bond length	1.541 Å	±0.002	±0.004
C-H bond length	1.130 Å	±0.005	±0.008
CCC angle	114.6°	±0.4	±0.6
HCH angle	99.6°	±3.3	±4.4
gauche CCCC dihedral angle	71.5°	±4.4	±4.4
C-C bonded amp	0.0562	±0.0025	±0.0055
C-H bonded amp	0.0845	±0.0056	±0.0101
1...3 C...C amp	0.0849	±0.0062	±0.0109
1...3 C...H amp	0.1154	±0.0077	±0.0114
1...4 C...C gauche amp	0.2023	±0.0460	±0.0507
Index of resolution $\sigma(I)/\langle I\rangle$ = 0.0018	0.9865	±0.0295	±0.0431

Table VII. Values of the Fixed[a] Amplitudes for n-Hexadecane (ΔG° = 296 cal/mol)

Amplitude	Value
1...3 H...H	0.21223
other (>1...) C...C	0.12789
1...4 C...H	0.18362
1...5 C...H	0.22900
1...4 H...H	0.32703
1...5 H...H	0.52463
1...4 C...C (trans)	0.10239

[a] These amplitudes were not varied with the independent parameters. Once a structure had been obtained for a given value of ΔG°, the independent parameters were fixed and the C...C, 1...3, H...H, and 1...4 C-H amplitudes were varied.

assumption that the important part of the autocorrelation curve has only one component, and that perhaps γ = 1A might be a better representation of the correlation of a significant component of the least squares residuals than γ = 2.7 A. Accordingly, γ = 1 A was used in the relationships to compute the bona fide error matrix. The values of the fixed average amplitudes are given in Table VII. The correlation matrix for the independent parameters is tabulated in Table VIII. The values shown in Tables VI, VII, and VIII were determined assuming ΔG° = 296 cal/mol, which was quite close to the value of 260 cal/mol which was found to give the best fit of the intensity data. Figure 5 shows the blended molecular intensity function and residuals while Figure 6 shows the corresponding radial distribution curve, again for ΔG° = 296 cal/mol.

A plot of the various values of $\sigma(I)/\langle I\rangle$ versus ΔG° is shown in Figure 7. The parabola which was fitted to the points is also shown. The vertex of the parabola is at ΔG° = 260 cal/mol. This value of ΔG° implies a gauche fraction of 47.7% (given the molecular model used). The uncertainty in ΔG° was determined using equation (1) and the parabola shown in Figure 7. A factor of three was used for $B_{\ell\ell}(B^{-1})_{\ell\ell}$. The uncertainty ($\pm\sigma$) in ΔG° is determined to be $\pm$ 260 cal/mol, which implies an uncertainty ($\pm\sigma$) of $\pm$ 6% in the value of the gauche fraction.

Table VIII. Correlation Matrix (zero-order) for the Independent Parameters of n-Hexadecane

	1	2	3	4	5	6	7
1	1.						
2	0.07	1.					
3	-0.48	0.	1.				
4	0.22	0.41	-0.34	1.			
5	0.03	-0.05	0.02	-0.07	1.		
6	0.11	-0.02	-0.04	0.17	0.02	1.	
7	0.10	0.09	-0.04	0.15	0.	0.19	1.
8	0.05	0.	-0.06	0.23	0.15	0.22	0.13
9	0.02	0.01	0.10	-0.01	-0.04	0.10	0.06
10	-0.09	-0.05	0.06	-0.19	0.09	-0.15	-0.10
11	0.15	0.03	-0.06	0.34	0.02	0.59	0.35

	8	9	10	11
1				
2				
3				
4				
5				
6				
7				
8	1.			
9	0.08	1.		
10	-0.10	-0.07	1.	
11	0.37	0.18	-0.26	1.

1. C-C bond length
2. C-H bond length
3. CCC angle
4. HCH angle
5. gauche CCCC dihedral angle
6. C-C bonded amplitude
7. C-H bonded amplitude
8. 1...3 C...C amplitude
9. 1...3 C...H amplitude
10. 1...4 C...C gauche amplitude
11. Index of resolution

Table VIII continued.

The zero-order standard deviations of the parameters are

1.	6.5×10^{-4}	7.	1.8×10^{-3}
2.	1.7×10^{-3}	8.	2.0×10^{-3}
3.	1.3×10^{-1} [a]	9.	2.5×10^{-3}
4.	5.9×10^{-1}	10.	1.5×10^{-2}
5.	1.4	11.	9.4×10^{-3}
6.	7.8×10^{-4}		

[a] This is the standard deviation of half of the HCH angle.

Figure 5. Experimental and Calculated Molecular Intensity Functions for n-Hexadecane.

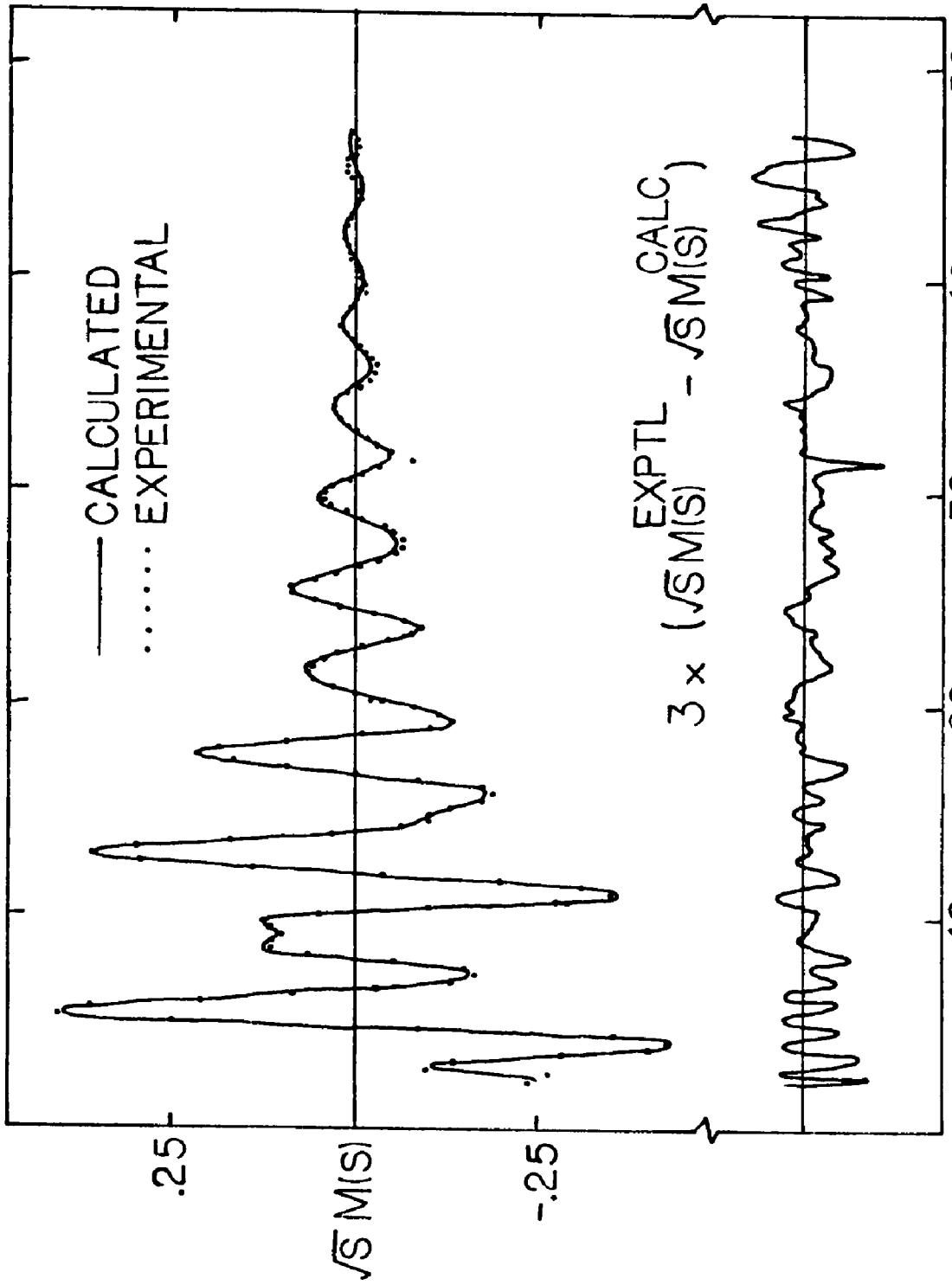

CALCULATED
EXPERIMENTAL
$3 \times (\sqrt{S}M(S)^{EXPTL} - \sqrt{S}M(S)^{CALC})$
$\sqrt{S}M(S)$
.25
-.25
10
20
30
40
50
S, Å^{-1}

Figure 5.

Figure 6. Experimental Radial Distribution Function for n-Hexadecane.

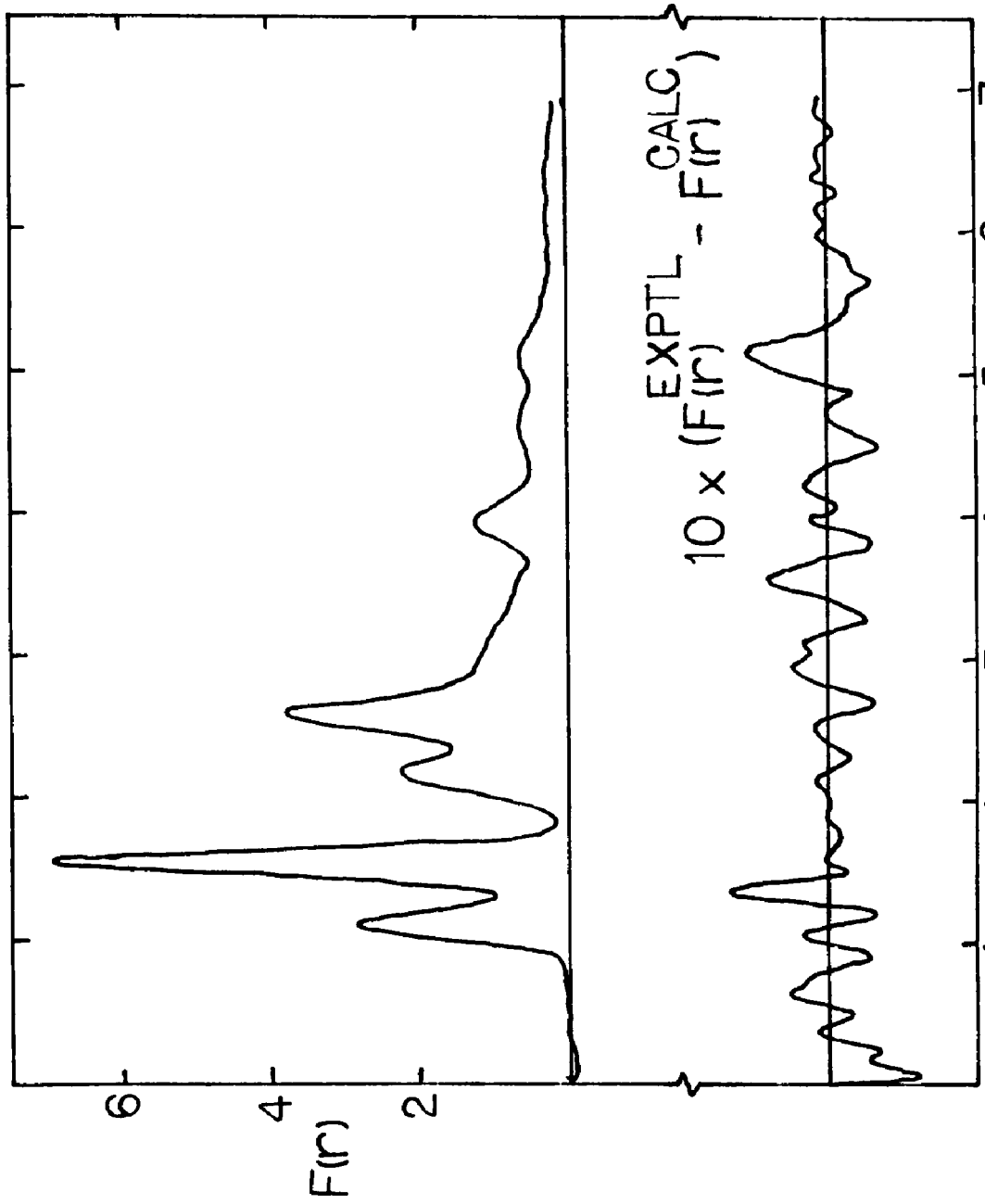


Figure 6.

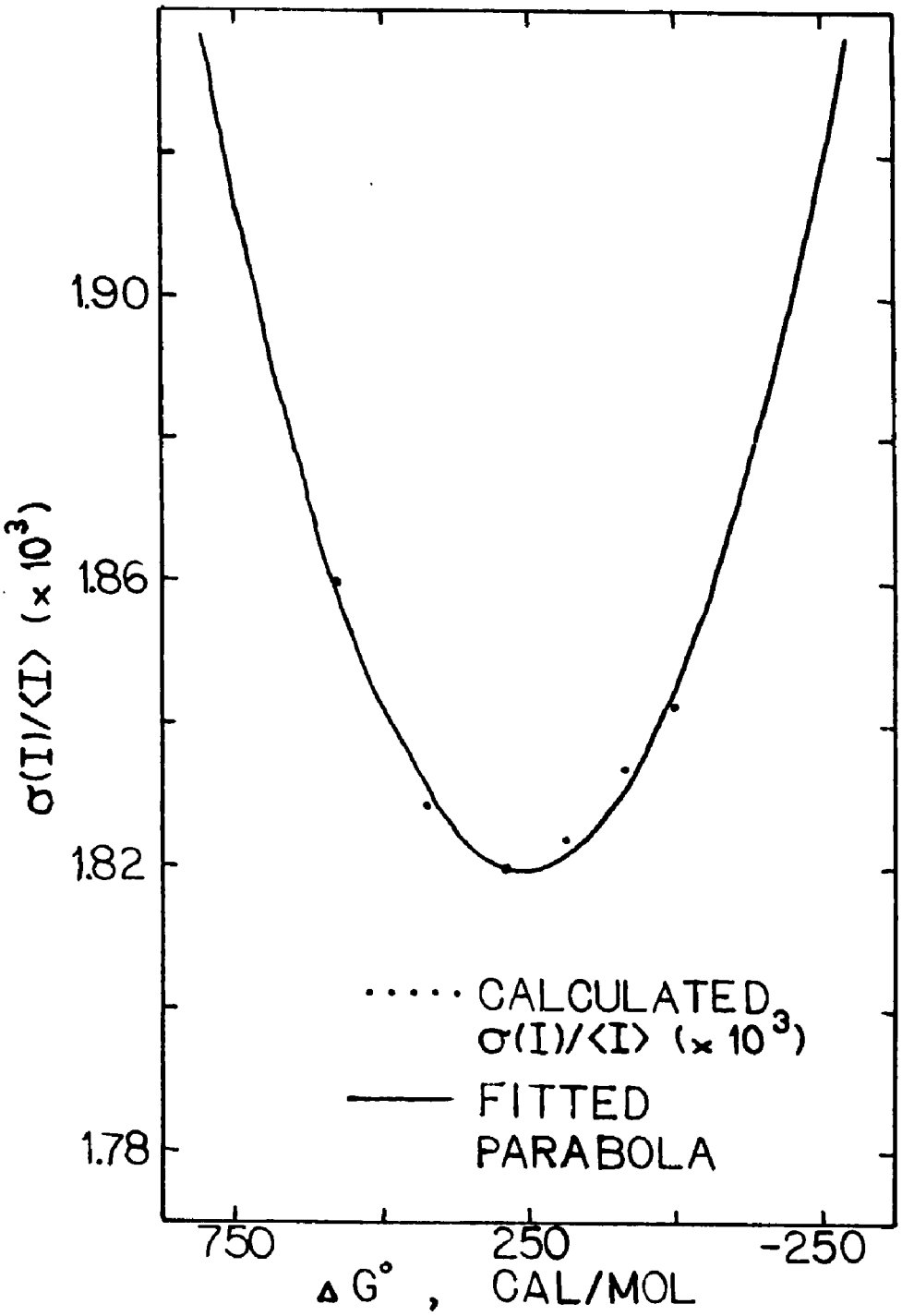


Figure 7. Standard Deviation of the Intensity as a Function of ΔG° (gauche-trans) for n-Hexadecane.

5. Discussion

As may be seen, the values determined for the n-hexadecane bond lengths in the course of this study are longer than the n-alkane bond lengths determined in a previous study.[5] There are good reasons to believe that the apparent increases in the bond lengths are real rather than effects of experimental errors or the particular molecular model used. All three sets of r^3 data, which were subjected to least squares analysis separately, indicated that the n-hexadecane bond lengths were longer than those of the shorter n-alkanes. The wavelength of the electrons used was checked by measuring the distance between lines of electron diffraction patterns of zinc oxide and was found to be within 0.1% of the computed value of the wavelength for 40 kV electrons, 0.06015 A. Finally, a second series of 21-cm r^3 plates were taken roughly three months after the first set. Analysis of this data yielded long bond lengths also, the increase in length over the bond lengths in the shorter n-alkanes being indistinguishable from that yielded by the other data sets. In short, the experimental equipment was operating properly, and the results obtained were reproducible.

That the increases in the bond lengths are artifacts of the molecular model used in the least squares analyses is highly unlikely. First, bond lengths do not depend upon the details of the molecular model used, as parameters such as the torsional angle may. Second, a number of different

molecular models was used in the data analysis before the model which was finally used was devised. Analyses done using the different models showed virtually no differences in the values obtained for the bond lengths. Hence, it may be concluded that the long bond lengths are not the result of a subtle bias in the handling of the data.

Neither are the bond length increases the result of the higher than customary sample temperature. Of course, it is impossible to determine the true temperature of the gas sample which diffracts the electrons because the amount of cooling of the gas upon expansion is unknown, but it is probable that the final temperature of the n-hexadecane sample is substantially higher than that of the shorter n-alkanes, because the initial temperature of the n-hexadecane sample was 150° C while that of the shorter n-alkanes was 32° C. If this were indeed the case and if the higher temperature had a sizeable effect upon the r_g bond length values determined, the bonded C-H and C-C amplitudes of vibration should be larger for n-hexadecane than they are for the shorter n-alkanes, for r_g is larger than r_e (which is not temperature dependent) by approximately $(3/2)\ al^2$. However, the C-C amplitude for n-hexadecane is within σ of the average value for the shorter n-alkanes, while the n-hexadecane C-H amplitude is within 2σ of the shorter n-alkane average value. These differences will not cause r_g differences of the magnitude observed.

The increase in the C-H bond length is not a firm

value, for the uncertainty in the C-H bond length value is comparatively high. The value of $\sigma_{\text{bona fide}}$ is ± 0.003 A; therefore, using Cruickshanks' criterion that differences in derived parameters of less than 3σ are not significant, the C-H bond length in n-hexadecane may be considered to be only marginally longer than the C-H bond lengths in shorter n-alkanes. However, if the increase is real, two possible explanations for it present themselves. The n-hexadecane C-H bond length should be close to the value appropriate for an n-alkane methylene C-H bond, for the n-hexadecane molecule has twenty-eight methylene hydrogens and six methyl hydrogens. The n-hexadecane structure study provides the first good indication of the value of the n-alkane methylene C-H bond length, for n-heptane, the longest n-alkane for which an electron diffraction structure has been published, has only ten methylene to six methyl hydrogens. It is interesting to note that the average C-H bond length in the series n-butane to n-heptane does appear to increase, though the size of the increase is not significant (the value of 1.108 A for the n-butane C-H bond length given by reference 5 is probably low; part A of this section gives a value of 1.117 ± 0.001 A). Taking another tack, examination of the n-hexadecane results shows that the geminal H...H distance is quite short, being shorter than the corresponding distance in the other n-alkanes by nearly 0.1 A. The uncertainty in the distance is fairly large, but the decrease appears to be significant. The

molecule will probably relax in some way to relieve the increased H...H repulsions. Experience with model force fields suggests that the HCH angle should open out before the C-H bonds would stretch, but is possible that the same forces which closed the HCH angle down in the first place are stronger than the forces which must be overcome if the C-H bond is to stretch. Therefore, it is possible that an increase in the C-H bond length is caused by the relaxation of the molecule to relieve geminal H...H repulsions.

Rationalizing the length of the C-C bond is somewhat more difficult, but there are indications that the n-alkane C-C bond length might be expected to increase as the chain gets longer. First, there is the fact that the n-hexadecane C-C bond length corresponds to the methylene-methylene C-C bond length. n-Hexadecane has thirteen methylene-methylene C-C bonds and two methyl-methylene C-C bonds; n-heptane has four of the former to two of the latter. Ab initio calculations indicate that a methyl-methylene C-C bond is longer than a methyl-methyl C-C bond; 4-31G calculations on ethane and propane make the difference about 0.001 ± 0.001 A, while STO-3G (a method somewhat less accurate than 4-31G) calculations make the difference 0.003 ± 0.001 A.[12] STO-3G calculations on n-butane indicate that the trans and gauche methylene-methylene C-C bonds are longer than the propane methyl-methylene bond by about 0.004 ± 0.002 and 0.006 ± 0.002 A, respectively.[12] Given the difference in the 4-31G and STO-3G results

listed above, it is obvious that the differences between the STO-3G methylene-methylene and methyl-methylene C-C bond lengths given above cannot be considered to be quantitatively reliable, but they do provide an indication that the methylene-methylene bond is longer than the methyl-methylene bond. The shorter n-alkane C-C bond lengths do not show a measurable increase as the chain length increases, but the experiments are not recent and the associated uncertainties are fairly large. Structural studies on cyclic alkanes would be expected to show methylene-methylene C-C bond lengths, so some of these were examined. The most recent study of cyclohexane,[13] which is an average of results from two laboratories, gives an r_g C-C bond length of ($\pm\sigma$) 1.536 ± 0.002 Å. A study of cyclodecane[14] gives an r_g C-C bond length of 1.545 ± 0.0015 Å (± 2σ). Cyclodecane is strained, whereas cyclohexane is not, for cyclodecane has a number of close H...H nonbonded distances. However, examination of molecular models suggests that cyclodecane can relieve these by internal rotation about various C-C bonds much more easily than by stretching C-C bonds. Of course, since there is evidence that internal rotation and bond stretching interact significantly, the torsional deformation would be expected to cause some increase in the C-C bond length. The magnitude of the torsionally-caused stretching is difficult to determine with a high degree of certainty, for it is postulated to be dependent upon the dihedral angles, and cyclodecane

consists of a number of different conformers, which makes specifying the dihedral angles rather difficult. However, dihedral angles given for the boat-chair-boat conformation, which a combined electron diffraction-molecular mechanics study[14] indicates is the predominant species, imply an average torsional lengthening of 0.003 A if the 4-31G estimate of the increase in the C-C bond length in eclipsed ethane (0.015 A) is used for δR in the expression

$$\Delta R = 1/2\delta R(1 + \cos 3\tau), \qquad (5)$$

where ΔR is the change in the bond length and τ is the dihedral angle. The cyclodecane C-C bond length corrected for the effects of torsional lengthening is thus 1.542 ± 0.0015 A, very close to the C-C bond length determined for n-hexadecane.

Molecular mechanics calculations were done for some longer n-alkanes using the force field MUB-2, which was described in part II of this thesis. It may be remembered the MUB-2 did an excellent job of reproducing trends in structural parameters. Therefore, it may be expected that most bond length differences calculated using MUB-2 are probably quantitatively significant. Due to considerations of simplicity and the expense of computer time, calculations were not done on the n-hexadecane molecule. Instead, sites consisting of two adjacent C-C bonds located well within the chain of methylene-methylene C-C bonds in the molecules n-octane and n-nonane were examined. Trans-

trans, trans-gauche, and gauche-gauche sites were chosen. The average C-C lengths for the three sites were 1.5362 A, 1.5371 A, and 1.5369 A, respectively. Using the percentages appropriate for a 47.7% gauche model, the above values imply an average bond length of 1.5368 A. The average methylene-methylene bond length calculated for the shorter n-alkanes (butane and pentane) was between 1.534 and 1.535 A (the methyl-methylene bond length calculated for n-propane was 1.533 A). Calculations done using MUB-2 would, therefore, seem to predict a lengthening of the average C-C bond as the chain is lengthened. It must be noted that the magnitude of the lengthening suggested by the results given above does not contain the possible effects of so-called long-range interactions which occur over fairly short nonbonded distances, for all conformations outside of the site of interest were assigned to be trans and therefore the n-alkane molecules examined in the course of the molecular mechanics calculations did not bend back upon themselves. Some of the n-hexadecane conformers present in the diffraction sample will be twisted so that one portion of the molecule will bend back upon another. The bonds may lengthen further to relieve strain brought about by the additional close nonbonded interactions present in such a conformation. Judging from the results and considerations detailed above, the MUB-2 calculations suggest a value of the n-hexadecane bond length which is similar to the one obtained from experiment.

The gauche-trans free energy difference determined for n-hexadecane is somewhat smaller than that determined for other n-alkanes.[6] However, the uncertainties in all ΔG° values determined by electron diffraction are high, so the differences between the values of ΔG° determined for the various n-alkanes are not significant. The value of ΔG° determined for n-hexadecane will be discussed further in the section below on the characteristic ratio of polymethylene.

6. Calculation of the Characteristic Ratio of Polymethylene

a. Introduction

The characteristic ratio of a polymer is defined as $\langle r^2 \rangle_o / nl^2$, where $\langle r^2 \rangle_o$ is the mean-square distance between the two ends of the polymer chain, corrected for the effects of excluded volume; n is the number of segments which the polymer chain contains; and l is the length of each segment. The ratio above becomes a constant for a given polymer type once the chains, whose individual conformations are distributed over the conformational states which the polymer molecule may assume, reach a certain length. It may be seen that the characteristic ratio is, in a sense, a measure of the degree of extension of the average polymer molecule. Values of the characteristic ratio may be computed from the results of measurement of the light scattered by polymer solutions. Of course, the value of the characteristic ratio is determined by the conformations of the polymer molecules,

which are dependent upon the solvent and the temperature of the solution. Most measurements of the characteristic ratio are made at the θ-point, which corresponds to that solution composition and temperature where the polymer favors neither solvent nor self contacts. Therefore, the conformation which a polymer assumes in a θ-solvent is its lowest free energy conformation in the bulk.

The characteristic ratio may also be computed using the structural parameters of the polymer and the free energy differences between various conformations. However, these quantities are not known. The approach, therefore, has been to use the characteristic ratio to evaluate various combinations of structural parameters and conformational energies, since the ratio is not dependent upon just one of these quantities. Reasonable estimates of the quantities needed for the characteristic ratio calculation have been taken from various structural studies, including a number on molecules in the gas phase.

Abe, Jernigan, and Flory[15] have calculated the polymethylene characteristic ratio using data obtained from gas-phase structural studies of small alkanes and from a simple model force field which was parameterized (by trial and error) to fit the assumed small alkane gauche-trans free energy difference of 500 cal/mol. The n-hexadecane structure study provides the parameters of a molecule which may be expected to be more like polymethylene than will small n-alkanes. Also, MUB-2 is a more firmly established

force field than the field used in reference 15, so the conformational energy differences calculated using MUB-2 are probably more trustworthy than those given in reference 15. Therefore, the n-hexadecane structure study and MUB-2 are sources of "better" parameters for the calculation of the characteristic ratio than were available to Abe, Jernigan, and Flory. Of course, the use of the structural parameters and conformational energy differences of n-alkanes which are appropriate for the gas-phase species for the calculation of the polymethylene characteristic ratio is valid only if neither long-range intramolecular nor intermolecular interactions induce sizeable changes in the structural parameters or energy differences. The calculation of the characteristic ratio using the n-hexadecane and MUB-2 data may provide some idea of the role of both types of interaction mentioned above in determining the conformation of polymethylene.

b. Theory

Two sets of relationships from which the characteristic ratio may be computed are given in reference 15. One of these is good for chains of any length, while the other is good for infinite chains only. The second set of relationships, that derived by Hoeve,[16] was used because (1) it was simpler than the first, and (2) there was no explicit dependence upon the bond length. This dependence could be a source of confusion, since the type of bond

length (r_g, r_e, r_α, or a host of others) to be used is unclear. The differences between the values of the different types of bond and torsional angles are generally assumed to be small, so the ambiguity about which type of angle is to be used does not provide any difficulties. The value of the characteristic ratio was computed using the following expression:

$$(\langle r^2\rangle_o/n\ell^2)_\infty = 1 + \{2(\underline{X}^* \times \underline{E}_3)||\underline{T}||[\underline{E}_{33} - (\underline{U} \times \underline{E}_3)\lambda^{-1}||\underline{T}||]^{-1}(\underline{X} \times \underline{E}_3)\}_{1,1}, \quad (6)$$

where $\underline{E}_3$ is the three-dimensional identity matrix ($\underline{E}_{3s}$ is the 3s-dimensional identity matrix), and "$\underline{A} \times \underline{B}$" means "take the direct product of $\underline{A}$ and $\underline{B}$." The $\underline{U}$ matrix is defined as

$$\underline{U} = \begin{pmatrix} 1 & \alpha & \alpha \\ & \alpha & \alpha\omega \\ & \alpha\omega & \alpha \end{pmatrix}, \quad (7)$$

where $\alpha = \exp(-E_g/RT)$ (E_g is the free energy difference between the gauche and trans conformations) and $\omega = \exp(-E_g + {}_g{}^-/RT)$ ($E_g + {}_g{}^-$ is the free energy difference between a gauche$^+$-gauche$^-$ conformation and a gauche$^+$-gauche$^+$ or gauche$^-$-gauche$^-$ conformation). $\underline{X}^*$ is the eigenrow of $\underline{U}$ corresponding to the maximum eigenvalue λ, and $\underline{X}$ is the corresponding eigencolumn. The $||\underline{T}||$ matrix is defined as

$$||\underline{T}|| = \begin{pmatrix} \underline{T}^{(1)} & & \\ & \underline{T}^{(2)} \cdot \cdot & \\ & & \underline{T}^{(r)} \end{pmatrix}, \qquad (8)$$

where $\underline{r}$ is the number of rotational states and the $\underline{T}^{(i)}$ are defined as

$$\underline{T}^{(i)} = \begin{pmatrix} \cos\theta_i & \sin\theta_i & 0 \\ \sin\theta_i\cos\phi_i & -\cos\theta_i\cos\phi_i & \sin\phi_i \\ \sin\theta_i\sin\phi_i & -\cos\theta_i\sin\phi_i & -\cos\phi_i \end{pmatrix}, \qquad (9)$$

where θ_i is the supplement of the bond angle and ϕ_i the displacement of the dihedral angle from trans for the $\underline{i}$th rotational state. Of the quantities needed for the calculation of $(\langle r^2\rangle_o/nl^2)_\infty$, E_g, the θ_i, and the ϕ_i are available from the structural study of $\underline{n}$-hexadecane. $E_{g^+g^-}$ was obtained from molecular mechanics calculations of the energies of $\underline{\text{gauche}}^+$-$\underline{\text{gauche}}^+$ and $\underline{\text{gauche}}^+$-$\underline{\text{gauche}}^-$ $\underline{n}$-nonane using the force field MUB-2.

Of course, the values of the parameters necessary for the calculation of the characteristic ratio will show variations from site to site within the molecule. However, average values of the parameters are all that are available, and indeed, average values must be assumed if the calculation is to be tractable. Simple three-state calculations of the characteristic ratio have been successful before. Also, the dependence of the calculated value of $(\langle r^2\rangle_o/$

$nl^2)_\infty$ upon the values of both E_g and the gauche ϕ_i is approximately linear over a fairly large range, and the dependence of the characteristic ratio upon the values of $E_{g^+g^-}$ and θ_i are fairly weak. Therefore, assumption of average values for the parameters should cause only minor uncertainties in the computed value of the characteristic ratio.

c. Results and Discussion

The MUB-2 calculations indicate that, for isomers having two adjacent gauche sites located in the center of an n-nonane chain, the gauche$^+$-gauche$^-$ rotamer will have an energy 3.0 kcal/mol above that of the gauche$^+$-gauche$^+$ rotamer. Of course, there are many possible ways to locate a gauche$^+$-gauche$^-$ site within a long chain; some of these may have a value of $E_{g^+g^-}$ which is less than 3 kcal/mol, but others will have $E_{g^+g^-}$ greater than 3 kcal/mol. Also, MUB-2 calculations on n-pentane give a value of 3.4 kcal/mol for $E_{g^+g^-}$. Therefore, 3 kcal/mol may be taken as a reasonable approximation of the value of $E_{g^+g^-}$ as predicted by MUB-2. The characteristic ratio was computed using equation (7) with E_g = 260 cal/mol, θ_i = 65.5°, ϕ_i = 0°, ± 108.5°, and $E_{g^+g^-}$ = 3 kcal/mol, the values implied by the n-hexadecane structure study and the MUB-2 results. The value obtained for the characteristic ratio was 9.1, which may be compared with the experimental value of 6.8 ± 0.3.[17] Of course, the parameters obtained from

the electron diffraction data have some uncertainty associated with them. Reference 16 shows that a decrease in the value of E_g or an increase in the gauche ϕ_i value will decrease the computed value of the characteristic ratio. Therefore, E_g was decreased and the gauche ϕ_i increased by roughly the standard deviations of each of these parameters, and values of $(\langle r^2\rangle_o/nl^2)_\infty$ were computed for the new sets of conformational parameters. The values $E_g = 0$, $\theta_i = 65.5°$, $\phi_i = 0°, \pm 108.5°$ and $E_{g^+g^-} = 3$ kcal/mol gave a characteristic ratio of 8.65, while the values $E_g = 260$ cal/mol, $\theta_i = 65.5°$, $\phi_i = 0°, \pm 110.3°$, and $E_{g^+g^-} = 3$ kcal/mol gave a value of 8.75. Since little, if any, correlation between the values of E_g and ϕ_i was evidenced during the course of the electron diffraction structure analysis, the above data implies that the standard deviation ($\pm\sigma$) of the computed value of the characteristic ratio is $\pm$ 0.6.

The computed value of the characteristic ratio is a bit difficult to interpret. It is within 4σ of the experimental value, so, according to Cruickshanks' criterion, it might be said that the difference between the computed and experimental values is marginally significant. However, such a conclusion would ignore the fact that the value given for the uncertainty in the computed value of the characteristic ratio is not well determined, since the uncertainties in the value of E_g and θ_i are not well determined. Subjective considerations would probably lead one to have some confidence in the value given for E_g: the

percentage of gauche sites, which is dependent upon the gauche-trans free energy difference, showed little if any dependence upon the large number of molecular models which were tested before the model finally used (that described above) was devised. However, the value of the gauche dihedral angle was dependent upon the model used (though the dependence was not strong--the value of the gauche ϕ_i was always less than 113°). The value of σ which comes out of the least squares analysis does not contain any of the dependence of the gauche ϕ_i upon the molecular model. Also, recent work[7] suggests that the σ obtained from conventional least squares analyses may constitute uncertainty estimates which are too small, especially for parameters like dihedral angles, which are strongly dependent upon a small portion of the experimental data. Also, the value of $E_{g^+g^-}$ used in the calculation has been assumed to have zero uncertainty, which certainly is not the case. Therefore, the difference between the experimental and computed values of the characteristic ratio cannot be considered to be significant. Hence, the results of this research suggest that so-called long range interactions and effects arising from the state of aggregation of polymethylene do not play a dominant role in determining its conformation.

One aspect of the results which looked somewhat puzzling was the failure of this research to produce a calculated value of the characteristic ratio which was closer to the experimental one than was that calculated by Abe,

Jernigan, and Flory in reference 15. Using the same three state model employed in this research, they calculated a value of 7.6 for the characteristic ratio, though one would expect that the sources of their parameters would provide poorer data for polymethylene than would the sources used in the present work. However, a change of a few (less than ten) degrees in the gauche dihedral angle, which, if not within the actual uncertainty in the electron diffraction parameter, could certainly occur upon the transition from a hypothetical gaseous to solid phase, would bring the computed value of the characteristic ratio down to the value of the experimental one. The characteristic ratio value calculated in reference 15 is smaller than the one calculated in this research because the reference 15 values of the gauche ϕ_i and $E_{g^+g^-}$ are larger and smaller, respectively, than the values assumed in this research. The uncertainty in the gauche ϕ_i has already been discussed. It has been pointed out that the value of 3 kcal/mol for $E_{g^+g^-}$ is only an estimate for the excess energy of a gauche$^+$-gauche$^-$ site in a gas-phase molecule; the effects of condensation could easily alter the value of $E_{g^+g^-}$ by several hundred calories.

The calculations detailed in reference 15 strongly suggest that if the polymethylene gauche dihedral angle is greater than 60°, as chemical intuition would suggest, E_g must be less than 500 cal/mol (if a reasonable value is assumed for $E_{g^+g^-}$). In this connection, the value of ΔG°

(gauche-trans) determined for n-hexadecane is quite interesting. As has been noted above, the value of 260 cal/mol determined for ΔG° in the course of the n-hexadecane structure study is smaller than the ΔG° values derived for smaller n-alkanes, all of which were reported to be around 600 cal/mol. If it is assumed that the entropy difference between single gauche and trans conformations is small, the gauche-trans energy difference seems to be fairly independent of the phase of the sample: liquid Raman studies[18] of the shorter n-alkanes give a value for ΔH (gauche-trans) of 500 cal/mol for most molecules studied. Therefore, data on the smaller n-alkanes suggests that E_g for polymethylene in a θ-solvent should be around 500 cal/mol. However, the n-hexadecane results suggest that the value may be somewhat smaller. The uncertainty in the value of ΔG° determined for n-hexadecane is high, so the indications that the polymethylene E_g may be lower than what would be expected from the short n-alkane data are only tentative. Still, the n-hexadecane results do provide some suggestion that a gauche dihedral angle greater than 60° and a low value of E_g may provide a correct account of the value of the characteristic ratio of polymethylene.

REFERENCES

1. W. F. Bradford, private communication.

2. W. F. Bradford, Thesis, The University of Michigan, 1975.

3. R. A. Bonham and L. S. Bartell, J. Amer. Chem. Soc., 81, 3491 (1959).

4. K. Kuchitsu, Bull. Chem. Soc. Japan, 32, 748 (1959).

5. R. A. Bonham, L. S. Bartell, and D. A. Kohl, J. Amer. Chem. Soc., 81, 4765 (1959).

6. L. S. Bartell and D. A. Kohl, J. Chem. Phys., 39, 3097 (1963).

7. L. S. Bartell, private communication.

8. I. Hargittai, J. Hernadi, M. Kolonito, G. Schultz, Rev. Sci. Instruments, 42, 546 (1971).

9. L. Schafer, A. C. Yates, and R. A. Bonham, J. Chem. Phys., 55, 3055 (1971).

10. V. Mastryukov, private communication.

11. L. S. Bartell and M. G. Anashkin, J. Mol. Struc., 17, 193 (1973).

12. W. J. Hehre, private communication.

13. O. Bastiansen et al., J. Mol. Struc., 18, 163 (1973).

14. R. L. Hilderbrandt, J. D. Weiser, and L. K. Montgomery, J. Amer. Chem. Soc., 95, 8598 (1973).

15. A. Abe, R. L. Jernigan, and P. J. Flory, J. Amer. Chem. Soc., 88, 631 (1966).

16. C. A. J. Hoeve, J. Chem. Phys., 35, 1266 (1961).

17. R. Chiang, J. Phys. Chem., 69, 1645 (1965).

18. N. Sheppard and G. J. Szasz, J. Chem. Phys., 17, 86 (1949).

APPENDIX I

Experimental Levelled Intensity and Background Intensity Functions for n-Butane

Of the 21-cm r^2 sector data set, the points from s = 2.513 to s = 6.912 were used to obtain the final blended intensity.

Of the 21-cm r^3 sector data set, the points from s = 4.398 to s = 21.049 were used to obtain the final blended intensity.

Of the 11-cm r^3 sector data set, the points from s = 14.451 to s = 39.584 were used to obtain the final blended intensity.

Table I. Experimental Levelled Intensity and Background Values for the 21-cm Camera Distance, r^2 Sector

s	I(s)	$I_B(s)$	s	I(s)	$I_B(s)$
1.885	1.6906	1.2623	7.226	1.6787	1.6938
2.199	1.2077	1.2809	7.540	1.6851	1.7054
2.513	1.185	1.3042	7.854	1.7069	1.7165
2.827	1.2282	1.3342	8.168	1.7384	1.7275
3.142	1.2771	1.3764	8.482	1.7631	1.7384
3.456	1.2960	1.4290	8.796	1.7777	1.7491
3.770	1.2951	1.4773	9.111	1.7914	1.7596
4.084	1.3152	1.5146	9.425	1.8005	1.7705
4.398	1.3854	1.5457	9.739	1.7957	1.7813
4.712	1.4958	1.5719	10.053	1.7750	1.7919
5.027	1.6125	1.5945	10.367	1.7473	1.8025
5.341	1.7015	1.6136	10.681	1.7265	1.8129
5.655	1.7446	1.6305	10.996	1.7223	1.8232
5.969	1.7430	1.6450	11.310	1.7429	1.8337
6.283	1.7262	1.6584	11.624	1.7823	1.8442
6.597	1.7079	1.6707	11.938	1.8351	1.8546
6.912	1.6893	1.6825			

Table II. Experimental Levelled Intensity and Background Values for the 21-cm Camera Distance, r^3 Sector

s	I(s)	$I_B(s)$	s	I(s)	$I_B(s)$
3.142	1.4131	1.5093	13.823	2.0550	2.0247
3.456	1.4503	1.6026	14.137	2.0164	2.0270
3.770	1.4334	1.6806	14.451	1.9980	2.0290
4.084	1.4683	1.7413	14.765	1.9904	2.0311
4.398	1.5620	1.7873	15.080	1.9828	2.0331
4.712	1.7248	1.8227	15.394	1.9723	2.0349
5.027	1.8881	1.8507	15.708	1.9659	2.0366
5.341	2.0093	1.8722	16.022	1.9753	2.0380
5.655	2.0525	1.8897	16.336	1.9972	2.0395
5.969	2.0470	1.9054	16.650	2.0263	2.0410
6.283	2.0160	1.9192	16.965	2.0596	2.0427
6.597	1.9793	1.9313	17.279	2.0916	2.0443
6.912	1.9453	1.9420	17.593	2.1141	2.0463
7.226	1.9241	1.9515	17.907	2.1180	2.0485
7.540	1.9294	1.9598	18.221	2.1010	2.0510
7.854	1.9560	1.9673	18.535	2.0698	2.0534
8.168	1.9915	1.9736	18.850	2.0387	2.0563
8.482	2.0174	1.9793	19.164	2.0207	2.0593
8.796	2.0297	1.9842	19.478	2.0200	2.0627
9.111	2.0368	1.9886	19.792	2.0301	2.0662
9.425	2.0341	1.9924	20.106	2.0477	2.0697
9.739	2.0156	1.9959	20.420	2.0675	2.0740
10.053	1.9763	1.9990	20.735	2.0817	2.0783
10.367	1.9280	2.0016	21.049	2.0976	2.0825
10.681	1.8890	2.0040	21.363	2.1102	2.0868
10.996	1.8731	2.0062			
11.310	1.8900	2.0084			
11.624	1.9370	2.0103			
11.938	2.0019	2.0123			
12.252	2.0705	2.0142			
12.566	2.1243	2.0162			
12.881	2.1484	2.0182			
13.195	2.1428	2.0202			
13.509	2.1051	2.0225			

Table III. Experimental Levelled Intensity and Background Values for the 11-cm Camera Distance, r^3 Sector

s	I(s)	$I_B(s)$	s	I(s)	$I_B(s)$
8.168	5.0506	5.0095	18.850	4.8043	4.8420
8.482	5.1054	5.0041	19.164	4.7463	4.8379
8.796	5.1152	4.9988	19.478	4.7324	4.8338
9.111	5.1382	4.9935	19.792	4.7496	4.8297
9.425	5.1290	4.9882	20.106	4.7797	4.8258
9.739	5.0514	4.9829	20.420	4.8104	4.8219
10.053	4.9186	4.9776	20.735	4.8332	4.8181
10.367	4.7762	4.9724	21.049	4.8502	4.8144
10.681	4.6527	4.9672	21.363	4.8525	4.8108
10.996	4.5839	4.9620	21.677	4.8445	4.8073
11.310	4.6212	4.9568	21.991	4.8321	4.8039
11.624	4.7462	4.9517	22.305	4.8174	4.8006
11.938	4.9231	4.9465	22.619	4.7998	4.7975
12.252	5.1037	4.9414	22.934	4.7756	4.7944
12.566	5.2418	4.9363	23.248	4.7466	4.7915
12.881	5.3084	4.9313	23.562	4.7269	4.7886
13.195	5.2728	4.9262	23.876	4.7256	4.7859
13.509	5.1578	4.9212	24.190	4.7457	4.7834
13.823	5.0087	4.9162	24.504	4.7783	4.7810
14.137	4.8865	4.9113	24.819	4.8086	4.7787
14.451	4.8209	4.9064	25.133	4.8263	4.7766
14.765	4.7921	4.9015	25.447	4.8325	4.7746
15.080	4.7586	4.8967	25.761	4.8246	4.7728
15.394	4.7183	4.8918	26.075	4.8041	4.7712
15.708	4.6941	4.8871	26.389	4.7758	4.7697
16.022	4.7075	4.8823	26.704	4.7509	4.7684
16.336	4.7592	4.8777	27.018	4.7331	4.7673
16.650	4.8313	4.8730	27.332	4.7229	4.7664
16.965	4.9134	4.8684	27.646	4.7237	4.7657
17.279	4.9864	4.8639	27.960	4.7265	4.7652

Table III continued.

s	I(s)	$I_B(s)$	s	I(s)	$I_B(s)$
17.593	5.0412	4.8594	28.274	4.7340	4.7649
17.907	5.0473	4.8550	28.588	4.7481	4.7648
18.221	4.9931	4.8506	28.903	4.7679	4.7650
18.535	4.8993	4.8463	29.217	7.7899	4.7653
29.531	4.8065	4.7659	34.872	4.8231	4.8196
29.845	4.8124	4.7668	35.186	4.8219	4.8257
30.159	4.8081	4.7679	35.500	4.8201	4.8322
30.473	4.7958	4.7692	35.814	4.8223	4.8392
30.788	4.7812	4.7709	36.128	4.8289	4.8465
31.102	4.7658	4.7728	36.442	4.8400	4.8543
31.416	4.7539	4.7749	36.757	4.8537	4.8625
31.730	4.7507	4.7774	37.071	4.8687	4.8711
32.044	4.7562	4.7801	37.385	4.8825	4.8802
32.358	4.7686	4.7832	37.699	4.8941	4.8897
32.673	4.7830	4.7866	38.013	4.9068	4.8996
32.987	4.7953	4.7903	38.327	4.9197	4.9101
33.301	4.8065	4.7943	38.642	4.9315	4.9210
33.615	4.8153	4.7986	38.956	4.9389	4.9324
33.929	4.8212	4.8033	39.270	4.9437	4.9444
34.243	4.8224	4.8084	39.584	4.9557	4.9568
34.558	4.8229	4.8138			

APPENDIX II

Experimental Levelled Intensity and Background Intensity Functions for n-Hexadecane

Of the 21-cm r^2 sector data set, the points from s = 2.199 to s = 9.425 were used to obtain the final blended intensity.

Of the 21-cm r^3 sector data set, the points from s = 6.597 to s - 18.850 were used to obtain the final blended intensity.

Of the 11-cm r^3 sector data set, the points from s = 13.195 to s = 40.212 were used to obtain the final blended intensity.

Of the 7-cm r^3 sector data set, the points from s = 39.584 to s = 46.810 were used to obtain the final blended intensity.

Table I. Experimental Levelled Intensity and Background Values for the 21-cm Camera Distance, r^2 Sector

s	I(s)	$I_B(s)$	s	I(s)	$I_B(s)$
2.199	0.8552	0.9964	6.597	1.4007	1.4162
2.513	0.8931	1.0428	6.912	1.3641	1.4248
2.827	1.0208	1.0913	7.226	1.3522	1.4320
3.142	1.0693	1.1440	7.540	1.3713	1.4385
3.456	1.0417	1.1956	7.854	1.4207	1.4442
3.770	1.0188	1.2393	8.168	1.4726	1.4492
4.084	1.0358	1.2744	8.482	1.5012	1.4537
4.398	1.1154	1.3023	8.796	1.5054	1.4579
4.712	1.2798	1.3267	9.111	1.5028	1.4621
5.027	1.4714	1.3470	9.425	1.5112	1.4662
5.341	1.5701	1.3648	9.739	1.5273	1.4699
5.655	1.5582	1.3805	10.053	1.5093	1.4734
5.969	1.4984	1.3944	10.367	1.4410	1.4771
6.283	1.4460	1.4063	10.681	1.3776	1.4807

Table II. Experimental Levelled Intensity and Background Values for the 21-cm Camera Distance, r^3 Sector

s	I(s)	$I_B(s)$	s	I(s)	$I_B(s)$
3.456	1.6024	1.8194	10.367	1.9089	1.9629
3.770	1.5616	1.8948	10.681	1.8289	1.9617
4.084	1.5893	1.9356	10.996	1.7966	1.9609
4.398	1.7055	1.9617	11.310	1.8166	1.9604
4.712	1.9329	1.9793	11.624	1.8690	1.9604
5.027	2.1625	1.9919	11.938	1.9420	1.9606
5.341	2.2769	2.0008	12.252	2.0234	1.9608
5.655	2.2470	2.0067	12.556	2.0916	1.9610
5.969	2.1575	2.0103	12.881	2.1167	1.9612
6.283	2.0620	2.0117	13.195	2.0901	1.9614
6.597	1.9874	2.0111	13.509	2.0341	1.9616
6.912	1.9279	2.0092	13.823	1.9747	1.9616
7.226	1.9009	2.0059	14.137	1.9351	1.9615
7.540	1.9189	2.0017	14.451	1.9177	1.9614
7.854	1.9663	1.9966	14.765	1.9181	1.9615
8.168	2.0189	1.9912	15.080	1.9101	1.9617
8.482	2.0467	1.9855	15.394	1.8942	1.9620
8.796	2.0398	1.9799	15.708	1.8897	1.9629
9.111	2.0250	1.9750	16.022	1.9048	1.9639
9.425	2.0267	1.9706	16.336	1.9340	1.9650
9.739	2.0297	1.9670	16.650	1.9577	1.9662
10.053	1.9931	1.9646	16.965	2.0033	1.9680
17.279	2.0330	1.9700	19.164	1.9377	1.9879
17.593	2.0492	1.9724	19.478	1.9448	1.9914
17,907	2.0435	1.9751	19.792	1.9623	1.9947
18.221	2.0137	1.9780	20.106	1.9811	1.9979
18.535	1.9759	1.9812	20.420	1.9966	2.0012
18.850	1.9477	1.9844			

Table III. Experimental Levelled Intensity and Background Values for 11-cm Camera Distance, r^3 Sector

s	I(s)	$I_B(s)$	s	I(s)	$I_B(s)$
9.425	4.3314	4.2166	19.478	4.0519	4.1421
9.739	4.3648	4.2161	19.792	4.0750	4.1394
10.053	4.2815	4.2158	20.106	4.1026	4.1367
10.367	4.0836	4.2151	20.420	4.1352	4.1340
10.681	3.9040	4.2144	20.735	4.1589	4.1315
10.996	3.8480	4.2137	21.049	4.1727	4.1288
11.310	3.8978	4.2129	21.363	4.1732	4.1264
11.624	4.0206	4.2119	21.677	4.1662	4.1239
11.938	4.1944	4.2108	21.991	4.1525	4.1214
12.252	4.3787	4.2095	22.305	4.1356	4.1187
12.566	4.5250	4.2081	22.619	4.1081	4.1159
12.881	4.5675	4.2064	22.934	4.0799	4.1133
13.195	4.4977	4.2044	23.248	4.0548	4.1107
13.509	4.3652	4.2022	23.562	4.0422	4.1083
13.823	4.2298	4.1997	23.876	4.0592	4.1057
14.137	4.1313	4.1969	24.190	4.0842	4.1031
14.451	4.0914	4.1941	24.504	4.1158	4.1006
14.765	4.0865	4.1912	24.819	4.1372	4.0981
15.080	4.0597	4.1879	25.133	4.1437	4.0956
15.394	4.0192	4.1845	25.447	4.1431	4.0932
15.708	4.0033	4.1812	25.761	4.1296	4.0909
16.022	4.0346	4.1777	26.075	4.1062	4.0888
16.336	4.0967	4.1742	26.389	4.0791	4.0868
16.650	4.1662	4.1706	26.704	4.0610	4.0847
16.965	4.2395	4.1671	27.019	4.0481	4.0828
17.279	4.3025	4.1636	27.332	4.0364	4.0809
17.593	4.3385	4.1601	27.646	4.0369	4.0791
17.907	4.3106	4.1568	27.960	4.0421	4.0776
18.221	4.2305	4.1537	28.274	4.0485	4.0762
18.535	4.1401	4.1507	28.588	4.0682	4.0747
18.850	4.0681	4.1478	28.903	4.0844	4.0736
19.164	4.0375	4.1448	29.217	4.0957	4.0725
29.531	4.0996	4.0716	35.186	4.0548	4.0685
29.845	4.0978	4.0707	35.500	4.0502	4.0687
30.159	4.0884	4.0699	35.814	4.0491	4.0689
30.473	4.0761	4.0693	36.128	4.0553	4.0691
30.778	4.0619	4.0688	36.442	4.0601	4.0693
31.102	4.0477	4.0684	36.757	4.0655	4.0696
31.416	4.0410	4.0861	37.071	4.0716	4.0699
31.730	4.0429	4.0679	37.385	4.0770	4.0702
32.044	4.0498	4.0678	37.699	4.0822	4.0705
32.358	4.0566	4.0678	38.013	4.0801	4.0709
32.673	4.0661	4.0678	38.327	4.0771	4.0714
32.987	4.0750	4.0678	38.642	4.0748	4.0719

Table III continued.

s	I(s)	$I_B(s)$	s	I(s)	$I_B(s)$
33.301	4.0801	4.0679	38.956	4.0725	4.0723
33.615	4.0850	4.0680	39.270	4.0620	4.0728
33.929	4.0843	4.0681	39.584	4.0655	4.0732
34.243	4.0858	4.0681	39.898	4.0742	4.0737
34.558	4.0729	4.0682	40.212	4.0819	4.0742
34.872	4.0639	4.0683			

Table IV. Experimental Levelled Intensity and Background Values for 7-cm Camera Distance, r^3 Sector

s	I(s)	$I_B(s)$	s	I(s)	$I_B(s)$
18.850	0.2454	0.2498	24.819	0.2418	0.2395
19.164	0.2433	0.2492	25.133	0.2421	0.2390
19.478	0.2434	0.2487	25.447	0.2414	0.2384
19.792	0.2445	0.2482	25.761	0.2402	0.2378
20.106	0.2462	0.2476	26.075	0.2385	0.2372
20.420	0.2473	0.2471	26.389	0.2367	0.2366
20.735	0.2477	0.2466	26.704	0.2349	0.2360
21.049	0.2476	0.2460	27.019	0.2336	0.2354
21.363	0.2482	0.2455	27.332	0.2327	0.2348
21.677	0.2473	0.2450	27.646	0.2321	0.2342
21.991	0.2458	0.2445	27.960	0.2317	0.2336
22.305	0.2441	0.2439	28.274	0.2320	0.2329
22.619	0.2425	0.2434	28.588	0.2324	0.2323
22.934.	0.2403	0.2428	28.903	0.2327	0.2316
23.248	0.2391	0.2423	29.217	0.2326	0.2310
23.562	0.2385	0.2417	29.531	0.2322	0.2303
23.876	0.2389	0.2412	29.845	0.2314	0.2296
24.190	0.2399	0.2407	30.159	0.2303	0.2289
24.504	0.2401	0.2401	30.473	0.2285	0.2282
30.778	0.2273	0.2275	39.270	0.2055	0.2060
31.102	0.2260	0.2268	39.584	0.2047	0.2051
31.416	0.2248	0.2261	39.898	0.2039	0.2043
31.730	0.2241	0.2254	40.212	0.2029	0.2034
32.044	0.2237	0.2246	40.527	0.2025	0.2026
32.358	0.2234	0.2239	40.841	0.2019	0.2017
32.673	0.2234	0.2231	41.155	0.2010	0.2009
32.987	0.2231	0.2224	41.469	0.2002	0.2000
33.301	0.2226	0.2216	41.783	0.1996	0.1992
33.615	0.2218	0.2208	42.097	0.1984	0.1983
33.929	0.2204	0.2201	42.412	0.1977	0.1975
34.243	0.2199	0.2193	42.726	0.1972	0.1967
34.558	0.2186	0.2185	43.040	0.1960	0.1959

Table IV continued.

s	I(s)	$I_B(s)$	s	I(s)	$I_B(s)$
34.872	0.2175	0.2177	43.354	0.1950	0.1950
35.186	0.2162	0.2169	43.668	0.1939	0.1942
35.500	0.2155	0.2161	43.982	0.1932	0.1934
35.814	0.2143	0.2153	44.296	0.1924	0.1926
36.128	0.2136	0.2144	44.610	0.1920	0.1919
36.442	0.2134	0.2136	44.925	0.1916	0.1911
36.757	0.2126	0.2128	45.239	0.1908	0.1903
37.071	0.2125	0.2119	45.553	0.1900	0.1896
37.385	0.2116	0.2111	45.867	0.1887	0.1889
37.699	0.2108	0.2102	46.181	0.1878	0.1882
38.013	0.2093	0.2094	46.496	0.1871	0.1875
38.327	0.2088	0.2086	46.810	0.1869	0.1868
38.642	0.2079	0.2077			
38.956	0.2066	0.2068			